Comparing the Impact of Control Strategies on Mathematical Models of *Clostridium difficile* Transmission

A Dissertation Presented for the

Doctor of Philosophy

Degree

The University of Tennessee, Knoxville

Brittany Christine Stephenson

August 2018

© by Brittany Christine Stephenson, 2018
All Rights Reserved.

I dedicate this dissertation and the completion of my degree to my incredibly giving and patient parents, selfless boyfriend, and supportive siblings. Without their unceasing love, encouragement, and guidance, I would never have made it this far. I thank them each for believing in me and pushing me to accomplish my goals even (and especially) when I doubted myself.

Acknowledgments

I must begin by acknowledging both of my advisors, Judy Day and Suzanne Lenhart, for their guidance and encouragement throughout the entirety of my time in graduate school. I will never be able to thank them enough for going above and beyond their duties to ensure my success. To Judy, thank you for all the pep talks and encouraging words you gave me over the course of our time together and thank you for the countless times you allayed my stress and reminded me of my capabilities. You were the perfect combination of motivating and encouraging, and I could not have asked for a better advisor or inspiration. Your care and compassion carried me through some of my most stressful days. To Suzanne, thank you for inspiring me every day with your dedication to your students and their success, ability to balance a large number of projects with such ease, enthusiasm for women in mathematics, and desire to impact future generations of mathematicians. Your passion and brilliance are evident, and I am honored to have had the chance to work with you.

I would also like to thank my "non-mathematics" advisor, Cristina Lanzas, for guiding me in my understanding of *C. difficile*. My project was motivated by Dr. Lanzas's previous work and was funded by the joint DMS/NIGMS Mathematical Biology Program through NIH award #R01GM113239, of which she is PI. None of this would have been possible without her or her expertise. To the other members of my committee, Drs. Mike Frazier and Nina Fefferman, thank you for the time you gave to thoughtfully evaluating my work and for your willingness to serve on my committee (especially to Dr. Frazier, who was on sabbatical at the time).

My time as a graduate student at the University of Tennessee was funded through a teaching assistantship and through the NIH award previously mentioned. I am very thankful to have worked in such a supportive and collaborative mathematics department. To Joan

Lind, thank you for your guidance and support in all of my pedagogical endeavors; I owe my growth as an instructor to you. To Pam Armentrout, you are invaluable. Thank you for all the times you talked me through stress and for all that you do for the mathematics department. To my fellow graduate students, Betsy, Lindsey, Maggie, Kylie, Camila, Mark, Grace, Kolin, Elise, Jimmy, and many others, thank you for all the chats, collaborations, venting sessions, and "non-math" activities. I also have to thank my undergraduate advisor, Dr. Ratnasingham Shivaji, without whom, I may not have pursued an advanced degree in mathematics.

To my unwaveringly supportive boyfriend, Thomas, thank you for all the laughs you bring me and for standing by me and encouraging me to continue throughout my time as a graduate student; I could not have done this without you. To my parents, Chris and Jud, I would not be the person I am today without your love, sacrifice, and support. Everything I do is because of and thanks to you. To my brother, Matt, my career in mathematics is thanks to your example and assistance, and you continue to inspire me every day. To my sister, Kayla, thank you for being a constant source of support, friendship, and happiness. To my best friends, Jaclyn, Megan, and Megan, your love and support have helped carry me through this process. Finally, to my two loving and loyal dogs, Rudy and Corky, thank you for never leaving my side during the late nights of work and for constantly bringing me joy, even through the stress.

Abstract

The spore-forming, gram-positive bacteria *Clostridium difficile* can cause severe intestinal illness. A striking increase in the number of cases of *C. difficile* infection (CDI) among hospitals has highlighted the need to better understand how to prevent its spread. In this dissertation, I discuss the development and structure of two different models of nosocomial *C. difficile* transmission that we used to evaluate the efficacy of various control strategies and to determine optimal interventions.

We begin with an update and modification of a compartmental model of nosocomial *C. difficile* transmission to include vaccination. We then apply optimal control theory on this epidemiological model to determine the time-varying optimal vaccination rate that minimizes a combination of (1) disease prevalence and spread in the hospital population and (2) the cost, in terms of time and money, associated with vaccination. Various hospital scenarios are considered, such as times of increased antibiotic prescription rates and periods of outbreak, to see how such scenarios affect the optimal vaccination rate. By comparing the values of our objective functional with constant vaccination rates to those with time-varying optimal vaccination rates, we illustrate the benefits of time-varying controls.

The second model is an agent-based model that also simulates the transmission of *C. difficile* in a healthcare setting. This model explicitly incorporates healthcare workers (HCWs) as vectors of transmission, tracks individual patient antibiotic histories, incorporates varying risk levels of antibiotics with respect to CDI, and tracks contamination levels of ward rooms by *C. difficile*. Using this model, we evaluated the efficacy of a variety of control interventions and combinations of interventions on reducing *C. difficile* nosocomial colonizations and infections. The control techniques included two forms of antimicrobial

stewardship, increased environmental decontamination through room cleaning, improved HCW compliance, and a preliminary assessment of vaccination.

Table of Contents

1 Introduction **1**

1.1 Background 1

1.2 Compartmental epidemiological model 4

1.2.1 Optimal control theory 4

1.3 Agent-based model 7

2 Compartmental model of nosocomial *C. difficile* transmission **9**

2.1 Introduction 9

2.2 ODE Model 10

2.3 Existence and uniqueness 15

2.4 Optimal control of vaccination rate 20

2.4.1 Existence of optimal control 21

2.4.2 Characterization of optimal control 23

2.5 Numerical results 25

2.5.1 Summary of exploration into weighting coefficient values 25

2.5.2 Determining the impact of vaccination 27

2.5.3 An increase in susceptible patients 29

2.5.4 Increasing transmission coefficients 32

2.6 Discussion 36

3 Agent-based model of nosocomial *C. difficile* transmission **38**

3.1 Introduction 38

3.2 Model overview 43

3.2.1 Model setting . . . 43
3.2.2 Model components . . . 44
3.2.3 Model processes . . . 48
3.3 Control interventions . . . 53
3.4 High-performance computing setup . . . 56
3.5 Results . . . 57
3.5.1 Baseline results . . . 57
3.5.2 Single control interventions . . . 60
3.5.3 Combination strategies . . . 63
3.5.4 Vaccination . . . 68
3.6 Discussion . . . 72
3.7 ODD Protocol: Overview . . . 77
3.7.1 Purpose . . . 77
3.7.2 Input data . . . 77
3.7.3 Entities, state variables, and scales . . . 78
3.7.4 Process overview and scheduling . . . 86
3.7.5 Initialization . . . 86
3.8 Submodels . . . 87
3.8.1 Admit HCWs . . . 87
3.8.2 Admit patients . . . 87
3.8.3 Update disease status . . . 90
3.8.4 Update room contamination levels . . . 92
3.8.5 Discharge patients . . . 92
3.8.6 Clean ward rooms . . . 92
3.8.7 Update patient time characteristics . . . 93
3.8.8 HCW movement . . . 93
3.8.9 Update HCW and room contamination levels . . . 94
3.8.10 HCW compliance . . . 97
3.8.11 Shift change and update of HCW time characteristics . . . 97
3.8.12 Antibiotic assignment . . . 97

3.8.13 Colonization probability assignment 97
3.8.14 Resistance-restoration probability assignment 98
3.8.15 Quarantine and treat 99
3.8.16 Patient length of stay 100

4 Future work **101**

Bibliography **103**

Appendices **114**

A Sensitivity analysis 115

Vita **119**

List of Tables

2.1 Patient transition states developed in [45] 10
2.2 Additional patient transition states for vaccinated patients 11
2.3 Model parameter descriptions and values 14
2.4 Exploration of a biologically feasible range of values for vaccination rate, v . 15
2.5 Comparison of $J(v)$ with constant vaccination rate to $J(v)$ with time-varying optimal vaccination rate, shown in Figure 2.4, for various upper bounds, M, on $v(t)$ 29
2.6 Comparison of $J(v)$ and total vaccinated with constant vaccination rate to $J(v)$ and total vaccinated with time-varying optimal vaccination rate, shown in Figure 2.5, for various antibiotic prescription rates, α 30
2.7 Comparison of $J(v)$ with constant vaccination rate to $J(v)$ with time-varying optimal vaccination rate, shown in Figure 2.7, for various transmission coefficients, β_c and β_d 32
2.8 Comparison of $J(v)$ with constant vaccination rate to $J(v)$ with time-varying optimal vaccination rate, shown in Figure 2.10, for various upper bounds, M, on $v(t)$ with increased $\beta_c, \beta_d = 0.007$ 35

3.1 Antimicrobial stewardship strategy: reduction in the overall number of antibiotics prescribed 55
3.2 Antimicrobial stewardship strategy: reduction in the proportions of antibiotics prescribed according to risk level with respect to CDI 55
3.3 Median percentage of patients admitted in each class who eventually become colonized during their hospital stay out of 100 iterations 59

3.4 Median percentage of patients admitted in each class who eventually become diseased during their hospital stay out of 100 iterations 59
3.5 Median numbers of nosocomial colonizations and nosocomial infections per year for 100 iterations, normalized to 10,000 admissions, for the individual control scenarios listed 64
3.6 Antimicrobial stewardship and ward room cleaning combination strategies numbered for easy reference, where the specific distributions of antibiotic-risk-level probabilities for each risk scenario are given in Table 3.2 66
3.7 Parameter combinations representing control interventions with increased HCW compliance (where 0.45 is baseline) combined with select combinations of antimicrobial stewardship and ward room cleaning (Scenarios 6, 15, 18, 22, and 25 from Table 3.6) 69
3.8 Parameter combinations representing control interventions with decreased probability of being immunocompromised (where 0.10 is baseline), combined with select combinations of improved HCW compliance, antimicrobial stewardship, and ward room cleaning (Scenarios 6.1, 6.2, 18.1, 18.2, 22.1, 22.2, 25.1, and 25.2 from Table 3.7) 73
3.9 Room state variable explanations and values 79
3.10 Patient state variable explanations and values 81
3.11 HCW state variable explanations and values 83
3.12 Global variable explanations and baseline values 85
3.13 Probabilities used to determine risk level of tasks performed by HCWs . . . 96
3.14 Probabilities of becoming colonized for each combination of antibiotic-risk and room-contamination level 99

A.1 List of parameters considered in the sensitivity analysis procedure with their corresponding intervals sampled and baseline values 117
A.2 PRCCs and corresponding p-values for each parameter 118

List of Figures

2.1 Summary of movement among patient transition states with corresponding parameters 13

2.2 Optimal vaccination rate v^* for $c_0 = 3$, $c_1 = 0.1$, $c_2 = c_5 = 15$, $c_3 = c_4 = 0.5$, $M = 0.3$, and $T = 30$ 27

2.3 Dynamics of patient transition states with optimal vaccination rate v^* shown in Figure 2.2 compared to those without vaccination for $c_0 = 3$, $c_1 = 0.1$, $c_2 = c_5 = 15$, $c_3 = c_4 = 0.5$, $M = 0.3$, and $T = 30$ 28

2.4 **(a)** Comparison of optimal vaccination rate v^* with upper bound $M = 0.3$ to that with the increased value of $M = 0.6$ with $c_0 = 3$, $c_1 = 0.1$, $c_2 = c_5 = 15$, $c_3 = c_4 = 0.5$, and $T = 30$ **(b)** View of (a) over a 3-day interval to observe the initial difference in v^* 29

2.5 Optimal vaccination rate v^* for increasing antibiotic prescription rate, α, and for $c_0 = 3$, $c_1 = 0.1$, $c_2 = c_5 = 15$, $c_3 = c_4 = 0.5$, $M = 0.3$, and $T = 30$ 31

2.6 Dynamics of patient transition states for increasing antibiotic prescription rate, α, and for $c_0 = 3$, $c_1 = 0.1$, $c_2 = c_5 = 15$, $c_3 = c_4 = 0.5$, $M = 0.3$, and $T = 30$ 31

2.7 Optimal vaccination rate v^* for increasing transmission coefficients, β_c, β_d, and for $c_0 = 3$, $c_1 = 0.1$, $c_2 = c_5 = 15$, $c_3 = c_4 = 0.5$, $M = 0.3$, and $T = 30$ 33

2.8 Dynamics of patient transition states for increasing transmission coefficients, β_c, β_d, and for $c_0 = 3$, $c_1 = 0.1$, $c_2 = c_5 = 15$, $c_3 = c_4 = 0.5$, $M = 0.3$, and $T = 30$ 34

2.9 Dynamics of patient transition states with vaccination rate shown in Figure 2.7 for the increased values of $\beta_c, \beta_d = 0.007$ compared to those without vaccination for $c_0 = 3$, $c_1 = 0.1$, $c_2 = c_5 = 15$, $c_3 = c_4 = 0.5$, $M = 0.3$, and $T = 30$ 34
2.10 Optimal vaccination rate v^* for increasing M with increased $\beta_c, \beta_d = 0.007$, $c_0 = 3$, $c_1 = 0.1$, $c_2 = c_5 = 15$, $c_3 = c_4 = 0.5$, and $T = 30$ 35
2.11 Dynamics of patient transition states with optimal vaccination rates shown in Figure 2.10 with various upper bounds M for the increased values of $\beta_c, \beta_d = 0.007$ for $c_0 = 3$, $c_1 = 0.1$, $c_2 = c_5 = 15$, $c_3 = c_4 = 0.5$, $M = 0.3$, and $T = 30$. 36

3.1 Snapshot of the graphical user interface of our model environment in NetLogo as a hospital with six wards that each have 35 rooms, where the dice represent patients, the people represent HCWs, and the colors represent the amount of contamination in that room (yellow indicates low contamination, green is medium contamination, and brown is high contamination) 44
3.2 Summary of movement among disease statuses of patients in agent-based model 47
3.3 Summary of ABM processes that are run at each 15-minute time-step 49
3.4 Summary of ABM processes that are run at each half-day time-step 52
3.5 Summary of modes of *C. difficile* transmission included in the ABM, where *prob-room-transfer* refers to the probability of an HCW picking up *C. difficile* spores from a room, *prob-HCW-transfer* refers to the probability of an HCW contaminating room surface(s) with spores, and *prob-becoming-colonized* represents the probability of a patient becoming colonized based on the contamination level of the room and on the risk level of the antibiotic received 53
3.6 Baseline parameter values: Number of (a) nosocomial colonizations and (b) nosocomial infections by *C. difficile*, normalized to 10,000 admissions, for 100 iterations over a one-year time period with baseline parameter values 58

3.7 Breakdown of (a) nosocomial colonizations and (b) nosocomial infections based on disease status at admission for 100 iterations over a one-year time period with baseline parameter values 59
3.8 Reducing the half-daily probability of receiving an antibiotic: Resulting number of (a) nosocomial colonizations and (b) nosocomial infections for baseline probability of receiving an antibiotic ($p = 0.27$) and for the the reduced probabilities of receiving an antibiotic (10% reduction and 20% reduction) described in Table 3.1, normalized to 10,000 admissions, for 100 iterations over a one-year time period 60
3.9 Reducing the proportion of very high-risk and high-risk antibiotics: Resulting number of (a) nosocomial colonizations and (b) nosocomial infections for each risk scenario (specifying proportions of low-risk, high-risk, and very high-risk antibiotics) described in Table 3.2, where Risk Scenario 1 is baseline, normalized to 10,000 admissions, for 100 iterations over a one-year time period 61
3.10 Increasing the probability of sufficiently cleaning ward rooms: Resulting number of (a) nosocomial colonizations and (b) nosocomial infections for increased probabilities of sufficiently cleaning ward rooms, where 0.5 is baseline, normalized to 10,000 admissions, for 100 iterations over a one-year time period 62
3.11 Increasing HCW compliance with all patients: Resulting number of (a) nosocomial colonizations and (b) nosocomial infections for increased probabilities of HCWs sufficiently cleaning their hands after visiting patients, where 0.45 is baseline, normalized to 10,000 admissions, for 100 iterations over a one-year time period 62
3.12 Increasing HCW contact compliance with quarantined patients: Resulting number of (a) nosocomial colonizations and (b) nosocomial infections for increased probabilities of HCW contact compliance when visiting quarantined patients, where 0.6 is baseline, normalized to 10,000 admissions, for 100 iterations over a one-year time period 63

3.13 Combination strategies involving antimicrobial stewardship and ward room cleaning: Resulting number of nosocomial colonizations for each of the 27 strategies listed in Table 3.6 that incorporate both antimicrobial stewardship and ward room cleaning as control interventions, normalized to 10,000 admissions, for 100 iterations over a one-year time period, where the x-axis gives the strategies listed in order from the most effective strategy to the least effective strategy for reducing nosocomial colonizations (a) based on conclusions from Bintz et al.'s model [5] and (b) based on the results from our model 65

3.14 Combination strategies involving antimicrobial stewardship and ward room cleaning: Resulting number of nosocomial infections for each of the 27 strategies listed in Table 3.6 that incorporate both antimicrobial stewardship and ward room cleaning as control interventions, normalized to 10,000 admissions, for 100 iterations over a one-year time period, where the x-axis gives the strategies listed (a) in order of increasing resulting median number of nosocomial colonizations determined in Figure 3.13b and (b) in order of increasing resulting median number of nosocomial infections 67

3.15 Combination strategies involving antimicrobial stewardship, ward room cleaning, and HCW compliance: Resulting number of nosocomial colonizations for each of the 15 strategies listed in Table 3.7 that incorporate antimicrobial stewardship, ward room cleaning, and HCW compliance as control interventions, normalized to 10,000 admissions, for 100 iterations over a one-year time period, where the x-axis (a) corresponds to the strategies in Table 3.7 with HCW contact compliance with quarantined patients equal to 0.6 and (b) corresponds to the strategies in Table 3.7 with HCW contact compliance with quarantined patients equal to 1 70

3.16 Combination strategies involving antimicrobial stewardship, ward room cleaning, and HCW compliance: Resulting number of nosocomial infections for each of the 15 strategies listed in Table 3.7 that incorporate antimicrobial stewardship, ward room cleaning, and HCW compliance as control interventions, normalized to 10,000 admissions, for 100 iterations over a one-year time period, where the x-axis (a) corresponds to the strategies in Table 3.7 with HCW contact compliance with quarantined patients equal to 0.6 and (b) corresponds to the strategies in Table 3.7 with HCW contact compliance with quarantined patients equal to 1 70

3.17 Reducing probability of being immunocompromised as a form of effective vaccination: Resulting number of (a) nosocomial colonizations and (b) nosocomial infections for decreasing probabilities of being immunocompromised, where 0.10 is baseline, normalized to 10,000 admissions, for 100 iterations over a one-year time period 72

3.18 Combination strategies involving antimicrobial stewardship, ward room cleaning, HCW compliance, and vaccination: Resulting number of nosocomial colonizations for each of the 24 strategies listed in Table 3.8 that incorporate antimicrobial stewardship, ward room cleaning, HCW compliance, and vaccination as control interventions, normalized to 10,000 admissions, for 100 iterations over a one-year time period, where the x-axis (a) lists the scenarios in the order presented in Table 3.8 and (b) lists the scenarios according to increasing number of colonizations 74

3.19 Combination strategies involving antimicrobial stewardship, ward room cleaning, HCW compliance, and vaccination: Resulting number of nosocomial infections for each of the 24 strategies listed in Table 3.8 that incorporate antimicrobial stewardship, ward room cleaning, HCW compliance, and vaccination as control interventions, normalized to 10,000 admissions, for 100 iterations over a one-year time period, where the x-axis lists the scenarios in the order presented in Table 3.8 75

3.20 Transfer functions used to determine the probability a room (or HCW) will transfer pathogen at a particular time-step 96

A.1 Resulting PRCCs for each of the parameters considered 117

Chapter 1

Introduction

1.1 Background

In the United States, one of the most common causes of healthcare-associated infections (HAIs) is the spore-forming, toxin-producing bacteria *Clostridium difficile* [50, 42]. In fact, *C. difficile* has surpassed *Staphylococcus aureus* as the leading cause of nosocomial infections [42]. Although *C. difficile* was first identified in the 1930s and has since been more intensely studied beginning in the 1970s, there is still difficulty diagnosing, treating, and preventing *C. difficile* infection (CDI) [19]. Between 2000 and 2010, the number of hospitalizations for CDI among adults in the U.S. doubled [50]. This increase in both incidence and severity coincided with the emergence of the epidemic NAP1/B1/027 strain, which is a highly virulent strain [56]. In 2011, *C. difficile* was estimated to cause approximately 453,000 incident infections and was linked to approximately 29,000 deaths [50]. For acute care facilities alone, the estimated costs associated with *C. difficile* infection are as much as $4.8 billion [50], which has placed a significant burden on healthcare facilities.

C. difficile spores are commonly found in the environment of healthcare facilities and are transmitted through the fecal-oral route [48]. Symptomatic and asymptomatic individuals shed *C. difficile* spores, and if ingested by a susceptible person, the spores can survive the acidity of the stomach and reach the large intestine, where *C. difficile* can colonize. Typically, the normal gut microbiota prevents *C. difficile* colonization by competing for nutrients and producing inhibitory compounds against *C. difficile*. Antibiotics disrupt the

normal gut microbiota, facilitating the colonization of *C. difficile*. Hence, use of antibiotics is the strongest risk factor for developing CDI, and almost all antibiotics have been linked to CDI [48]. With advanced age comes an increased risk of contracting CDI [48]. Toxins A and B are responsible for most of the clinical manifestations of CDI including diarrhea, abdominal pain, and bloating [48]. Once *C. difficile* reaches large numbers in the colon, both toxins A and B are produced by *C. difficile* [19]. In response, some people will be able to mount their own immune response and fight off the toxins. These individuals will become asymptomatic carriers and never experience clinical symptoms [45].

Strategies to control and prevent CDI include antimicrobial usage restriction and stewardship and methods to prevent the patient from exposure to *C. difficile* [18]. Current practice includes identifying patients who have clinical CDI, putting them into isolation, and taking proper contact precautions such as wearing gloves and gown, as well as vigilant hand-washing with soap [18]. *C. difficile* cannot be eliminated by routine surface cleaning nor by alcohol-based hand sanitizers, but washing with soap and water has been shown to decrease *C. difficile* spores [48]. Worth noting is the fact that the large increase in CDI in the early 2000s coincides with the expanded use of alcohol-based hand sanitizers in healthcare settings [19].

In spite of these current practices, a notable difficulty in studying nosocomial *C. difficile* transmission arises because many colonized patients, who also shed *C. difficile* in their feces and contribute to transmission, are asymptomatic. Over the years, there have been discrepancies in determining the relative contributions of asymptomatic carriers versus those of symptomatic patients. In the 1980s, studies were conducted by [9] that concluded symptomatic CDI patients were the main source of *C. difficile* transmission. Therefore, protocol often focused on isolating and taking proper contact precautions with only symptomatic CDI patients. Such protocol included healthcare workers' wearing gloves and gowns when interacting with symptomatic patients and the intense cleaning of their hospital rooms after symptomatic patients were discharged [48]. However, since these studies were completed, changes in the epidemiology of *C. difficile* may have altered the relative contributions of symptomatic CDI patients and asymptomatic carriers [45, 80]. Typically, healthcare facilities are unable to readily identify asymptomatic patients, so their

contribution to the spread of *C. difficile* is often more significant than that of symptomatic patients because healthcare workers may not follow proper contact protocol when interacting with them [19]. Therefore, it would be beneficial to identify not only symptomatic patients, but also asymptomatic ones. There are two types of asymptomatic patients: those who are able to mount an immune response and avoid infection and those who are unable to mount an immune response, which leaves them vulnerable to contracting CDI.

Current treatment for patients experiencing CDI symptoms includes antimicrobial therapy, specifically with metronidazole or vancomycin [73]. Data have indicated that symptoms are resolved in 80% of patients treated with one of these antibiotics [45]. However, the antibiotics may also disrupt the normal gut microbiota and lead to recurrence of CDI upon cessation of treatment [73]. Therefore, it is often recommended that all antibiotic usage be stopped if possible to allow the gut microbiota to return to normal, which is often sufficient for controlling *C. difficile* [73]. Active vaccination is also being considered with the current clinical trial testing of three toxoid vaccines that would fight off the main virulence factors of *C. difficile*, toxins A and B. Initial trial phases have shown signs of efficacy [84], and the hope is for at least one of these vaccines to be approved for implementation.

Since *C. difficile* infection and colonization have been acknowledged as a significant burden to healthcare facilities [73], there is a strong need to better understand the transmission and subsequent infection by *C. difficile* in order to prevent its spread. Mathematical models have been used to successfully amalgamate theory with procedures and data in order to simulate disease dynamics and predict emerging behaviors [46]. The goal of my work is to develop mathematical models of *C. difficile* transmission in order to gain insight into the dynamics of its spread, explore the role of the environment in its transmission, and to assess optimal intervention strategies. Because the majority of CDI cases are nosocomial [48], this dissertation focuses on modeling the within-hospital transmission of *C. difficile*. Two different types of models are considered, and each incorporate different underlying assumptions about how *C. difficile* is spread.

1.2 Compartmental epidemiological model

The first model we developed is a modification of the compartmental model of *C. difficile* nosocomial transmission in [45], consisting of ordinary differential equations (ODEs) that group patients into classes based on their disease status (similar to the classic SIR model [6]). The focus of this ODE model is on assessing the impact of vaccination on CDI transmission. With a *C. difficile* toxoid vaccine still in testing, this model was our first exploration into how a vaccine could theoretically affect the spread of CDI in a healthcare setting. A major underlying assumption of this model is the direct transmission of *C. difficile* from an infected patient to a susceptible patient, i.e., without the explicit modeling of an environmental reservoir or healthcare workers.

Using this model, we aimed to determine the optimal time-varying rate of vaccination that minimized both the cost associated with a vaccination program and the overall impact of the disease, including the prevalence, incidence, and transmission. Obtaining the optimal rate of vaccination involves assessing trade-offs between vaccinating a large number of patients to control the disease while also keeping the associated cost low. To answer this, we used optimal control theory to find the optimal rate of vaccination that minimized our objective functional subject to the system of ordinary differential equations that simulated transmission. We formulated the objective functional to represent our goal of controlling the vaccination rate in a way that minimizes the cost and the overall impact of disease. This model and the corresponding optimal control problem are detailed in Chapter 2. An overview of optimal control theory is given in the following section.

1.2.1 Optimal control theory

Optimal control theory involves steering a dynamical system to a desired state by adjusting the values of a control or multiple controls [70, 49]. The underlying dynamic system being steered can be represented by ordinary differential equations, partial differential equations, discrete equations, stochastic differential equations, integro-difference equations, or a combination of discrete and continuous systems [49]. We will focus on an underlying

system represented by ODEs. In the 1950s, Pontryagin and his collaborators developed the theory of optimal control of systems of ODEs [70].

Suppose $u(t)$ denotes a control and $x(t)$ represents the underlying state dynamics and is dependent on the control $u(t)$. Then, we define $x(t)$ by the differential equation:

$$x'(t) = g(t, x(t), u(t)). \tag{1.1}$$

This dependence of the state system on the control means that a change in the control value engenders a change in the state solution [49]. An optimal control problem involves solving for the time-varying control, $u(t)$, and corresponding state, $x(t)$, that maximize the objective functional, formulated to balance the tradeoffs being assessed [49]. In general, we want to find the optimal control, $u^*(t)$, that satisfies the following:

$$J(u^*) = \sup_{u \in U^*} J(u), \tag{1.2}$$

where U^* is the set of admissible controls and

$$J(u) = \left[\phi(x(t_1)) + \int_{t_0}^{t_1} f(t, x(t), u(t))dt\right], \tag{1.3}$$

subject to (1.1) with $x(t_0) = x_0$ and $x(t_1)$ unrestricted. $J(u)$ represents the objective functional. If an optimal solution exists and is unique, we refer to it as the *optimal control* and denote it by $u^*(t)$. The solution to the state system that corresponds to the optimal control is denoted $x^*(t)$ and is referred to as the *optimal state*. Together, $(u^*(t), x^*(t))$ are referred to as an *optimal pair* [49].

Solving an optimal control problem involves solving a set of necessary conditions. First, one must establish that an optimal control exists. If it is determined an optimal pair exists, then Pontryagin's Maximum Principle [70] provides necessary conditions for solving for $(u^*(t), x^*(t))$. Pontryagin's Maximum Principle introduces an adjoint variable(s), denoted $\lambda(t)$, to link the state equation(s) to the objective functional, $J(u)$. This concept is similar to the idea of introducing Lagrange multipliers to solve constrained optimization problems in multivariable calculus. The Maximum Principle takes the original problem of finding $u \in U^*$

that maximizes $J(u)$ subject to the state equation (1.1) with specified initial conditions and transforms it into the problem of maximizing what is referred to as the Hamiltonian with respect to u, pointwise. The formal statement of the Maximum Principle follows below for continuously differentiable functions f, g, and ϕ in their arguments and f and g concave in u.

Theorem 1.1. *Pontryagin's Maximum Principle ([70]): If $(u^*(t), x^*(t))$ are an optimal solution pair to (1.2) with (1.1), then there exists an adjoint variable, $\lambda(t)$, such that*

$$H(t, x^*(t), u(t), \lambda(t)) \leq H(t, x^*(t), u^*(t), \lambda(t)), \tag{1.4}$$

for all $u(t) \in U^*$ at each time t, where

$$H(t, x(t), u(t), \lambda(t)) = f(t, x(t), u(t)) + \lambda(t) \cdot g(t, x(t), u(t)) \tag{1.5}$$

is called the Hamiltonian and

$$\lambda'(t) = -\frac{\partial H(t, x^*(t), u^*(t), \lambda(t))}{\partial x}, \quad \lambda(t_1) = \frac{d\phi}{dx}(x^*(t_1)). \tag{1.6}$$

Pontryagin's Maximum Principle can also be extended to a system of n state differential equations: $x_1, ..., x_n$. In this case, there would be n adjoint differential equations: $\lambda_1, ..., \lambda_n$, one for each state equation. The Hamiltonian would be defined as

$$\begin{aligned} H(t, x_1(t), ..., x_n(t), u(t), \lambda_1(t), ..., \lambda_n(t)) &= f(t, x_1(t), ..., x_n(t), u(t)) \\ &+ \lambda_1(t) \cdot g_1(t, x_1(t), ..., x_n(t), u(t)) + ... \\ &+ \lambda_n(t) \cdot g_n(t, x_1(t), ..., x_n(t), u(t)), \end{aligned} \tag{1.7}$$

where g_i refers to the right-hand side of the i^{th} state differential equation, $x_i'(t)$. The adjoint differential equations and corresponding transversality conditions would then be defined as

$$\lambda_i(t) = -\frac{\partial H}{\partial x_i}, \quad \lambda_i(t_1) = \frac{d\phi}{dx_i}(x_1(t_1), ..., x_n(t_1)), \tag{1.8}$$

at $u^*, x_1^*, ..., x_n^*$.

1.3 Agent-based model

The simplifying assumption of direct transmission of *C. difficile* from an infected individual to a susceptible individual did not allow us to explicitly evaluate the role of a pathogen environmental reservoir. Since *C. difficile* spores can survive for extended periods of time, even years, in healthcare facilities [28], *C. difficile* in the environment plays a significant role in transmission. Therefore, our second model, discussed in Chapter 3, incorporates the role of environmental transmission through the explicit inclusion of the dynamics of healthcare workers (HCWs). We then are able to assess the impact of various intervention strategies while considering the contribution to transmission from an environmental pathway.

Often, models include simplifying assumptions that restrict their complexity in order to maintain their mathematical tractability [72]. With agent-based models (ABMs), we can remove many of these simplifying assumptions through the use of computer simulation. Rather than modeling just the average behavior of a population, ABMs allow individuals within a population to each be characterized by specific traits and events to be defined and simulated on an individual-to-individual basis. These individual behaviors are then simulated to observe overall system dynamics that arise over time, often referred to as emergent behavior [72]. Interactions among agents (or individuals) are typically defined locally, which adds a spatial component to the model. ABMs allow us to discern how the overall behavior of a system is linked to individual behaviors. Another benefit of ABMs is that they allow us to model processes that may be too complex to represent in a more traditional equations-based model [72]. We have the freedom to include as much detail as we want when developing ABMs; however, decisions and assumptions have to be made about which individual characteristics, behaviors, and interactions to incorporate in the model and which are not as influential on the overall system dynamics [72].

Of primary importance to pathogens with environmental reservoirs is spatial heterogeneity. Exposure to *C. difficile* depends on the varying survival and growth of the pathogen on different hospital surfaces [34, 52], and control interventions often include a spatial

component. For example, we may want to more stringently clean a room from which a symptomatic patient was discharged than a room from which a healthy individual was discharged. Not all rooms in healthcare settings receive the same frequency of contact and level of cleaning and disinfection [15, 7, 22], so a more detailed assessment of control interventions for environmentally transmitted pathogens necessitates a spatially explicit model, such as an ABM.

The level of compliance of HCWs to proper hand-washing and contact protocol differs by individual, and the level of environmental cleaning is also variant. ABMs allow for the incorporation of varying individual compliance levels and are inherently stochastic in nature. Thus, different outcomes at the population level can arise from similar starting conditions due to the stochasticity of individual behaviors.

In Chapter 3, we describe the ABM we developed to include environmental transmission in the spread of *C. difficile* in a healthcare setting. By modifying and expanding an ABM originally created by Bintz et al. [5], we developed an ABM that includes individual antibiotic histories of patients, environmental contamination of individual rooms, and HCWs as vectors of transmission. The explicit addition of HCWs allows us to consider individual HCW behaviors and to assess the impact of increased overall HCW compliance on the spread of *C. difficile* spores. We use this model to explore the effect of individual intervention strategies as well as to assess if there is an optimal combination of intervention strategies for reducing nosocomial infection incidence and colonization by *C. difficile*. Investigating how an environmental reservoir affects transmission of a pathogen is an ongoing assessment, and with this work, we aim to gain traction in pinpointing where control efforts should be concentrated.

Chapter 2

Compartmental model of nosocomial *C. difficile* transmission

2.1 Introduction

Many healthy individuals have antibodies against *C. difficile* toxins A and B, and these antibodies have a protective effect against clinical disease [85]. In a prospective study, patients with low levels of IgG antibodies against toxin A were at greater risk of developing *C. difficile*-induced diarrhea [43]. Vaccination can be an important addition to the current intervention strategies against *C. difficile*. Currently, several toxoid vaccines (i.e., vaccines that confer immunity against *C. difficile* toxins) are being tested in clinical studies for efficacy, effectiveness, and safety [51]. Toxoid vaccines can provide protection against clinical diseases but not against *C. difficile* colonization. In [47], a simulation study looking at *C. difficile* vaccination was found to be cost-effective for a range of risk, vaccine efficacies, and vaccine cost in two populations: a target vaccination for patients with CDI undergoing antibiotic treatment and universal vaccination on at-risk patients. Vaccination as an infection control measure was not evaluated. Although vaccination with a toxoid vaccine may not prevent colonization, it may reduce transmission in hospital settings.

In this chapter, our goal is to better understand how vaccination would affect the transmission and prevention of CDI in a healthcare setting and also to determine the most cost-effective way to implement a vaccination strategy. In order to accomplish this goal,

Table 2.1: Patient transition states developed in [45]

State	Infection status
R	resistant to colonization
S	susceptible to colonization
C^-	asymptomatically colonized without protection against CDI
C^+	asymptomatically colonized with protection against CDI
D	diseased (with CDI)

we use techniques of optimal control on a system of ordinary differential equations (ODEs). See [27, 53, 16, 2, 30, 24, 61] for examples of the use of optimal control theory to design vaccination strategies in ODE models of infectious diseases.

We begin in Section 2.2 by developing a compartmental model that describes the movement of hospital patients in and out of seven CDI-related states. A control variable representing the vaccination rate is incorporated into the system. Then, in Section 2.4, we utilize optimal control techniques to determine the time-varying optimal rate at which hospitals should vaccinate in order to minimize the disease prevalence, disease transmission, and the related cost, in terms of both time and money. In Section 2.5, we discuss the results of our numerical simulations. In particular, we determine optimal vaccination strategies for various hospital statuses, such as times of high transmission of *C. difficile* and periods of increased administration of antibiotic prescriptions. We also compare the value of the objective functional with a time-varying vaccination rate to that with a constant vaccination rate to determine the benefits of varying the vaccination rate with time. Finally, in Section 2.6, we discuss our conclusions based on the numerical results.

2.2 ODE Model

Because mathematical models of disease transmission provide a solid framework for understanding the spread of disease, we begin by extending the mathematical model of *C. difficile* transmission developed by [45] to include vaccination. The original model is a system of ODEs that depicts *C. difficile* transmission within a hospital setting, where all patients are divided into five transition states, measured in number of patients, according to infection status as listed in Table 2.1.

Table 2.2: Additional patient transition states for vaccinated patients

State	Infection status
V	vaccinated for CDI and not colonized
C_v^+	asymptomatically colonized and vaccinated

Resistant patients (R) have not received antimicrobial treatment and have a normal intestinal microbiota [39]. It is assumed that patients with a normal intestinal microbiota are resistant to colonization since patients with a normal flora have a significantly lower risk of developing CDI [45]. Susceptible patients (S) have received antimicrobial treatment and are therefore susceptible to colonization. Colonized patients may or may not mount a protective response. Those who are colonized, asymptomatic, and unable to mount an immune response are labeled C^- and could potentially develop CDI. C^+ patients are also colonized and asymptomatic, but they are able to mount an immune response and do not become diseased. All C^- and C^+ patients are assumed to be colonized during their entire stay at the hospital [58, 77], and both can transmit the disease to the susceptible population. Diseased patients (D) are treated with antibiotics and either become susceptible again or remain infected if treatment is unsuccessful.

In addition to the classes in the original model by [45], we will also consider two additional transition states for vaccinated patients, listed in Table 2.2. In our model, vaccination will be performed on patients in S, C^-, and C^+. As previously stated, vaccination does not eliminate colonization from those who are in C^- or C^+. Because colonized patients, even asymptomatic ones, contribute to the transmission of disease, it is important to distinguish between those who are vaccinated and those who are vaccinated but also colonized. For this reason, we consider two classes of vaccinated patients. It should also be noted that although C^+ patients are not at risk of contracting CDI, we still vaccinate them because there is not a practical and quick method for distinguishing between C^- and C^+ patients when deciding who needs vaccinating. Therefore, C^+ and C_v^+ have the same infection status, but both of these classes are necessary in the model to keep track of who has been vaccinated and to prevent the same patient from being vaccinated multiple times. Because they have the same infection status, we assume the transmission coefficients for C_v^+ and C^+ are equivalent.

Patients can be discharged and admitted in any of the seven states, but in all cases presented in this chapter, we assume that none of the patients are already vaccinated when admitted. All transitions are modeled deterministically as the system of ODEs given in (2.1), an extension of the model developed by [45]:

$$\begin{aligned}
\frac{dR}{dt} &= a_r\delta N + \theta S - (\alpha + k_r)R \\
\frac{dS}{dt} &= a_s\delta N + \alpha R + p\varepsilon D - (\theta + \lambda + k + v)S \\
\frac{dC^-}{dt} &= a_{cn}\delta N + (1-f)\lambda S - (\phi + k + v)C^- \\
\frac{dC^+}{dt} &= a_{cp}\delta N + f\lambda S - (k + v)C^+ \\
\frac{dD}{dt} &= a_d\delta N + \phi C^- - (p\varepsilon + k_d)D \\
\frac{dV}{dt} &= a_v\delta N + vS - (\lambda + k)V \\
\frac{dC_v^+}{dt} &= a_{cv}\delta N + v(C^+ + C^-) + \lambda V - kC_v^+,
\end{aligned} \tag{2.1}$$

where the transmission rate is

$$\lambda = \beta_c(C^- + C^+ + C_v^+) + \beta_d D$$

and

$$N = R + S + C^- + C^+ + D + V + C_v^+.$$

To maintain a constant total population, we define δN similarly to that in [45], which allows discharges to be balanced with admissions:

$$\delta N = k_r R + kS + kC^- + kC^+ + k_d D + kV + kC_v^+. \tag{2.2}$$

The movement among states described by the system in (2.1) is illustrated in Figure 2.1. Details about each parameter are listed in Table 2.3; a similar table is found in the work completed by [45] with a few modifications and updates made here. Parameter values are based on hospital data or published literature. In particular, the restoration rate of

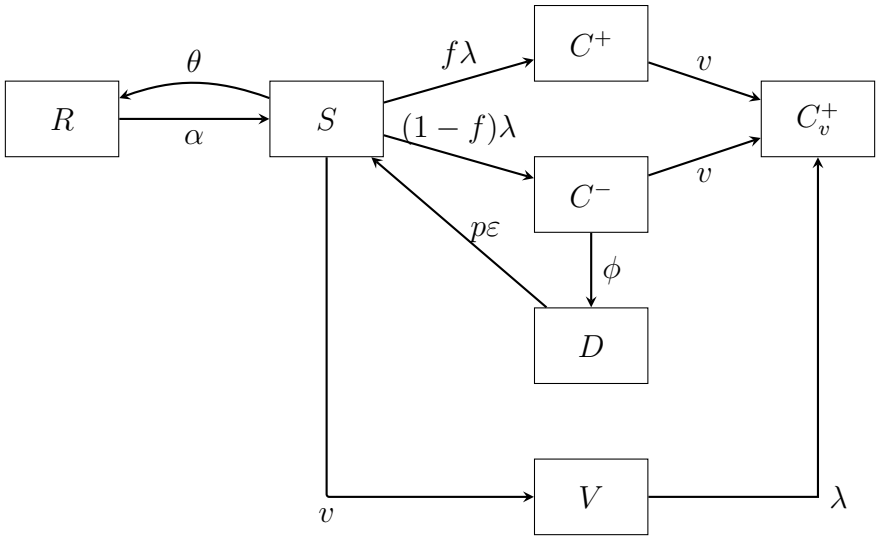


Figure 2.1: Summary of movement among patient transition states with corresponding parameters

colonization resistance, θ, is taken from [71]. The fraction of colonized patients that mount an immune response, f, comes from [44], and both the treatment rate, ε, and the probability of successful treatment, p, are taken from [57]. All remaining parameters are either based directly on hospital data or are an adjustment of hospital data to reflect observed disease incidence. More details on these adjustments are given in the following paragraphs.

At the time [45] developed their model, hospital data indicated that the proportion of admitted patients that were asymptomatically colonized totaled 2%. Therefore, in [45], $a_{cn} = a_{cp} = 0.01$. Since this time, new research in [1] has indicated that approximately 15% of admitted patients were observed to be asymptomatically colonized upon arrival. We divided this updated percentage into 9% admitted with protective response, a_{cp}, and 6% without protective response, a_{cn}. Once these values were determined, the admission proportion for susceptible patients was accordingly decreased by 13% from the value of 22% used in [45], which updated a_s to 0.09 as listed in Table 2.3. The values for a_v and a_{cv} were assumed to be 0 for all results presented. Once the admission percentages were all adjusted to match updated observed rates, the transmission coefficients, β_c and β_d, and the clinical disease rate, ϕ, were then adjusted so that the average number of observed incident cases of CDI per month per ward was comparable to the value of 2.2 given in [45].

Table 2.3: Model parameter descriptions and values

Symbol	Description, units	Baseline Value
a_r	Proportion of admitted patients that are resistant, dimensionless	0.75
a_s	Proportion of admitted patients that are susceptible, dimensionless	0.09
a_{cn}	Proportion of admitted patients that are colonized without protective response, dimensionless	0.06
a_{cp}	Proportion of admitted patients that are colonized with protective response, dimensionless	0.09
a_d	Proportion of admitted patients with *C. difficile* infection, dimensionless	0.01
a_v, a_{cv}	Proportion of admitted patients who are vaccinated and vaccinated who are colonized, respectively, dimensionless	0
α	Antibiotic prescription rate, per day	0.5
θ	Restoration rate of colonization resistance, per day	0.033
β_c, β_d	Transmission coefficients for asymptomatic carriers and diseased patients, respectively, per individual-day	10^{-6}
f	Fraction of colonized patients that mount immune response, dimensionless	0.6
ε	Treatment rate, per day	0.1
p	Probability of successful treatment, dimensionless	0.8
ϕ	Clinical disease rate, per day	0.06
k_r	Discharge rate for resistant patients, per day	0.33
k	Discharge rate for susceptible, colonized, and vaccinated patients, per day	0.15
k_d	Discharge rate for diseased patients, per day	0.068
v	Vaccination rate, per day	varied

Table 2.4: Exploration of a biologically feasible range of values for vaccination rate, v

v	% effectively vaccinated out of total admitted (in 30 days)
2	73.46%
1	67.51%
0.5	58.07%
0.3	48.91%
0.1	27.24 %
0.05	16.33%

We define the vaccination rate v to be the *effective* vaccination rate, which encompasses both effort and efficacy. To estimate a feasible range of values for the effective vaccination rate v, we solved the system in (2.1) numerically for various v values and noted the resulting percentage of patients who were effectively vaccinated out of the total number of patients admitted over a 30-day period. A few of these scenarios are summarized in Table 2.4. While determining this range for the vaccination rate, we decided for most simulations to not consider cases in which significantly more than 50% of those admitted in 30 days were effectively vaccinated. Therefore, we concentrate most of our focus on $0 \leq v \leq 0.3$. Because of the short time frame evaluated, we do not consider waning immunity.

For our simulations, we assume a hospital setting containing five wards of 30 beds each for a total population of $N = 150$ patients, which is kept constant by assumption (2.2). The initial conditions used were based on the admission proportions given in the list of parameter values shown in Table 2.3; that is, we set $R(0) = 112$, $S(0) = 14$, $C^-(0) = 9$, $C^+(0) = 13$, $D(0) = 2$, $V(0) = 0$, and $C_v^+(0) = 0$.

2.3 Existence and uniqueness

In this section, we will provide results about the existence, uniqueness, and non-negativity of solutions to our system in (2.1) for a given initial condition vector in $\mathbb{R}_+^7$. To begin, consider the general initial value problem

$$x'(t) = f(x(t)) \tag{2.3}$$
$$x(t_0) = \phi,$$

where $f : C \to \mathbb{R}^n$ is continuous, $C \subset \mathbb{R}^n$ is open, and $\phi \in \mathbb{R}^n$. Define R to be the following rectangular region:

$$R = R((t_0, \phi), a, b)) = \{(t, x) : |t - t_0| \leq a, |x - \phi| \leq b\}, \tag{2.4}$$

where a and b are two positive numbers. Recall that a function $f : C \to \mathbb{R}^n$ is Lipschitz if there exists a constant $L > 0$ such that

$$||f(x) - f(y)|| \leq L||x - y||, \tag{2.5}$$

for all $x, y \in C$. We will use the following theorem, taken from [35], to prove the existence and uniqueness of a solution to our initial value problem formed by (2.1) with specified initial conditions.

Theorem 2.1. *(Modified from [35]) If the entries of f are real-valued and continuous on a rectangular region R and if f satisfies the Lipschitz condition on R, then there exists a unique solution to the initial value problem (2.3) for all t within a given distance of t_0.*

The next theorem (a simplified case of a theorem from [79]) specifies conditions on f which ensure that non-negative initial conditions will guarantee non-negative solutions to (2.3).

Theorem 2.2. *([79]: Simpler case of Theorem 2.1, Chapter 5) Assume that when $\phi \in \mathbb{R}^n$ satisfies $\phi \geq 0$ with $\phi_i(0) = 0$ for some i, then $f_i(\phi) \geq 0$. Then, if $\phi \in \mathbb{R}^n$ satisfies $\phi \geq 0$, the solution of (2.3) satisfies $x(t) \geq 0$ for all $t \geq t_0$.*

We now use Theorem 2.2 to prove non-negativity of solutions to (2.1) with non-negative initial conditions, assuming a solution exists, and Theorem 2.1 to prove the existence and uniqueness of a solution to our system.

Theorem 2.3. *For any vector of initial conditions $\phi = (R_0, S_0, C_0^-, C_0^+, D_0, V_0, (C_v^+)_0) \geq 0$, the system in (2.1) has a non-negative solution.*

We check the hypotheses of Theorem 2.2.

1. Assume $\phi = (0, S_0, C_0^-, C_0^+, D_0, V_0, (C_v^+)_0) \geq 0$. Then,

$$f_1(\phi) = a_r(kS_0 + kC_0^- + kC_0^+ + k_d D_0 + kV_0 + k(C_v^+)_0) + \theta S_0 \geq 0.$$

2. Assume $\phi = (R_0, 0, C_0^-, C_0^+, D_0, V_0, (C_v^+)_0) \geq 0$. Then,

$$f_2(\phi) = a_s(k_r R_0 + kC_0^- + kC_0^+ + k_d D_0 + kV_0 + k(C_v^+)_0) + \alpha R_0 + p\varepsilon D_0 \geq 0.$$

3. Assume $\phi = (R_0, S_0, 0, C_0^+, D_0, V_0, (C_v^+)_0) \geq 0$. Then,

$$\begin{aligned} f_3(\phi) = a_{cn}(k_r R_0 + kS_0 + kC_0^+ + k_d D_0 + kV_0 + k(C_v^+)_0) \\ +(1-f)S_0(\beta_c C_0^+ + \beta_c (C_v^+)_0 + \beta_d D_0) \geq 0. \end{aligned}$$

4. Assume $\phi = (R_0, S_0, C_0^-, 0, D_0, V_0, (C_v^+)_0) \geq 0$. Then,

$$\begin{aligned} f_4(\phi) = a_{cp}(k_r R_0 + kS_0 + kC_0^- + k_d D_0 + kV_0 + k(C_v^+)_0) \\ +fS_0(\beta_c C_0^- + \beta_c (C_v^+)_0 + \beta_d D_0) \geq 0. \end{aligned}$$

5. Assume $\phi = (R_0, S_0, C_0^-, C_0^+, 0, V_0, (C_v^+)_0) \geq 0$. Then,

$$f_5(\phi) = a_d(k_r R_0 + kS_0 + kC_0^- + kC_0^+ + kV_0 + k(C_v^+)_0) + \phi C_0^- \geq 0.$$

6. Assume $\phi = (R_0, S_0, C_0^-, C_0^+, D_0, 0, (C_v^+)_0) \geq 0$. Then,

$$f_6(\phi) = a_v(k_r R_0 + kS_0 + kC_0^- + kC_0^+ + kD_0 + k(C_v^+)_0) + vS_0 \geq 0.$$

7. Assume $\phi = (R_0, S_0, C_0^-, C_0^+, D_0, V_0, 0) \geq 0$. Then,

$$\begin{aligned} f_7(\phi) = a_{cv}(k_r R_0 + kS_0 + kC_0^- + kC_0^+ + kD_0 + kV_0) + v(C_0^- + C_0^+) \\ +V_0(\beta_c C_0^- + \beta_c C_0^+ + \beta_d D_0) \geq 0. \end{aligned}$$

Therefore, whenever $\phi \geq 0$ (with $\phi_i(0) = 0$ for some i), we have $f_i(\phi) \geq 0$. By Theorem 2.2, if a solution, $X(t)$, to (2.1) exists for $\phi \geq 0$, the solution is non-negative for all $t \geq 0$. $\square$

Observe that

$$\frac{dR}{dt} + \frac{dS}{dt} + \frac{dC^-}{dt} + \frac{dC^+}{dt} + \frac{dD}{dt} + \frac{dV}{dt} + \frac{dC_v^+}{dt} = 0.$$

This implies $R(t) + S(t) + C^-(t) + C^+(t) + D(t) + V(t) + C_v^+(t) = \bar{c}$, for some constant $\bar{c} \geq 0$. If a solution to the system exists, then each component of the state solution must be less than or equal to $\bar{c}$ for all $t \geq t_0$, which (combined with the results of Theorem 2.3) means

$$0 \leq R(t), S(t), C^-(t), C^+(t), D(t), V(t), C_v^+(t) \leq \bar{c}, \tag{2.6}$$

for all $t \geq t_0$. Thus, if a solution exists, then our states are uniformly bounded.

Theorem 2.4. *There exists a unique solution to the initial value problem formed by (2.1) with specified initial conditions.*

Proof: First, we denote $X(t) = (R(t), S(t), C^-(t), C^+(t), D(t), V(t), C_v^+(t))$ and define

$$\begin{aligned}
\frac{dR}{dt} &= f_1(X(t)) \\
\frac{dS}{dt} &= f_2(X(t)) \\
\frac{dC^-}{dt} &= f_3(X(t)) \\
\frac{dC^+}{dt} &= f_4(X(t)) \\
\frac{dD}{dt} &= f_5(X(t)) \\
\frac{dV}{dt} &= f_6(X(t)) \\
\frac{dC_v^+}{dt} &= f_7(X(t)),
\end{aligned} \tag{2.7}$$

with $X(0) = X_0 = (R_0, S_0, C_0^-, C_0^+, D_0, V_0, (C_v^+)_0)$. Observe that the entries of f are all real-valued and continuous. We now show $f = (f_1, f_2, f_3, f_4, f_5, f_6, f_7)$ is Lipschitz. We will proceed by showing each component of f is Lipschitz. First, note that if a function of one real variable has a bounded derivative, it is Lipschitz. If we can show that f_i is Lipschitz in each of its seven inputs, then f_i is Lipschitz. To show each f_i is Lipschitz with respect to

a single input variable, we must show that the derivative of f_i with respect to the i^{th} state variable is bounded. In particular, to show f_1 is Lipschitz, we must show its derivative with respect to each input variable is bounded. The partial derivatives of f_1 with respect to each of the state variables are as follows:

$$\begin{aligned}
\frac{\partial f_1}{\partial R} &= a_r k_r - (\alpha + k_r) \\
\frac{\partial f_1}{\partial S} &= a_r k + \theta \\
\frac{\partial f_1}{\partial C^-} &= \frac{\partial f_1}{\partial C^+} = \frac{\partial f_1}{\partial V} = \frac{\partial f_1}{\partial C_v^+} = a_r k \\
\frac{\partial f_1}{\partial D} &= a_r k_d.
\end{aligned}$$

For f_3, we have

$$\begin{aligned}
\frac{\partial f_3}{\partial R} &= a_{cn} k_r \\
\frac{\partial f_3}{\partial S} &= a_{cn} k + (1-f)[\beta_c (C^+ + C^- + C_v^+) + \beta_d D] \\
\frac{\partial f_3}{\partial C^-} &= a_{cn} k + (1-f) S \beta_c - (\phi + k + v) \\
\frac{\partial f_3}{\partial C^+} &= a_{cn} k + (1-f) S \beta_c \\
\frac{\partial f_3}{\partial D} &= a_{cn} k_d + (1-f) S \beta_d \\
\frac{\partial f_3}{\partial V} &= a_{cn} k \\
\frac{\partial f_3}{\partial C_v^+} &= a_{cn} k + (1-f) S \beta_c.
\end{aligned}$$

The resulting partial derivatives of f_i with respect to each of the state variables for $i = 2, 4, 5, 6$, and 7 are similar to the ones illustrated above in that they depend only on products of parameter values and of parameter values with state variables. Thus, each partial derivative is bounded. On compact subsets of C, each f_i is Lipschitz in each of its inputs for every i; thus, f is Lipschitz. Since the entries of f in (2.1) are real-valued and continuous and since f is Lipschitz, by Theorem 2.1, there exists a unique solution to the initial value problem formulated by (2.1) with specified initial conditions. □

2.4 Optimal control of vaccination rate

We implement optimal control on the vaccination rate v to determine the time-varying, optimal rate of vaccination over a particular time period because the cost-effectiveness of a vaccine, in terms of both monetary and time resources, is so important. Our goal is to minimize not only the overall impact of the disease but also the cost associated with vaccination over a given period of time, $[0, T]$ for $T > 0$. The objective functional that represents this goal is shown in (2.8).

$$\begin{aligned} J(v) := c_0 C^-(T) + \int_0^T \Big[& \; c_1 v(t)\Big(S(t) + C^-(t) + C^+(t)\Big) + c_2\big(v(t)\big)^2 \\ & + \; c_3 D(t) + c_4 C^-(t) + c_5 \lambda(t)\Big(S(t) + V(t)\Big)\Big] dt \end{aligned} \tag{2.8}$$

The first term in the objective functional, $c_0 C^-(T)$, counts the number of patients asymptomatically colonized without protection at the final time and also ensures that the value of the control is not forced to zero for some $t \in [0, T]$, as further explained in Section 2.5.1. The next term, $c_1 v(t)\big(S(t) + C^-(t) + C^+(t)\big)$, represents the linear cost associated with the vaccination process while $c_2\big(v(t)\big)^2$ represents the nonlinear cost that arises from difficulties faced when implementing a successful vaccination program. The objective functional also accounts for the number of diseased patients with the term $c_3 D(t)$; by including this term, the disease prevalence in the population will be minimized. Additionally, the objective functional includes terms for the number of C^- patients, $c_4 C^-(t)$, and for nosocomial disease transmission, $c_5 \lambda(t)\big(S(t) + V(t)\big)$. Recall the transmission rate $\lambda(t) = \beta_c\big(C^-(t) + C^+(t) + C_v^+(t)\big) + \beta_d D(t)$. The coefficients $c_i \geq 0$, $0 \leq i \leq 5$, represent weights on the different terms of the objective functional. For some $M > 0$, the control set is

$$V^* := \{v : [0, T] \to [0, M] : v \text{ Lebesgue measurable}\}.$$

The goal is to characterize the optimal control v^* satisfying

$$\inf_{v \in V^*} J(v) = J(v^*),$$

subject to the state system (2.1) with specified non-negative initial conditions for R, S, C^-, C^+, D, V, and C_v^+. In order to use Pontryagin's Maximum Principle (Theorem 1.1, [70]) to characterize an optimal control, we must first prove that an optimal control exists.

2.4.1 Existence of optimal control

Theorem 2.5. *There exists an optimal control v^* that minimizes the objective functional $J(v)$ in (2.8) subject to the state system in (2.1) with specified non-negative initial conditions.*

Proof. By (2.6) and Theorem 2.3, we know our state solutions are uniformly bounded for all $t \in [0, T]$. This, together with the boundedness of our control, implies that $J(v)$ is bounded below by 0, and, therefore, a minimum exists. Let $\{v_n\}_{n=1}^{\infty}$ be a minimizing sequence such that

$$\min_{v \in V} J(v) = \lim_{n \to \infty} J(v_n),$$

where $X_n = (R_n, S_n, C_n^-, C_n^+, D_n, V_n, (C_v^+)_n)$ are the state sequences corresponding to v_n and $V = \{v : [0, T] \to [0, M] | v \text{ Lebesgue measurable}\}$.

The boundedness of the state sequences and control sequence imply that $\frac{dR_n}{dt}$, $\frac{dS_n}{dt}$, $\frac{dC_n^-}{dt}$, $\frac{dC_n^+}{dt}$, $\frac{dD_n}{dt}$, $\frac{dV_n}{dt}$, $\frac{d(C_v^+)_n}{dt}$ are each bounded for all $t \in [0, T]$. Bounded derivatives imply Lipschitz continuity; thus, each state sequence is Lipschitz continuous, and the state sequences are, therefore, also equicontinuous. The Arzela-Ascoli Theorem states that every uniformly bounded, equicontinuous sequence on a compact set has a uniformly convergent subsequence. Therefore, each state sequence has a uniformly convergent subsequence:

$$R_{n_k} \to R^* \in [0, N], S_{n_k} \to S^* \in [0, N], ..., (C_v^+)_{n_k} \to (C_v^+)^* \in [0, N].$$

Now, because $|v_n(t)| \leq M$ for all $n \in \mathbb{N}$ and for all $t \in [0,T]$, we know $v_n \in L^2(0,T)$, and for some constant $C_1 \geq 0$,

$$||v_n||_{L^2} \leq C_1, \tag{2.9}$$

for all $n \in \mathbb{N}$. As a consequence of the Banach-Alaoglu Theorem [25], every bounded sequence in L^2 has a weakly convergent subsequence; that is, there exists v^* such that $v_{n_k} \rightharpoonup v^*$ in L^2. Using lower-semicontinuity of L^2 norms with respect to weak convergence (see Theorem 4.10.7 in [25]), we have

$$||v^*||_{2(0,T)} \leq \liminf_{k\to\infty} ||v_{n_k}||_{2(0,T)}. \tag{2.10}$$

Let $\lambda_{n_k} = \beta_c(C^-_{n_k} + C^+_{n_k} + C^+_{v_{n_k}}) + \beta_d D_{n_k}$ and $\lambda^* = \beta_c(C^{-^*} + C^{+^*} + C^{+^*}_v) + \beta_d D^*$. Note that because $J(v_n)$ converges to $\min_v J(v)$, any subsequence of $J(v_n)$ must converge to that same limit. Additionally, because the state sequences and control sequence are L^∞-bounded, $v_{n_k} \rightharpoonup v^*$ in L^2, and the state subsequences converge uniformly in L^2,

$$\int_0^T v_{n_k}\left(S_{n_k} + C^-_{n_k} + C^+_{n_k}\right) dt \to \int_0^T v^*(S^* + C^{-*} + C^{+*})dt.$$

We then have the following:

$$\begin{aligned}
\min_v J(v) &= \lim_{n\to\infty} J(v_n) = \lim_{k\to\infty} J(v_{n_k}) \\
&= \liminf_{k\to\infty} J(v_{n_k}) \\
&\geq \liminf_{k\to\infty} \int_0^T \left[c_1 v_{n_k}(S_{n_k} + C^-_{n_k} + C^+_{n_k}) + c_3 D_{n_k} + c_4 C^-_{n_k} + c_5 \lambda_{n_k}\left(S_{n_k} + V_{n_k}\right)\right] dt \\
&\quad + \liminf_{k\to\infty} c_0 C^-_{n_k}(T) + \liminf_{k\to\infty} c_2 ||v_{n_k}||^2_{2(0,T)} \\
&\geq \int_0^T \left[c_1 v^*(S^* + C^{-*} + C^{+*}) + c_3 D^* + c_4 C^{-*} + c_5 \lambda^*\left(S^* + V^*\right)\right] dt \\
&\quad + c_0 C^{-*}(T) + ||v^*||^2_{2(0,T)} \\
&= J(v^*).
\end{aligned}$$

Thus, $\min_v J(v) = J(v^*)$, so v^* is optimal. $\square$

2.4.2 Characterization of optimal control

Now that we have established existence, we can apply Pontryagin's Maximum Principle (Theorem 1.1, [70]) to derive necessary conditions on the optimal control.

Theorem 2.6. *Given an optimal control v^* and solutions to the corresponding state system in (2.1), there exist adjoint variables λ_i, $i = 1, ..., 7$, satisfying*

$$
\begin{aligned}
\lambda_1' &= -\lambda_1(a_r k_r - \alpha - k_r) - \lambda_2(a_s k_r + \alpha) - k_r(\lambda_3 a_{cn} + \lambda_4 a_{cp} + \lambda_5 a_d) \\
&\quad -k_r(\lambda_6 a_v + \lambda_7 a_{cv}) \\
\lambda_2' &= -c_1 v - c_5\lambda - \lambda_1(k a_r + \theta) - \lambda_2(a_s k - \theta - k - \lambda - v) \\
&\quad -\lambda_3[a_{cn}k + (1-f)\lambda] - \lambda_4(a_{cp}k + f\lambda) - \lambda_5 a_d k \\
&\quad -\lambda_6(k a_v + v) - \lambda_7 a_{cv} k \\
\lambda_3' &= -c_1 v - c_4 - c_5\beta_c(S+V) - \lambda_1 a_r k - \lambda_2(k a_s - \beta_c S) \\
&\quad -\lambda_3[a_{cn}k + (1-f)\beta_c S - \phi - k - v] - \lambda_4(f\beta_c S + k a_{cp}) \\
&\quad -\lambda_5(k a_d + \phi) - \lambda_6(k a_v - \beta_c V) - \lambda_7(\beta_c V + k a_{cv} + v) \\
\lambda_4' &= -c_1 v - c_5\beta_c(S+V) - \lambda_1 a_r k - \lambda_2(k a_s - \beta_c S) - \lambda_3[a_{cn}k + (1-f)\beta_c S] \\
&\quad -\lambda_4(f\beta_c S + k a_{cp} - k - v) - \lambda_5 a_d k - \lambda_6(k a_v - \beta_c V) \qquad (2.11) \\
&\quad -\lambda_7(\beta_c V + k a_{cv} + v) \\
\lambda_5' &= -c_3 - c_5\beta_d(S+V) - \lambda_1 a_r k_d - \lambda_2(p\varepsilon - \beta_d S + a_s k_d) \\
&\quad -\lambda_3[a_{cn}k_d + (1-f)\beta_d S] - \lambda_4(f\beta_d S + a_{cp}k_d) - \lambda_5(a_d k_d - p\varepsilon - k_d) \\
&\quad -\lambda_6(a_v k_d - \beta_d V) - \lambda_7(\beta_d V + a_{cv}k_d) \\
\lambda_6' &= -c_5\lambda - \lambda_1 a_r k - \lambda_2 k a_s - \lambda_3 a_{cn} k - \lambda_4 a_{cp} k - \lambda_5 a_d k \\
&\quad -\lambda_6(a_v k - k - \lambda) - \lambda_7(a_{cv}k + \lambda) \\
\lambda_7' &= -c_5\beta_c(S+V) - \lambda_1 a_r k - \lambda_2(k a_s - \beta_c S) - \lambda_3[a_{cn}k + (1-f)\beta_c S] \\
&\quad -\lambda_4(f\beta_c S + k a_{cp}) - \lambda_5 a_d k - \lambda_6(k a_v - \beta_c V) - \lambda_7(\beta_c V + k a_{cv} - k), \\
\lambda_i(T) &= 0, \quad \textit{for} \quad i \neq 3 \\
\lambda_3(T) &= c_0.
\end{aligned}
$$

Furthermore, v^* is represented as

$$v^* = \min\{M, \max\{0, \hat{v}\}\}, \tag{2.12}$$

where

$$\hat{v} = \frac{\lambda_2 S + \lambda_3 C^- + \lambda_4 C^+ - \lambda_6 S - \lambda_7 (C^+ + C^-) - c_1 (S + C^+ + C^-)}{2c_2}. \tag{2.13}$$

Proof. The Hamiltonian is given by

$$\begin{aligned} H &= c_1 v(S + C^- + C^+) + c_2 v^2 + c_3 D + c_4 C^- + c_5 (S + V)\lambda \\ &\quad + \lambda_1 \frac{dR}{dt} + \lambda_2 \frac{dS}{dt} + \lambda_3 \frac{dC^-}{dt} + \lambda_4 \frac{dC^+}{dt} + \lambda_5 \frac{dD}{dt} + \lambda_6 \frac{dV}{dt} + \lambda_7 \frac{dC_v^+}{dt}. \end{aligned}$$

Pontryagin's Maximum Principle (Theorem 1.1, [70]) gives the existence of adjoint variables satisfying the system in (2.11) using

$$\lambda_1' = -\frac{\partial H}{\partial R}, \quad \lambda_2' = -\frac{\partial H}{\partial S}, \quad \lambda_3' = -\frac{\partial H}{\partial C^-}, \quad \lambda_4' = -\frac{\partial H}{\partial C^+}, \quad \lambda_5' = -\frac{\partial H}{\partial D},$$

$$\lambda_6' = -\frac{\partial H}{\partial V}, \quad \text{and} \quad \lambda_7' = -\frac{\partial H}{\partial C_v^+},$$

with transversality conditions $\lambda_i(T) = 0$ for $i \neq 3$ and $\lambda_3(T) = c_0$. We then have

$$\frac{\partial H}{\partial v} = c_1(S + C^- + C^+) + 2c_2 v - \lambda_2 S - \lambda_3 C^- - \lambda_4 C^+ + \lambda_6 S + \lambda_7 (C^- + C^+).$$

On the interior of the control set, $\frac{\partial H}{\partial v}\big|_{v^*} = 0$. Thus, we can solve for the optimal control on the interior:

$$v^*(t) = \frac{\lambda_2 S + \lambda_3 C^- + \lambda_4 C^+ - \lambda_6 S - \lambda_7 (C^+ + C^-) - c_1 (S + C^+ + C^-)}{2c_2}.$$

Note that on $\{t | v^*(t) = 0\}$, $\frac{\partial H}{\partial v} \geq 0$ and on $\{t | v^*(t) = M\}$, $\frac{\partial H}{\partial v} \leq 0$. Combining all three cases leads to the characterization of our optimal control given in (2.12). □

2.5 Numerical results

The optimality system, which consists of the state system in (2.1) with initial conditions, adjoint system in (2.11) with transversality conditions, and characterization of the optimal control in (2.12), is solved using a Forward-Backward Sweep method [33, 49]. This is an iterative method that solves the system using a fourth-order Runge-Kutta (RK4) scheme. We start with an initial guess for our control value and then use RK4 and the given initial conditions to solve the state system in (2.1) forward in time. Then, we use the initial control guess, the transversality conditions given for our adjoints, and the values for the state system solution to solve the adjoint system in (2.11) backward in time. Next, our control value v is updated by entering the new state and adjoint values into the characterization of the control in (2.12). Finally, convergence is checked, and the process is repeated until values converge sufficiently.

Unless otherwise stated, $M = 0.3$ per day so that $0 \leq v(t) \leq 0.3$ as discussed at the end of Section 2.2. Additionally, we set $T = 30$ so that we are considering 30-day intervals. Short periods of time are considered because the hospital will change states, thereby potentially shifting some parameter values, and the vaccination strategy will need to be reevaluated after the 30 days and possibly modified in response to this shift.

2.5.1 Summary of exploration into weighting coefficient values

Before any results were determined, we first gained an understanding of how changing the values of our weighting coefficients, c_i, affected the optimal control, v^*. Because vaccination against CDI is still in testing, we do not have data that details the cost associated with such a program. Once this data is known, it can be incorporated into the appropriate weighting coefficient values. For now, to establish how a particular weighting coefficient changes the optimal vaccination rate, we varied the value for one weighting coefficient while keeping all other coefficients fixed, some at 0. Additionally, we compared the relative size of each term, without being multiplied by the corresponding weighting coefficient, in the objective functional $J(v)$ given in (2.8). In particular, we observed that the nonlinear cost

associated with vaccination, given as v^2, and the transmission, $\lambda(S+V)$, are relatively small in comparison to the other terms. Therefore, we allow their corresponding weighting coefficients, c_2 and c_5, to be relatively large in comparison to the remaining coefficients.

After considering various scenarios in which we varied one weighting coefficient value while keeping the others fixed, we made several conclusions. First, we concluded that if control cost coefficient c_1 exceeds some threshold value, then $v^*(t) = 0$ for all $t \in [0, T]$. Since we do not want to consider a case in which vaccination is too costly to implement at all, we keep c_1 relatively small. Note that because the nonlinear cost term is smaller than the linear cost term in the objective functional, increasing c_2 does not force v^* to be 0 for the entire time period in the way that increasing c_1 does.

Next, note that if c_0, the weighting coefficient on the final time condition, is 0, the optimal vaccination rate will always drop down to 0 at some point in our time period no matter what the values are for the remaining weighting coefficients. In fact, there exists some threshold value $\hat{c_0}$ such that for $c_0 < \hat{c_0}$, $v^*(t) = 0$ for $t \in [\hat{t}, T]$, for some $\hat{t} \in [0, T]$. This is because if $c_0 = 0$, then $\lambda_i(T) = 0$ for $i = 1, ..., 7$, which means $\hat{v}$, in (2.13), is negative at the final time, and by the characterization of the optimal control in (2.12), this implies $v^*(T) = 0$. It is not practical to have to drop down to a vaccination rate of 0 in every scenario; therefore, we considered values for c_0 large enough to prevent this forced decrease to 0. Finally, note that an increase in c_3 or c_4 adds emphasis to our desire to minimize the overall impact of the disease and thereby leads to an increased v^*. The last term in $J(v)$, $c_5\lambda(S+V)$, involves a bit of a balancing act. We want to increase the number of vaccinated patients V while also minimizing this term as part of the objective functional. Thus, depending on the value of V, increasing c_5 may decrease v^* or increase v^*.

The exploration of values summarized in this section provided us with an idea of how to set weighting coefficient values in the simulations to come. The weighting coefficient values chosen are as follows: $c_0 = 3$, $c_1 = 0.1$, $c_2 = c_5 = 15$, and $c_3 = c_4 = 0.5$, and the resulting v^* obtained using this combination of weighting coefficients is shown in Figure 2.2.

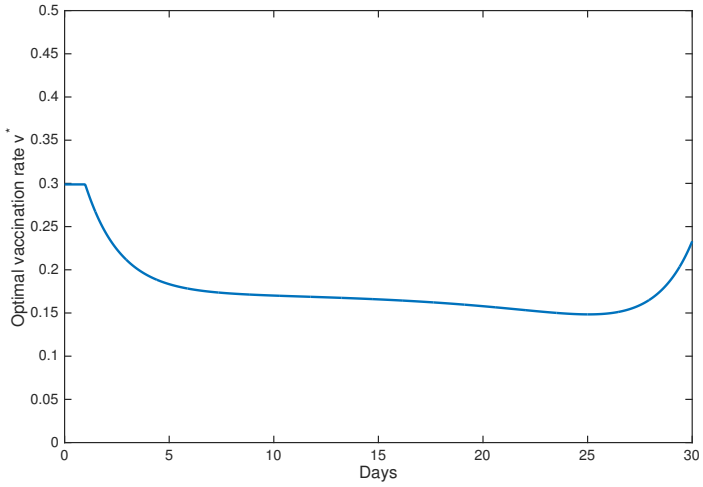


Figure 2.2: Optimal vaccination rate v^* for $c_0 = 3$, $c_1 = 0.1$, $c_2 = c_5 = 15$, $c_3 = c_4 = 0.5$, $M = 0.3$, and $T = 30$

2.5.2 Determining the impact of vaccination

In this section, we compare the population behavior with no vaccination to its behavior with vaccination implemented using optimal control and observe the differences. In Figure 2.3, the optimal states that correspond to the time-varying optimal vaccination rate v^* illustrated in Figure 2.2 are plotted alongside the states corresponding to no vaccination. We see from Figure 2.3 that without vaccination, each of the classes reaches its steady state before the 30 days have expired. Furthermore, Figure 2.3 illustrates that this particular vaccination rate v^* decreases the number of patients in C^- by approximately 4 in 30 days and the number of patients in D by approximately 2. Figure 2.3 also shows that the total number of colonized patients remains approximately the same (a difference of less than 1 person) when this optimal time-varying vaccination rate is implemented. Additionally, vaccination also leaves the hospital with a significantly lower number of patients who are susceptible to becoming colonized (approximately 47 fewer), which is significant since *C. difficile* spores can survive for extended time periods on various hospital surfaces.

Because the restriction of $M = 0.3$ per day is not a strict one, we also considered an increased upper bound on v. Figures 2.4(a) and 2.4(b) compare the optimal vaccination rate v^* for $M = 0.3$ per day to that in the increased case of $M = 0.6$ per day with the same

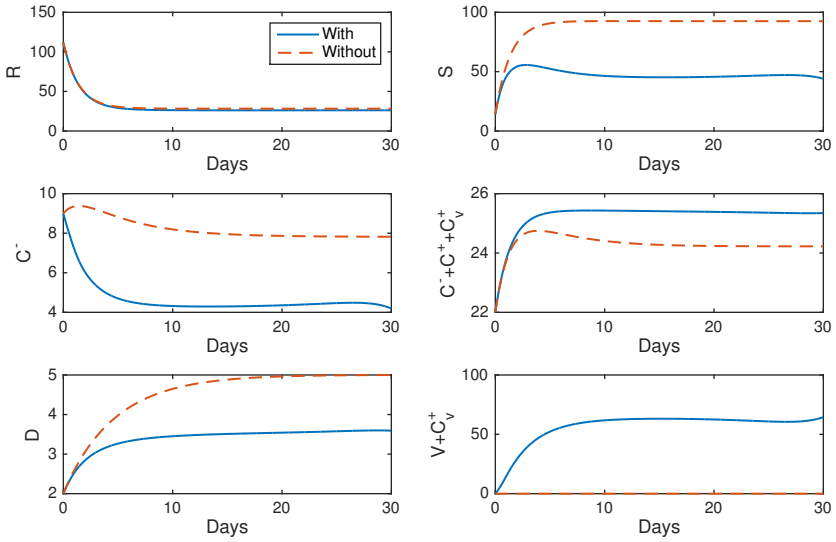


Figure 2.3: Dynamics of patient transition states with optimal vaccination rate v^* shown in Figure 2.2 compared to those without vaccination for $c_0 = 3$, $c_1 = 0.1$, $c_2 = c_5 = 15$, $c_3 = c_4 = 0.5$, $M = 0.3$, and $T = 30$

weighting coefficient values previously considered. Observe from Figure 2.4(a) that for this case, an increase in M only initially alters v^*. Figure 2.4(b) zooms in on this initial change in v^* by displaying an interval of only 3 days. Additionally, note that the v^* obtained for $M = 0.6$ produces the exact same corresponding state populations for all 30 days that the v^* with $M = 0.3$ produces (results not shown).

To determine the impact of using a time-varying vaccination rate, we compare the value of the objective functional, $J(v)$ in (2.8), obtained with our time-varying optimal vaccination rate to that obtained with a constant vaccination rate of 0.3 per day for the entire time period. For the particular case of weighting coefficient values illustrated in Figures 2.2 and 2.3 and for the case with an increased upper bound (shown in Figure 2.4), various $J(v)$ values are compared in Table 2.5. First, observe that whether $M = 0.3$ or $M = 0.6$, a time-varying optimal vaccination rate engenders a savings over a constant rate. Furthermore, if M is increased to 0.6 per day, then a time-varying vaccination rate leads to a much more notable savings over the case of a constant rate than the $M = 0.3$ case does. Thus, if we allow for

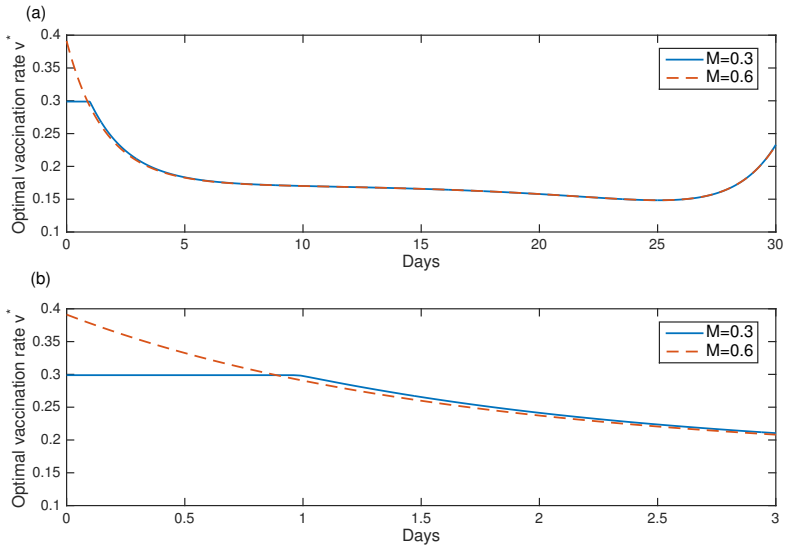


Figure 2.4: **(a)** Comparison of optimal vaccination rate v^* with upper bound $M = 0.3$ to that with the increased value of $M = 0.6$ with $c_0 = 3$, $c_1 = 0.1$, $c_2 = c_5 = 15$, $c_3 = c_4 = 0.5$, and $T = 30$ **(b)** View of (a) over a 3-day interval to observe the initial difference in v^*

Table 2.5: Comparison of $J(v)$ with constant vaccination rate to $J(v)$ with time-varying optimal vaccination rate, shown in Figure 2.4, for various upper bounds, M, on $v(t)$

M	$J(v)$ with constant $v(t) = M$	$J(v)$ with time-varying optimal v^*
0.3	203	192
0.6	305	192

an increased upper bound on the vaccination rate, then we see a more stark difference and impact of time-varying vaccination versus that of constant vaccination.

2.5.3 An increase in susceptible patients

In this section, we explore the question of how hospitals should modify their vaccination strategy in order to handle a larger number of susceptible patients. To do this, we consider alternate hospital statuses in which an increased number of patients have either received antibiotics after admission or taken them prior to admission.

First, if a particular hospital is prescribing high-risk antibiotics at an increased rate, this corresponds to an increase in α and thereby also an increase in the number of susceptible patients since more patients will have an altered intestinal microbiota. Assessing the effect of varying α on the resulting optimal control is also an interesting scenario because we showed

Table 2.6: Comparison of $J(v)$ and total vaccinated with constant vaccination rate to $J(v)$ and total vaccinated with time-varying optimal vaccination rate, shown in Figure 2.5, for various antibiotic prescription rates, α

α	$J(v)$ with constant $v(t) = 0.3$	$J(v)$ with time-varying optimal v^*	Total vaccinated with constant $v(t) = 0.3$	Total vaccinated with time-varying optimal v^*
0.5	203	192	405	319
1	201	187	447	332
5	199	181	493	338

that our objective functional, (2.8), was particularly sensitive to α (see Appendix A). For all simulations thus far, $\alpha = 0.5$ per day as listed in Table 2.3. Figure 2.5 illustrates how v^* changes for increasing α. Note that as α is increased, v^* decreases. To understand this downward shift, we first compare the patient population dynamics for the various α values, shown in Figure 2.6. From this, we see that when α is increased, we are able to reduce C^- and D to approximately the same number seen for the lower α-value of 0.5, but we do so with a lower v^* and therefore also a lower value of J. Additionally, with the higher antibiotic prescription rate, we observe that the total colonized population is also decreased.

Note that the number of susceptible patients vaccinated per day is given by vS. Since S is increased in this scenario, v^* can correspondingly decrease to lead to the same, or even a slightly increased, number of susceptible patients being vaccinated per day. Essentially, because there is an increased number of susceptible patients available to vaccinate due to the increase in α, we are able to vaccinate more patients (even at a lower rate). This increase in V engenders the decrease in the number of C^- and D patients. From Table 2.6, observe that we vaccinate more patients as α is increased whether we use a constant vaccination rate or a time-varying one. Furthermore, Table 2.6 also indicates that time-varying rates of vaccination in this scenario may be more economical than constant rates.

Another way for a hospital to experience an increase in susceptible patients is to have more upon admission due to a greater number of patients taking antibiotics before entering the hospital. We considered this case by increasing the proportion of susceptible patients admitted, a_s, and thereby also increasing the initial number of susceptible patients by adjusting the remaining admission proportions and initial conditions to reflect the change.

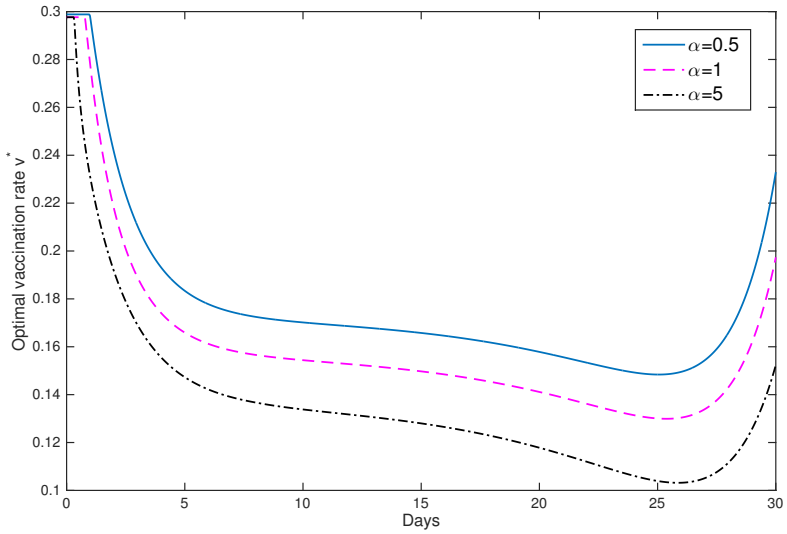


Figure 2.5: Optimal vaccination rate v^* for increasing antibiotic prescription rate, α, and for $c_0 = 3$, $c_1 = 0.1$, $c_2 = c_5 = 15$, $c_3 = c_4 = 0.5$, $M = 0.3$, and $T = 30$

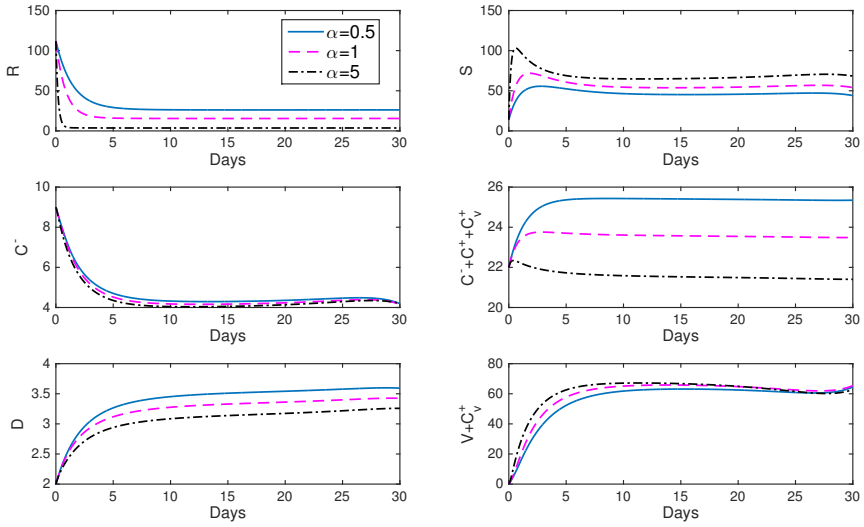


Figure 2.6: Dynamics of patient transition states for increasing antibiotic prescription rate, α, and for $c_0 = 3$, $c_1 = 0.1$, $c_2 = c_5 = 15$, $c_3 = c_4 = 0.5$, $M = 0.3$, and $T = 30$

Table 2.7: Comparison of $J(v)$ with constant vaccination rate to $J(v)$ with time-varying optimal vaccination rate, shown in Figure 2.7, for various transmission coefficients, β_c and β_d

β_c, β_d	$J(v)$ with constant $v(t) = 0.3$	$J(v)$ with time-varying optimal v^*
10^{-6}	203	192
0.0007	1,224	1,216
0.007	6,416	6,416

This scenario produced results that were similar to those obtained when increasing α and are omitted here.

2.5.4 Increasing transmission coefficients

Another scenario we considered is the case of an outbreak, meaning an increase in the transmission coefficients, β_c and β_d. Such an increase in transmission coefficients could occur for a multitude of reasons, one of which being an understaffed hospital in which workers may not be following proper protocol such as adequate washing of hands and wearing of gloves when necessary. Additionally, note that the system in [45] was found to be particularly sensitive to β_c and our objective functional, (2.8), was found to be sensitive to β_c and β_d (see Appendix A), so we determined the case of changing β_c and β_d was one worth exploring. Recall that thus far $\beta_c = \beta_d = 10^{-6}$.

Figure 2.7 shows how such an increase in β_c and β_d affects the optimal vaccination rate. As expected, in such a scenario, we should increase the vaccination rate in order to contain the outbreak. As β_c and β_d are increased, a time-varying optimal vaccination rate is just barely more cost-effective than a constant vaccination rate since v^* is increased closer to its maximum allowed rate of 0.3 per day. The savings in $J(v)$ are decreased as β_c and β_d are increased, as shown in Table 2.7. In a particularly bad outbreak, the optimal vaccination rate is constant at the upper bound of $M = 0.3$, as shown in Figure 2.7 for $\beta_c, \beta_d = 0.007$.

The resulting patient state dynamics for each set of transmission coefficient values considered in Figure 2.7 are illustrated in Figure 2.8. For the increased transmission coefficient values of $\beta_c, \beta_d = 0.007$, a comparison of the state dynamics with no vaccination to those with vaccination implemented using optimal control is shown in Figure 2.9. In this

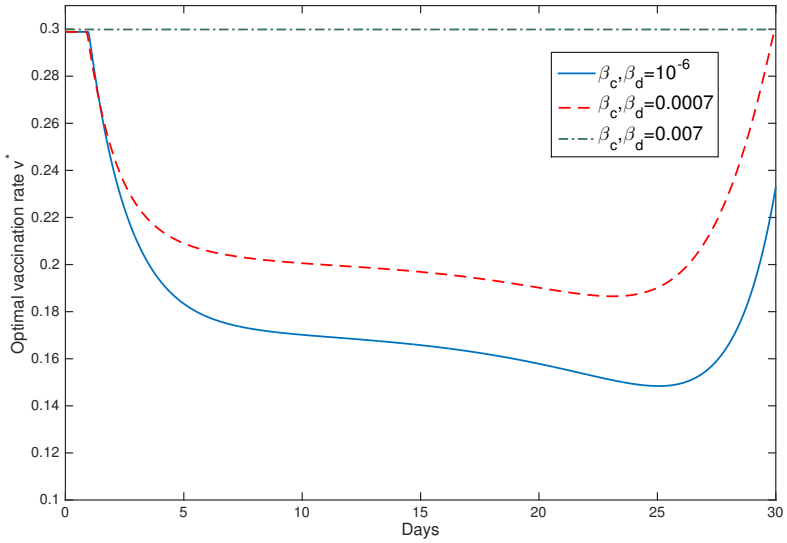


Figure 2.7: Optimal vaccination rate v^* for increasing transmission coefficients, β_c, β_d, and for $c_0 = 3$, $c_1 = 0.1$, $c_2 = c_5 = 15$, $c_3 = c_4 = 0.5$, $M = 0.3$, and $T = 30$

case, observe that vaccination has a much more significant impact than the scenario shown in Figure 2.2, and in 30 days decreases the number of C^- patients by approximately 20 and the number of D patients by approximately 10.

We also considered scenarios in which we increased the clinical disease rate ϕ while simultaneously increasing the transmission coefficients β_c and β_d. Note that in this case, the trend remains essentially the same to that when only β_c and β_d are increased. The only difference is that there is an increase in D when ϕ is also increased, which is expected. Because the results were similar, they are omitted.

Note that an increase in the upper bound M on the vaccination rate may be reasonable for some hospitals depending on a combination of factors. One such factor is how many people a hospital can manage to vaccinate in a day. If staff increases its efforts, the hospital may be able to handle an increase in vaccination rate. Additionally, if it becomes easier to convince persons to be vaccinated, such a scenario would also call for an increase in M. Since the most extreme outbreak, with $\beta_c, \beta_d = 0.007$, forces v^* to become constant at its upper bound, we also wanted to explore how v^* would change with an increase in the upper bound M to 0.6. The resulting v^* is illustrated in Figure 2.10 alongside v^* with $M = 0.3$. The corresponding state trajectories are given in Figure 2.11 for $M = 0.3$ and 0.6. This figure

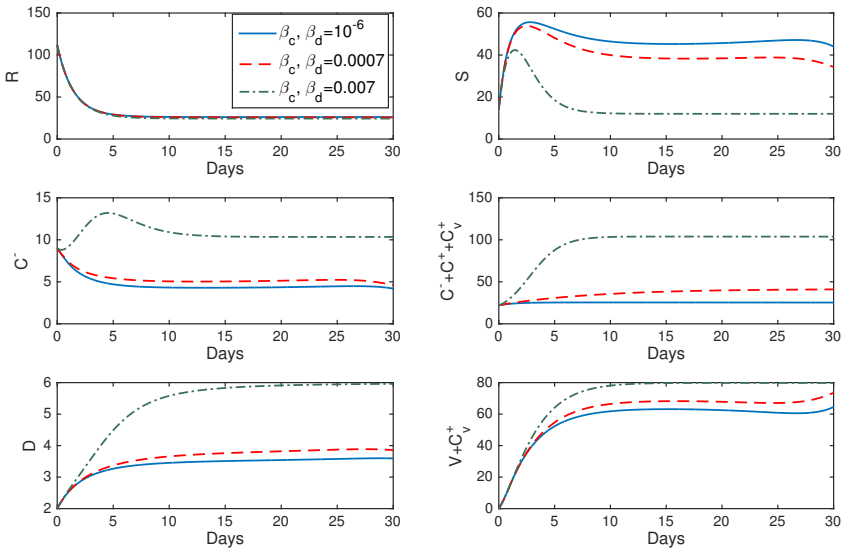


Figure 2.8: Dynamics of patient transition states for increasing transmission coefficients, β_c, β_d, and for $c_0 = 3$, $c_1 = 0.1$, $c_2 = c_5 = 15$, $c_3 = c_4 = 0.5$, $M = 0.3$, and $T = 30$

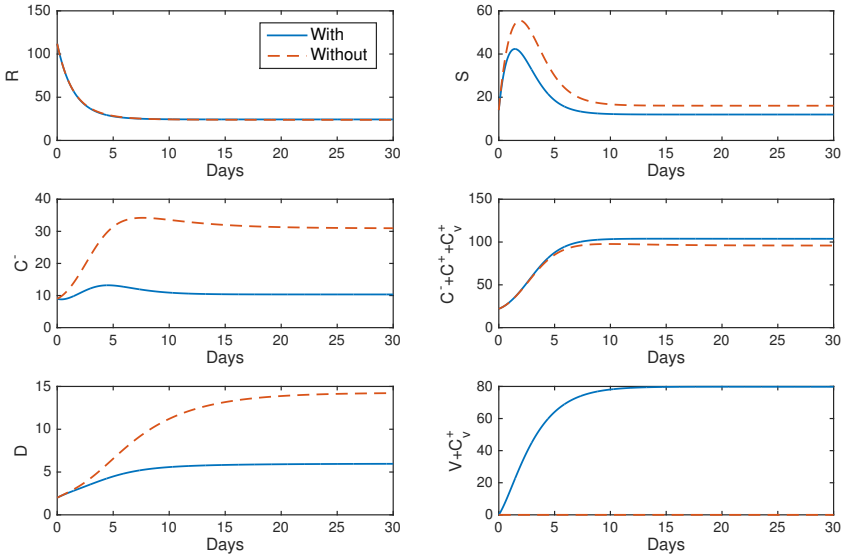


Figure 2.9: Dynamics of patient transition states with vaccination rate shown in Figure 2.7 for the increased values of $\beta_c, \beta_d = 0.007$ compared to those without vaccination for $c_0 = 3$, $c_1 = 0.1$, $c_2 = c_5 = 15$, $c_3 = c_4 = 0.5$, $M = 0.3$, and $T = 30$

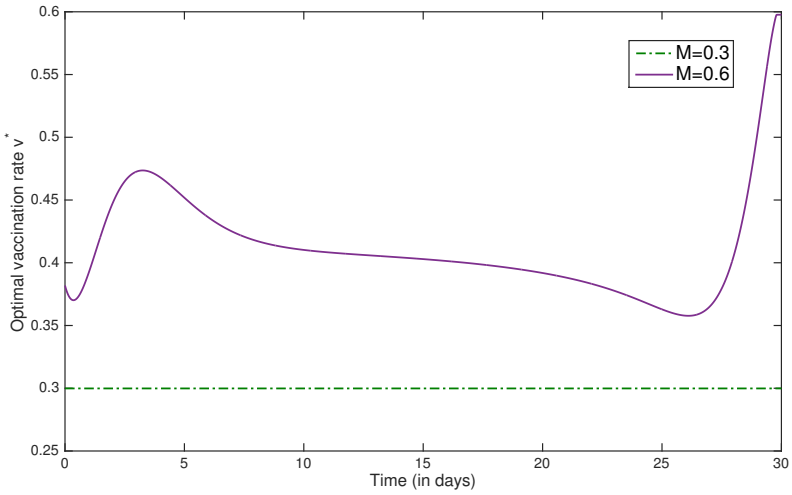


Figure 2.10: Optimal vaccination rate v^* for increasing M with increased $\beta_c, \beta_d = 0.007$, $c_0 = 3$, $c_1 = 0.1$, $c_2 = c_5 = 15$, $c_3 = c_4 = 0.5$, and $T = 30$

Table 2.8: Comparison of $J(v)$ with constant vaccination rate to $J(v)$ with time-varying optimal vaccination rate, shown in Figure 2.10, for various upper bounds, M, on $v(t)$ with increased $\beta_c, \beta_d = 0.007$

M	$J(v)$ with constant $v(t) = M$	$J(v)$ with time-varying optimal v^*
0.3	6,416	6,416
0.6	6,433	6,398

shows that D and C^- are decreased more in the case when $M = 0.6$ than when $M = 0.3$. Furthermore, from Table 2.8, observe that in the case of the increased upper bound, there is a notable benefit to using time-varying control over a constant rate of vaccination for all 30 days. Notably, the value of $J(v)$ for the optimal v^* corresponding to $M = 0.6$ is smaller than the value of $J(v)$ for the optimal v^* corresponding to $M = 0.3$. Thus, allowing for an increase in the upper bound on $v(t)$ could lead to an overall savings and a greater impact on reducing disease prevalence and incidence. We conclude that time-varying vaccination could be beneficial in more extreme outbreak scenarios (i.e., $\beta_c, \beta_d = 0.007$) with this upper bound increase, whereas without this increase, a constant rate of vaccination would be preferred.

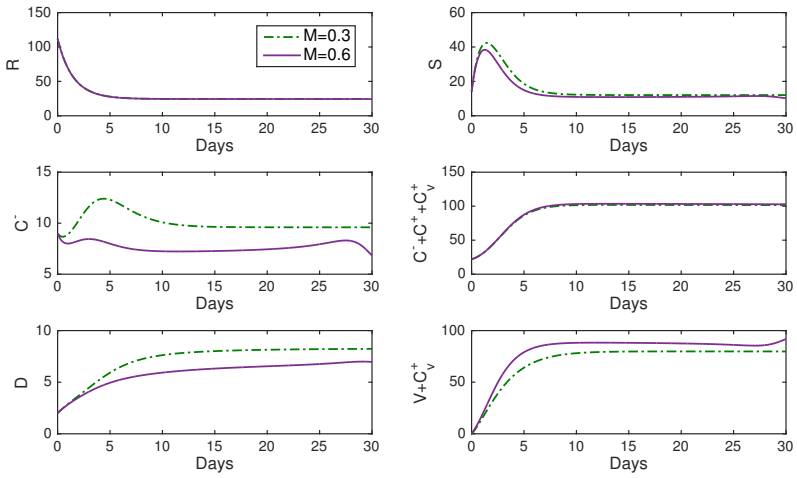


Figure 2.11: Dynamics of patient transition states with optimal vaccination rates shown in Figure 2.10 with various upper bounds M for the increased values of $\beta_c, \beta_d = 0.007$ for $c_0 = 3$, $c_1 = 0.1$, $c_2 = c_5 = 15$, $c_3 = c_4 = 0.5$, $M = 0.3$, and $T = 30$

2.6 Discussion

The recent striking growth in the prevalence of *Clostridium difficile* infection (CDI) in healthcare facilities highlights the need for finding effective strategies for prevention. A new potential prevention strategy is being considered as two international studies are underway to test the effectiveness of a vaccine against the toxins produced by *C. difficile* [48]. In anticipation of this vaccine, we have extended and updated a mathematical model of *C. difficile* transmission in hospitals to include vaccination. We then employed optimal control theory in order to find the time-varying optimal rate at which hospitals should vaccinate patients that minimizes disease prevalence and transmission while also minimizing the cost associated with vaccination.

In this chapter, our simulations considered 30-day time periods since vaccination strategies will need to be reevaluated after this due to parameter values that may change during this period. We considered different hospital statuses and compared time-varying rates to constant rates in order to determine in which scenarios a time-varying rate would be preferred. First, we considered a scenario in which hospitals have an increased number of susceptible patients due to more high-risk antibiotics being given either prior to or after

admission. We saw that with this increase in the number of susceptible patients, the optimal vaccination rate decreased. In this scenario, hospitals could reduce all colonized populations (asymptomatic and symptomatic) by the same amount (or slightly more), with a lower vaccination rate and lower objective functional value. This is because there are more patients available to be vaccinated in this scenario. In this case, a time-varying rate of vaccination was shown to be more beneficial.

Another situation that hospitals commonly experience is that of an outbreak. In this scenario, we saw that an increase in transmission coefficients led to a simultaneous increase in the optimal vaccination rate. Because part of our main goal is to minimize disease prevalence and transmission, as *C. difficile* spores are being transmitted at a higher rate, we must vaccinate more to control this outbreak. Once the transmission coefficients increased to some threshold value, the optimal vaccination rate became constant at its upper bound. Therefore, in more severe outbreaks a constant vaccination rate is optimal to accomplish our goal rather than a time-varying one, unless we allow for an increase in the upper bound on the vaccination rate.

It is important to note that the upper bound of 0.3 we imposed on the vaccination rate is not a strict upper bound. For this reason, we also considered how an increased upper bound changed our results. In particular, we observed that in some cases of severe outbreak a time-varying optimal vaccination rate is more economical when the upper bound is increased.

Chapter 3

Agent-based model of nosocomial *C. difficile* transmission

3.1 Introduction

Since the early 2000s, a notable increase in the incidence and severity of CDI has placed a substantial burden on healthcare facilities [41, 40, 84]. In particular, the North American population has experienced a fivefold increase in CDI incidence with an eightfold increase in the elderly [68], and the cost associated with CDI in United States acute-care facilities alone has been estimated to be as much as $4.8 billion annually [20]. These increases are due, in part, to significant changes in the epidemiology of *C. difficile* with the emergence of a new hypervirulent strain [40]. Thus, there is a critical need to better identify primary sources of transmission in order to determine optimal methods for prevention.

Mathematical and computational models provide a mechanism for evaluating the complex interactions driving transmission and for making recommendations about disease control and surveillance. Models using differential equations have previously been developed to represent nosocomial transmission [6, 86, 45, 36, 88, 81]. Using a compartmental model of *C. difficile* transmission in a healthcare setting, Lanzas et al. [45] concluded that asymptomatic patients are significant contributors to within-ward transmission. Increased awareness of the role of environmental transmission in the spread of some pathogens has led to the development of models that incorporate environmental components [38, 83, 74]. Updated studies have

indicated that the primary reservoirs of CDI are both colonized individuals (asymptomatic and symptomatic) and contaminated environments [39, 8, 75]. Because of this, we aim to expand our modeling assumptions to explicitly include the additional transmission pathway of environmental contamination.

Evidence has linked the acquisition of nosocomial pathogens to their presence on hospital surfaces, and *C. difficile*, in particular, has been found on beds, sinks, toilets, walls, rails, call buttons, and stretchers [28]. *C. difficile* spores can survive for extended periods of time, even years, on these hospital surfaces and are resistant to drying, heat, exposure to air, and most disinfectants and detergents [28]. Because the persistence time of *C. difficile* in the environment is often longer than the duration of pathogen shedding by infectious individuals, the risk of a susceptible individual becoming colonized greatly depends on the level of pathogen in the surrounding environment [18]. The survival of *C. difficile* spores on hospital surfaces makes healthcare workers (HCWs) important vectors of transmission, particularly if they exhibit poor hand-hygiene practices [28].

Antibiotic use has been shown to be the primary risk factor for contracting CDI since antibiotics disrupt the normal gut microbiota [63], allowing *C. difficile* to proliferate and colonize [3]. Certain antibiotics may make individuals more susceptible to colonization by *C. difficile* than others. This depends on the spectrum, duration, and number of antibiotics received [78, 14, 5]. Prolonged duration of antibiotic use and use of multiple antimicrobial agents are both linked to increased risk of contracting CDI [40]. Broad-spectrum antibiotics, such as amoxicillin, work against a broad range of bacteria, which results in more significant gut microbiota disturbance and, thereby, an increased risk for *C. difficile* colonization [67].

Strategies have been implemented to reduce the transmission of *C. difficile* in healthcare environments. Such strategies include antimicrobial usage restriction and stewardship, isolation of patients with CDI, environmental decontamination of rooms with bleach, and improved HCW hand-hygiene and contact protocol [18]. Antimicrobial stewardship involves an overall reduction in the number of antibiotics prescribed and/or a reduction targeted specifically at the proportion of antibiotics prescribed that are associated with a higher chance of contracting CDI, such as broad-spectrum antibiotics [23, 82, 5]. Current hospital practice calls for the identification and subsequent isolation of patients with CDI so that

proper contact precautions can be implemented to decrease the chances of pathogen spread [18]. Assessments of hospital cleaning practices have shown that routine disinfection is often not performed efficiently and as a result, it is ineffective at eradicating nosocomial pathogens [28]. Therefore, more purposeful cleaning with bleach can be an important strategy for reducing the pathogen level in a healthcare setting [29]. HCWs' hands can become contaminated after touching surfaces with *C. difficile* spores [60, 17], and studies have shown that adherence to best hand-hygiene and contact protocol practices have been difficult to maintain [64, 10]. Because the spread of nosocomial pathogens has been linked to poor hand-hygiene practices [28], improved adherence of HCWs to proper hand-washing and contact protocols is also an important control measure. Vaccination may soon be an addition to the current control strategies since early results of clinical trials of a *C. difficile* toxoid vaccine show efficacy in preventing CDI [84]. Although this vaccine does not prevent colonization by *C. difficile*, it may be effective for reducing transmission in hospital settings.

Studies have been completed to determine the individual impact of these control measures on the spread of *C. difficile* [55, 31, 66, 21], and several computational models [75, 10, 13, 5] have been designed to determine the optimal combination of intervention strategies for reducing *C. difficile* transmission. Agent-based and individual-based models allow us to define a system based on individual behaviors and interactions. These individual behaviors are simulated to observe emergent behaviors of the entire system [72]. Agent-based models (ABMs) also allow us to incorporate spatial heterogeneity, consider a variety of transmission pathways, and incorporate individual patient characteristics that are significant in determining transmission. ABMs also inherently have stochastic components that can result in different outcomes from similar starting conditions.

D'Agata et al. [13] used an individual-based model to determine the key contributing factors to nosocomial transmission of a general antimicrobial-resistant bacteria. Their model focused on the admission and exit of patients, infection of patients by HCWs, and contamination of HCWs by patients; however, their study did not include an environmental reservoir. They also analyzed the role of antibiotics, including the duration of treatment and the scheduling of treatment initiation. One drawback of considering a general antimicrobial-resistant bacteria is the inability to incorporate characteristics specific to a single type of

bacteria. By only monitoring one individual patient characteristic (the bacterial load during antibiotic treatment), this model ignores other individual patient characteristics that are especially relevant to CDI incidence, such as disease status at admission. In particular, patients colonized at admission significantly contribute to *C. difficile* transmission [12], so tracking patient disease status at admission is important when modeling CDI transmission.

The ABM created by Codella et al. [10] specifically considered *C. difficile* and included patients, HCWs, and visitors. The agents were able to interact with each other and the environment as possible sources of transmission. Neither this model nor the one created by D'Agata et al. [13] considered within-hospital patient history, such as the level of risk of *C. difficile* colonization associated with the particular antibiotics prescribed. Additionally, it is important to track when antibiotic treatment began since both the spectrum and duration of antimicrobial treatment affect the probability of a susceptible patient becoming colonized. The ABM of *C. difficile* transmission developed by Rubin et al. [75] does group antibiotics into classes based on the level of risk; however, none of the three ABMs mentioned evaluated antimicrobial stewardship as a control measure. This is notable because antimicrobial stewardship has been linked with the greatest evidence for preventing CDI in healthcare environments [37].

The ABM of *C. difficile* transmission created by Bintz et al. [5] focused on evaluating the efficacy of various control measures aimed at "reducing environmental contamination and mitigating the effects of antibiotic use on transmission" of *C. difficile* in order to reduce colonization and infection incidence within the hospital. Their model accounts for the heterogeneity of the environment and of the antibiotics prescribed. They denote various risk levels for antibiotics, according to the degree of microbiota disturbance they cause, and, consequently, the likelihood of colonization by *C. difficile*. By accounting for both the type and number of antibiotics each patient receives while in the hospital, they were able to simulate antimicrobial stewardship programs. In addition to considering antimicrobial stewardship as a control measure, they also considered environmental decontamination strategies. They tracked many individual patient characteristics that are relevant for determining the probability of colonization, such as disease status at admission, risk level of the antibiotic received, and the local contamination level. A major assumption of their

model is that the impact of HCWs on transmission can be estimated without explicitly incorporating HCWs as agents in the model. Bintz et al. [5] implicitly incorporate the impact of HCWs by considering ward-level contamination in addition to room-level contamination, but they do not consider HCWs as agents.

In this study, we develop an ABM of the spread of *C. difficile* in healthcare environments that includes environmental transmission and explicitly includes HCWs as vectors of transmission. The goal of our work is to build on the ideas formulated by Bintz et al. [5] in order to create an ABM of *C. difficile* transmission that incorporates specific patient histories, antibiotic histories, and antibiotic risk levels and that *explicitly* incorporates HCWs as agents. Using this model, we aim to evaluate various control strategies, such as environmental cleaning, antimicrobial stewardship, improved HCW hand-hygiene practices, and vaccination in order to determine the optimal combination of strategies for reducing nosocomial *C. difficile* colonization and infection incidence. Specifically, we hope to answer questions that the previous model [5] with only implicit HCWs was unable to answer, such as the effectiveness of improved HCW hand-hygiene practices as a control intervention. It is worth noting that none of the ABMs previously mentioned considered vaccination as a control measure. With positive early results of *C. difficile* toxoid vaccine trials [84], we saw benefit in performing a preliminary assessment of vaccination both individually as an intervention strategy and coupled with other interventions.

In Section 3.2, we give an overview of the structure of and components in our ABM, including a description of patient-HCW-environment interactions and specific characteristics tracked for HCWs, patients, and rooms. In Section 3.3, we discuss the control interventions and the combinations of interventions that we evaluated. Section 3.4 describes the computational methods we used to obtain our results, and Section 3.5 summarizes the results of our simulations and intervention comparisons. A discussion of implications and conclusions follows in Section 3.6. Specific details about the model structure and implementation are described using the standard Overview, Design Concepts, and Details (ODD) protocol [72] in Section 3.7.

3.2 Model overview

In this section, we give an overview of the structure of and components in our ABM of nosocomial *C. diffcile* transmission. For all the specific details about model design and implementation in their entirety, see the ODD protocol in Section 3.7 and the descriptions of the submodels in Section 3.8. Our ODD protocol follows the standard formatting originally developed by Grimm, Railsback, and their collaborators [32].

3.2.1 Model setting

We developed our ABM using NetLogo, a coding language primarily used for the creation of ABMs. Our model is a modification and extension of the ABM originally created by Bintz et al. [5]. The model environment is a hospital consisting of six wards, each with 35 patient rooms. A snapshot of the graphical user interface of our model environment in NetLogo is shown in Figure 3.1. We assume these are all single-patient rooms, so there can be at most 210 patients in the hospital at a time. For simplicity and to ensure we never have more patients than available rooms, we maintain a constant occupancy level. That is, the number of new patients admitted at a given time always equals the number of patients discharged at the previous time. The number of HCWs in the hospital is chosen to maintain a 3:1 ratio of patients to HCWs, and each time an HCW leaves the hospital, a new one arrives to maintain a constant total population of HCWs.

The model has two types of agents: patients and HCWs, and the environmental patches represent ward rooms. We track behaviors and characteristics specific to each individual agent and each individual patch. The individual characteristics and interactions can give rise to interesting overall population dynamics, and the resulting outputs of model simulations will vary based on the individual behaviors. Patient interactions and characteristics are updated at every half-day time-step, which mimics the time-scale of the ABM in [5], while HCW interactions and characteristics are updated at every 15-minute time-step. Many of the values for the parameters used in the model were taken from a dataset originally used in [45] that was collected from Barnes-Jewish Hospital in St. Louis, Missouri.

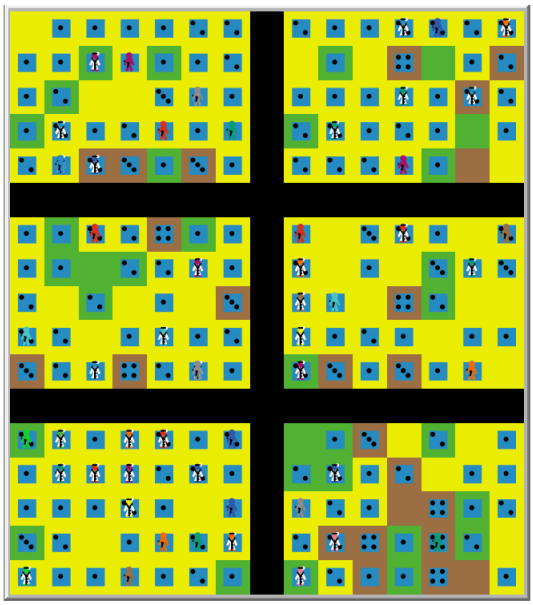


Figure 3.1: Snapshot of the graphical user interface of our model environment in NetLogo as a hospital with six wards that each have 35 rooms, where the dice represent patients, the people represent HCWs, and the colors represent the amount of contamination in that room (yellow indicates low contamination, green is medium contamination, and brown is high contamination)

3.2.2 Model components

For each ward room, we track its contamination level over time. The more surfaces in a room contaminated by *C. difficile* spores, the higher the room's contamination level. Pathogen shedding of both symptomatic and asymptomatic patients will increase the contamination level of a room. However, we assume that the shedding of symptomatic patients contributes more to room contamination than that of asymptomatic carriers since it has been shown that those with CDI shed more *C. difficile* in their stool [18], which leads to more environmental contamination. Patients who are not colonized by *C. difficile* will have no effect on the contamination level of the room in which they are residing.

For all patients, we assign a length of stay in the hospital based on their disease status upon admission and on data for the lengths of stays of patients at Barnes-Jewish Hospital [45, 5]. We also track each patient's time since admission, and once the time since admission reaches the preassigned length of stay, that patient is discharged from the hospital.

All patients, regardless of their disease status with respect to *C. difficile*, have a

probability of receiving an antibiotic (for treating illnesses not related to *C. difficile*) at each half-day time-step. Because different types of antibiotics result in varying degrees of microbiota disturbance and, therefore, varying risks of colonization by *C. difficile* [78, 14], we group antibiotics into three risk levels with respect to *C. difficile*: low-, high-, and very high-risk [5]. The risk level of an antibiotic directly affects the time until restoration of a normal gut microbiota and a patient's incubation period (the time between exposure to *C. difficile* and the onset of symptoms). In particular, higher risk antibiotics are associated with shorter incubation periods and longer periods until successful restoration of the gut microbiota. The model tracks the associated risk level of each antibiotic a patient receives and the number of antibiotics each patient receives while in the hospital. Additionally, the amount of time each patient spends on a particular antimicrobial therapy is tracked. Because of this, we are able to incorporate the impact of the antibiotic type, duration of treatment, and number of antibiotics on the risk of colonization and subsequent infection by *C. difficile*.

Throughout a patient's stay, we track the progression of his or her disease status, and we begin by noting the patient's disease status at admission. There are four possible disease statuses of patients: resistant, susceptible, (asymptomatically) colonized, and diseased. Upon admission, a patient's disease status is determined based on the admission proportions for each disease class. We use the same admission proportions here as we used in our ODE model in Chapter 2, in which the proportions were based on hospital data with modifications made to the colonized admission proportion because of updated data given by Alasmari et al. [1].

All possible transitions among disease states are represented in Figure 3.2. Because antibiotic use is widely recognized as the most significant risk factor for colonization by *C. difficile* [48, 40], we make the same assumption here that we made in our ODE model (Chapter 2): a patient only becomes susceptible to colonization after beginning antimicrobial therapy. Those who have not recently undergone antimicrobial therapy are considered resistant to colonization and will not be affected by exposure to *C. difficile* spores. Since, on average, a patient's microbiota will return to normal after 30 days [45], our model allows susceptible patients to return to resistant if they are not exposed to *C. difficile* while susceptible or if they do not receive an additional antibiotic in those 30 days. However,

the susceptible individuals who do come into contact with *C. difficile* spores have a chance of becoming colonized. Each individual susceptible patient has his or her own probability of becoming colonized that changes at each 15-minute time-step and depends on the risk level of the antibiotic prescribed and on the contamination level of his or her room. The more contamination in a room, the greater the chances of exposure and subsequent colonization. Similarly, the higher the antibiotic risk level with respect to *C. difficile*, the greater the chances of colonization.

Upon colonization, patients are randomly assigned as either immunocompromised or not immunocompromised, indicating whether or not they mount their own immune response against the toxins produced during colonization. In keeping with the values used by Bintz et al. [5], there is a 10% chance a colonized individual will be immunocompromised. All colonized patients have a chance of receiving one or more additional antibiotics (for the treatment of illnesses not related to *C. difficile*). For those who are not immunocompromised and receive an additional antibiotic, it is possible they will clear their colonization but still have an altered gut microbiota. Therefore, this subset of colonized patients may return to susceptible. For colonized patients who are not immunocompromised and do not receive an additional antibiotic, they may clear their colonization and also have their gut microbiota return to normal. This subset of colonized patients will return to the resistant class. Finally, those colonized who are immunocompromised will contract CDI. If they receive an additional antibiotic prior to becoming diseased, this will shorten their incubation period and cause them to experience CDI symptoms more quickly than they would have otherwise. Our model includes screening of symptomatic patients for CDI with the turnaround time for the screening test and the sensitivity of the screening test also incorporated. After the turnover time for the screening test has elapsed, the symptomatic patients who were unsuccessfully screened are tested again. Those diseased patients who are successfully screened for CDI will be quarantined, and their symptoms will be treated with one of the typical antibiotics used to treat CDI. There is an 80% chance of successful treatment and resolution of symptoms [45] that will allow diseased patients to return to the susceptible class.

Upon arrival to the hospital, each HCW is assigned a shift length. For simplicity, we consider either 8-hour or 12-hour shifts, with a 50% chance of each. We track each HCW's

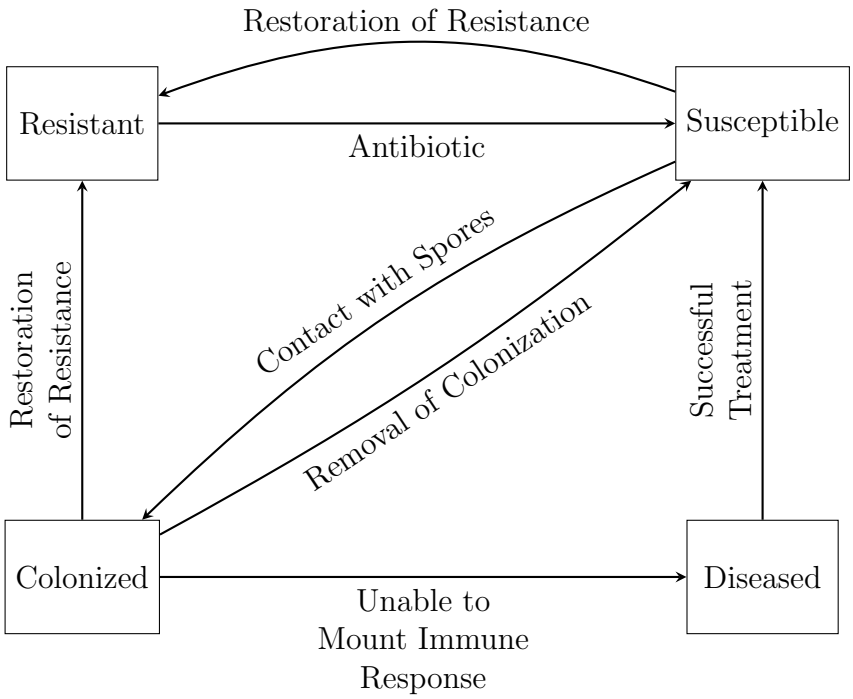


Figure 3.2: Summary of movement among disease statuses of patients in agent-based model

time since beginning a shift, and once this time surpasses the total shift length assigned, that HCW leaves the hospital. We divide HCWs into two groups: Type 1 and Type 2. Type 1 HCWs are assumed to be completing more routine, less time-consuming tasks and, therefore, move from patient to patient every 15 minutes. In contrast, Type 2 HCWs spend more time with the patients they visit and only move from patient to patient every 45 minutes. Our model assumes that no HCW will visit a vacant room and that HCWs of the same type will never be in the same room simultaneously; however, a Type 1 and Type 2 HCW may visit the same patient at the same time.

HCWs have individual contamination levels that represent the amount of *C. difficile* they are carrying. We do not track *C. difficile* colonization or infection of HCWs and view them only as vehicles of pathogen spread from room to room. Because *C. difficile* is primarily acquired nosocomially [48], we assume each HCW has a contamination level of zero upon entry into the hospital. However, we should note that there has been a significant increase in community-acquired infection by *C. difficile* [48], so this parameter can be varied to mimic contamination from this increase. Each time an HCW visits a patient, the chances

of becoming contaminated by *C. difficile* depends on the type of task being performed on the patient and on the amount of contamination in the room. For this reason, we divide the types of tasks HCWs complete into three groups: low-, medium-, and high-risk. The risk associated with a particular task depends on the invasiveness of the task and the likelihood of coming into contact with a large number of surfaces in the room. For example, we consider a task such as giving a patient a scrub bath to put an HCW more at risk of becoming contaminated than taking a patient's temperature does. Although both types of HCWs can perform any level of task, we assume Type 1 HCWs have a greater chance of performing low-risk tasks while Type 2 HCWs have a greater chance of performing high-risk tasks.

3.2.3 Model processes

Before beginning simulations, the model environment is first initialized. In this process, we populate the hospital with enough patients to meet the specified occupancy level. The disease status of these patients upon admission is based on the admission proportions: a_r, a_s, a_c, and a_d, whose values are given in Table 3.12. The room contamination levels are then initialized based on the disease status of the patient in the room. Rooms with resistant or susceptible patients will have a contamination level of zero. Because colonized and diseased patients will shed *C. difficile* spores, the contamination level of their rooms will be increased to reflect this. The exact process for determining the amount of increase is the same as that described in Section 3.8.4, where each submodel of the ABM is outlined. The hospital is next populated with enough HCWs to maintain a 3:1 ratio of patients to HCWs, and the contamination level of all HCWs is initialized to zero. In this initialization process, HCWs are randomly assigned a length of time remaining on their shift, varying from 0 to 12 hours. We let the model run for a three-week time period before recording outputs to ensure the resulting outputs are not significantly dependent on the specified initial conditions.

After initialization, the model executes the following processes, in the order presented below, at every 15-minute time-step. The flow of these processes is also illustrated in Figure 3.3.

1. New HCWs arrive to begin their shifts.

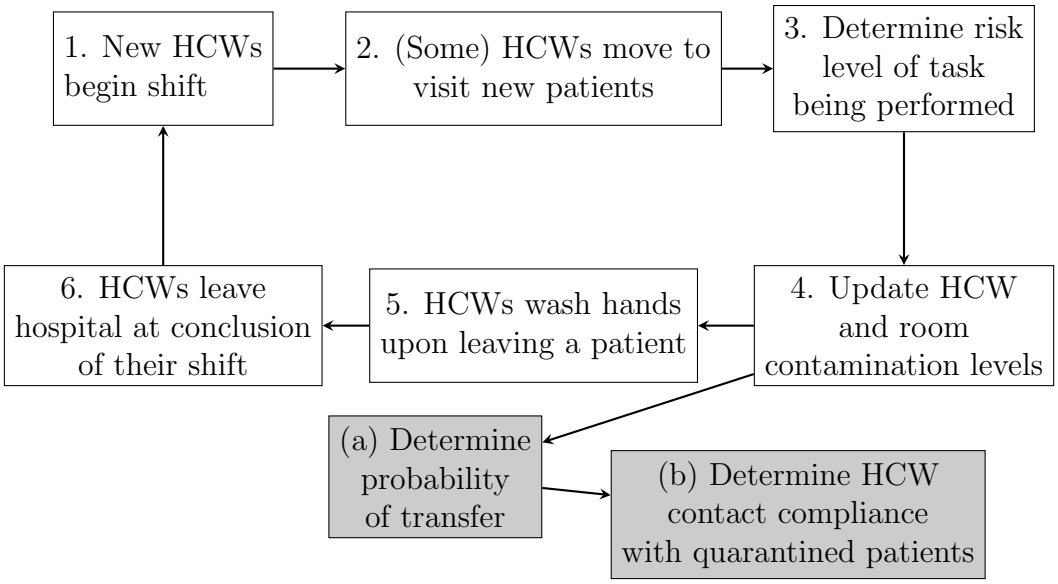


Figure 3.3: Summary of ABM processes that are run at each 15-minute time-step

2. If it is time to do so, HCWs move to begin a visit with a new patient; otherwise, they do not move and continue their visit with the current patient.

3. Risk level of task being performed is determined.

4. HCW contamination levels and room contamination levels are updated based on the transfer of *C. difficile*.

   (a) The probabilities of transfer from HCW to room and vice versa are first determined.

   (b) Separate probabilities of transfer are determined for HCWs visiting quarantined patients.

5. HCWs wash their hands at the conclusion of their patient visit.

6. HCWs who have completed their shifts leave the hospital.

To update the contamination levels of rooms and HCWs, we first determine the probability of pathogen transfer occurring. When HCWs visit rooms, they have a chance of picking up *C. difficile* spores, which would add to the existing contamination on their hands, and they also have a chance of transferring *C. difficile* spores already on their hands to the

room. The probability of an HCW picking up pathogen when visiting a room depends on the amount of contamination in the room and the risk level of the task being performed. The greater the room contamination and the higher the risk associated with the task, the more likely an HCW will pick up pathogen from the room. Similarly, the probability of an HCW transferring pathogen from his or her hands to a room surface depends on the contamination level of the HCW and on the risk level of the task being performed. The more *C. difficile* on an HCW's hands and the higher the risk of the task, the more likely an HCW will transfer pathogen to the room. We refer to the chance of HCWs picking up pathogen from the room as *prob-room-transfer* and refer to the chance of HCWs transferring some of their existing contamination to the room as *prob-HCW-transfer*. To calculate these probabilities at each 15-minute time-step for each HCW and room, we use three transfer functions, one for each task risk level. When determining prob-room-transfer, we consider these transfer functions to be functions of the room contamination level, and when determining prob-HCW-transfer, we consider them to be functions of the HCW contamination level. For more details and to see the specific functions used, refer to Section 3.8.9. Based on these probabilities, the model then determines whether or not transfer will occur between a room and an HCW.

Note that the process of determining the probability of transfer between a room and an HCW is different for quarantined patients. For these patients who were successfully identified with CDI and then placed in isolation, there is either a 100% chance of transfer or 0% chance of transfer between their room and the visiting HCW. We incorporate this into the model to reflect the fact that HCWs are likely to behave differently when they know they are visiting a patient quarantined with *C. difficile*. In fact, data shows a greater likelihood of HCWs adhering to contact protocol when visiting patients in isolation. We refer to the likelihood of HCWs complying with proper hand-hygiene and contact protocol when visiting quarantined patients as *hcw-contact-compliance* and set its baseline value to 0.6, based on data given by Rubin et al. [75]. If HCWs properly comply, there is a 0% chance of pathogen transfer between that room and the HCW; if they do not, there is a 100% chance of transfer.

After determining whether transfer will occur for each HCW-room combination, the model next updates HCW and room contamination levels to reflect the transfer. In particular, if an HCW picks up pathogen from a room, we decrease the room contamination

level by 10% and increase the HCW contamination level by that same amount to represent the transfer. Similarly, if an HCW transfers pathogen to a room, we decrease the HCW contamination level by 90% and increase the room contamination level by the same amount. These percentages were chosen to reflect the fact that ward rooms contain many surfaces, so one HCW is likely to only pick up a small percentage of the total contamination in the room during one visit. In contrast, we are only tracking the contamination of HCWs on their hands, so they are likely to transfer a vast majority of their total contamination to the room if it is determined that a transfer will occur.

HCWs may decrease their contamination levels by following proper hand-washing and contact protocols. Our model includes HCW routine hand-washing after every patient visit with a 45% chance that the hand-washing was effective at reducing contamination. This value was obtained by averaging the adherence percentage after patient contact of nurses and physicians given by Rubin et al. [75]. We refer to this compliance as *hcw-compliance* and set its baseline value to 0.45 (Table 3.12).

In addition to the processes run at each 15-minute time-step, the model will run the following processes, in the order presented, at each half-day time-step. These processes are also illustrated in the flow diagram in Figure 3.4.

1. Update the disease status of patients.
    (a) Determine if each patient will receive an antibiotic (based on the global variable for the overall probability of patients receiving antibiotics).
    (b) Determine each patient's probability of becoming colonized.
    (c) Screen symptomatic patients for CDI.
    (d) Quarantine and treat patients who tested positive for CDI.
2. Update the contamination level of rooms based on contributions from symptomatic and asymptomatically colonized patients.
3. Discharge patients from the hospital (once their time since admission equals their assigned length of stay).

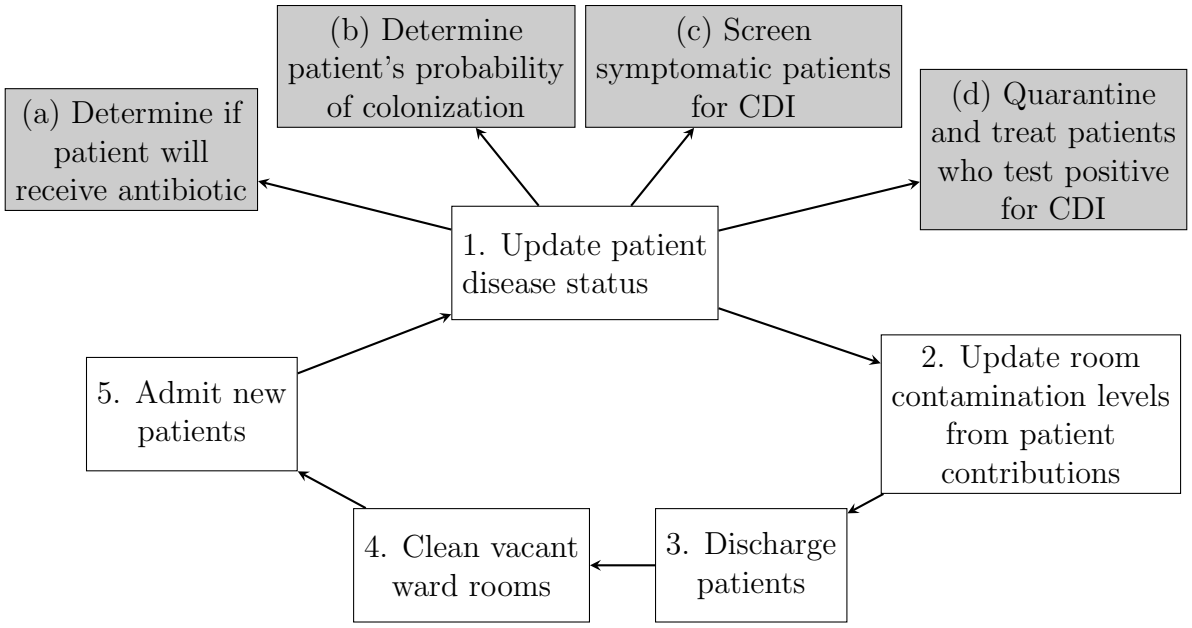


Figure 3.4: Summary of ABM processes that are run at each half-day time-step

4. Clean vacant ward rooms.

5. Admit new patients to replace those who were discharged.

At each half-day time step, all patients have a 27% chance of receiving an antibiotic. This number was chosen by Bintz et al. [5] so that the output for the total number of antibiotic treatments per patient matched the data from the hospital. Whether or not a patient receives an antibiotic will affect his or her disease status, as described in Section 3.2.2. When the model updates each patient's disease status, it first determines if that patient will receive an antibiotic and then determines the risk level of the antibiotic given. In this step, the model also updates the number of antibiotics each patient receives. The changes to disease status were all described in Section 3.2.2 and are described in the most detail in Section 3.8.3.

After patient disease statuses are updated, the room contamination levels are updated based on contributions from patients. As described in the initialization process, patients with CDI and asymptomatically colonized patients contribute to the contamination level of a room by shedding *C. difficile* spores in their feces. Resistant and susceptible patients will not contribute. Note that our model does not explicitly include pathogen transfer directly from HCW to patient or vice versa; rather, we model the transfer between HCWs and rooms and

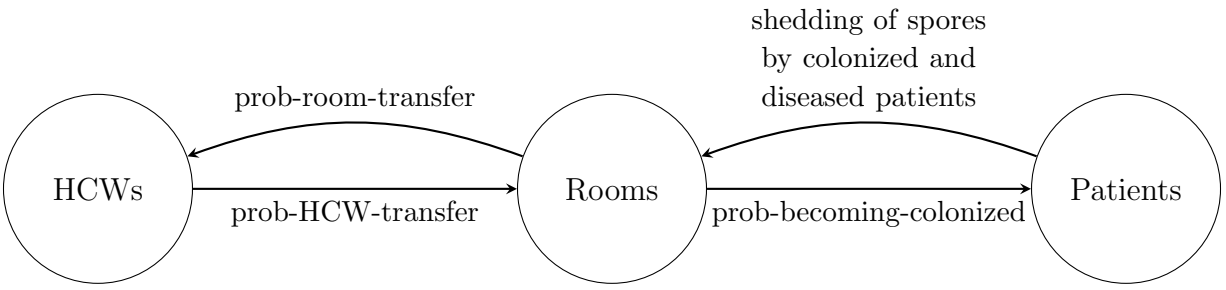


Figure 3.5: Summary of modes of *C. difficile* transmission included in the ABM, where *prob-room-transfer* refers to the probability of an HCW picking up *C. difficile* spores from a room, *prob-HCW-transfer* refers to the probability of an HCW contaminating room surface(s) with spores, and *prob-becoming-colonized* represents the probability of a patient becoming colonized based on the contamination level of the room and on the risk level of the antibiotic received

between patients and rooms. Transfer between patients and HCWs is considered implicitly as a result of the spread between rooms and HCWs and between rooms and patients. A summary of all possible *C. difficile* transfer routes is represented in Figure 3.5.

Once the disease status of patients and room contamination levels are updated, patients whose time since entering the hospital exceeds their length of stay assigned at admission are discharged. After this, the model admits new patients to replace those who were just discharged. This admission of patients is run in the same way patients were admitted during the initialization process. When new patients are admitted, we assign them a disease status and initialize all other patient characteristics that we are tracking. A complete list of these patient characteristics is given in Section 3.7.3 of the ODD protocol, and a detailed description of the admission of patients process run by the model is given in Section 3.8.2.

3.3 Control interventions

Our goal is to compare the impact of various control interventions, and combinations of control interventions, on the transmission of and subsequent infection by *C. difficile*. We consider the following intervention strategies:

1. Antimicrobial stewardship

2. Increased HCW adherence to hand hygiene and contact protocol (with all patients and specifically with quarantined patients)

3. Improved environmental decontamination

We consider antimicrobial stewardship in two forms (using the same techniques described in [5]): (1) an overall reduction in the number of antibiotics prescribed and/or (2) a reduction targeted at the proportions of high-risk and very high-risk antibiotics prescribed. To implement an overall reduction in the number of antibiotics prescribed, we reduce the half-daily probability of a patient receiving an antibiotic by a certain proportion. At baseline, this reduction is assumed to be 0% so that there is a 27% chance of patients receiving an antibiotic each half-day, as described by the global variable *prob-antib* listed in Table 3.12. The intervention scenarios considered include a reduction of this probability by 10% and by 20%, resulting in a 24.3% and a 21.6% chance, respectively, of patients receiving an antibiotic each half-day. For easy reference, these values are given in Table 3.1.

To implement the second form of antimicrobial stewardship, we alter the probabilities of the antibiotic prescribed being low risk, high risk, or very high risk with respect to CDI. The scenarios considered here are the same as those used by Bintz et al. [5] and are listed in Table 3.2. In the baseline scenario, we set the proportion of low-risk antibiotics prescribed to be 0.4, the proportion of high-risk to be 0.26, and the proportion of very high-risk to be 0.34. We will refer to this as Risk Scenario 1. The second risk scenario considered involves reducing the probability of very high-risk antibiotics being prescribed by half, and as a result, increasing the probability of high-risk antibiotics being prescribed by that same amount. The third and final risk scenario considered involves replacing both half of the proportion of very high-risk antibiotics prescribed with high-risk antibiotics and half of the high-risk antibiotics prescribed with low-risk antibiotics. As noted by Bintz et al. [5], these particular antimicrobial stewardship strategies and values were chosen to represent programs that could feasibly be implemented; more extreme values, such as a 0% chance of receiving an antibiotic, are not realistic. Data indicate that even when hospitals were successfully able to reduce the number of unnecessary antibiotics prescribed, there were always still some unavoidable prescriptions, even at the very high-risk level, remaining [5].

Table 3.1: Antimicrobial stewardship strategy: reduction in the overall number of antibiotics prescribed

	Probability of receiving antibiotic
baseline	0.27
10% reduction	0.243
20% reduction	0.216

Table 3.2: Antimicrobial stewardship strategy: reduction in the proportions of antibiotics prescribed according to risk level with respect to CDI

Risk scenario	1	2	3
proportion of low-risk	0.4	0.4	0.53
proportion of high-risk	0.26	0.43	0.3
proportion of very high-risk	0.34	0.17	0.17

The next intervention strategy considered involves the increased adherence of HCWs to hand-hygiene and contact protocols. To increase HCW compliance, a hospital might need to have additional HCWs due to the time spent adequately sanitizing. Our model does not explicitly account for the time HCWs spend adequately washing, but this is something that could be further explored in the future. We consider both improved HCW hand-hygiene compliance after each patient visit and improved HCW compliance when visiting quarantined patients. The baseline value for HCW compliance after completing a routine visit with a patient is 0.45, as mentioned in Section 3.2.3 to be taken from data given in [75], and is referred to as *hcw-compliance*. To assess the impact of improved HCW adherence on transmission and infection, we consider values greater than 0.45, including 0.65, 0.75, 0.85, and 1. Although a compliance of 100% is not the most likely scenario, this extreme case allows us to determine the impact of this particular control intervention. In addition to this more routine HCW compliance, we also consider an increase in compliance when visiting quarantined patients, referred to as *hcw-contact-compliance*. As mentioned in Section 3.2.3, the baseline value for this compliance is 0.6, and we increase it by various amounts up to, and including, 1 to assess the impact of this control strategy.

The third control intervention strategy considers improved environmental decontamination. Different types of cleaning and disinfection strategies will have varying impacts on

the removal of *C. difficile* spores in the environment. Thus, we incorporate a probability of sufficient cleaning into our model with a baseline value of 0.5 [5] that represents the effectiveness of routine cleaning. An increased value of this probability indicates the implementation of a more stringent and effective cleaning strategy that targets *C. difficile*. For now, we only consider terminal cleaning of rooms after patients are discharged rather than routine daily cleaning of all rooms.

3.4 High-performance computing setup

Because of the stochasticity embedded in ABMs, to best assess the impact of the control intervention strategies, we ran our model for 100 iterations over a one-year simulated time period with each combination of parameter values (representing different control strategies). Since our model is on a 15-minute time-step, this requires simulating the model for over 35,000 ticks, 100 times each, for more than 40 different parameter combinations. It proved to be very ineffective and time-consuming to run these computations on a single machine. A common approach for dealing with such a large number of parameter combinations and high numbers of iterations is to use computing clusters to enable parallelization and speed up execution time. Therefore, we ran all simulations via the computing cluster available at the Advanced Computing Facility (ACF), a high-performance computing facility available for use by students and faculty at the University of Tennessee.

In order to submit jobs to the cluster efficiently, we worked closely with Eduardo Ponce Mojica, a graduate student in the Department of Electrical Engineering and Computer Science, to create a process for submission and for organizing the resulting outputs. The process begins with the BehaviorSpace tool in NetLogo. This built-in NetLogo tool allows us to specify the various parameter combinations we want to simulate and the resulting outputs of interest. We then use the code created by BehaviorSpace to write a setup file. To submit the job to the cluster, we use a PBS file that does the following: (1) specifies the file path for the ABM, NetLogo, and the setup file, (2) calls the specified setup file, (3) specifies a maximum run-time and number of nodes to use, and (4) includes code for calling the Python file that orders and organizes the resulting simulation outputs according

to each parameter combination. For a more thorough description of this method, Mojica has submitted a conference proceedings paper entitled "PaPaS: A Lightweight and Generic Framework for Parallel Parameter Studies" [62] that outlines the details of the process for a general NetLogo ABM to serve as a reference for those interested in doing something similar.

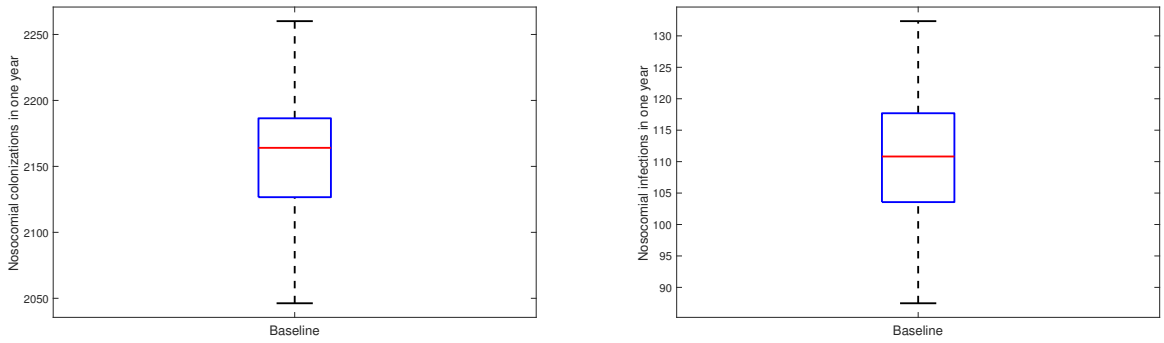
3.5 Results

To assess the impact of the control interventions, we examine the resulting number of nosocomial colonizations and nosocomial infections over a year's time period under each particular control strategy. Because simulations result in varying numbers of total patient admissions per year, we normalize all of the outputs to 10,000 admitted patients per year for comparison. Without this normalization, comparison of colonization and disease incidence can be misleading [5].

3.5.1 Baseline results

The baseline parameter values are given in Table 3.12 of Section 3.7.3, and the resulting numbers of nosocomial colonizations and infections for the 100 iterations of the baseline case are shown in the box plots in Figure 3.6. Note that the median values of nosocomial colonizations and infections for the 100 iterations are indicated by the red lines, and each box (outlined in blue) represents the inter-quartile range, which includes the middle 50% of output values. Specifically, the median number of nosocomial colonizations per year at baseline, normalized to 10,000 admissions, was 2,161, and the median number of nosocomial infections per year normalized to 10,000 was 111. Our numbers of nosocomial colonizations per year are significantly lower than the numbers obtained in [5]; we adjusted select parameters purposely (details in Section 3.8.13) so that our numbers of nosocomial colonizations matched updated data indicating that nosocomial colonization incidence affects 20% of admitted patients [11, 40].

To obtain a better understanding of the types of patients becoming colonized and/or diseased while hospitalized, we split up the total nosocomial colonizations and infections according to each patient's disease status at admission, with the results shown in Figure

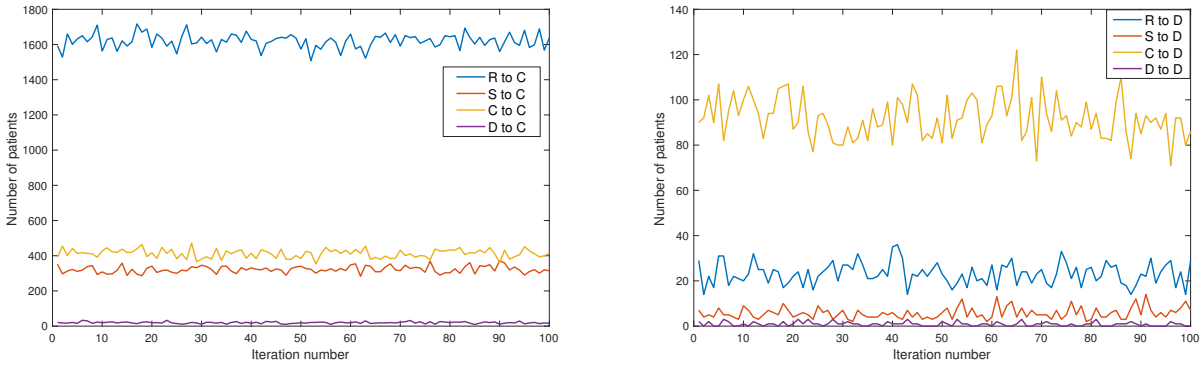


(a) Baseline nosocomial colonizations

(b) Baseline nosocomial infections

Figure 3.6: Baseline parameter values: Number of (a) nosocomial colonizations and (b) nosocomial infections by *C. difficile*, normalized to 10,000 admissions, for 100 iterations over a one-year time period with baseline parameter values

3.7. Figure 3.7a indicates that the majority of nosocomial colonizations are coming from those who were resistant at admission while Figure 3.7b illustrates that the majority of nosocomial infections come from those who are admitted colonized. The high number of resistant patients becoming colonized while in the hospital is likely a result of the fact that there is a 75% chance of patients being admitted resistant, so the number of resistant patients hospitalized is much higher than that of any other disease status. In fact, only approximately 19.64% of the total number of admitted resistant patients become colonized (Table 3.3). Still, the higher number of nosocomial colonizations coming from resistant patients suggests that restricting antibiotic prescriptions in a way that keeps resistant patients from becoming susceptible will be an important control strategy. Table 3.3 also indicates that the percentage of admitted susceptible patients who become colonized is the highest of any admission class (though not by a significant amount). This suggests that controlling the amount of *C. difficile* in the environment and reducing possible exposure pathways will be an important control strategy. Table 3.4 indicates that the largest percentage of admitted patients who will contract CDI are those who are colonized upon admission.



(a) Nosocomial colonizations

(b) Nosocomial infections

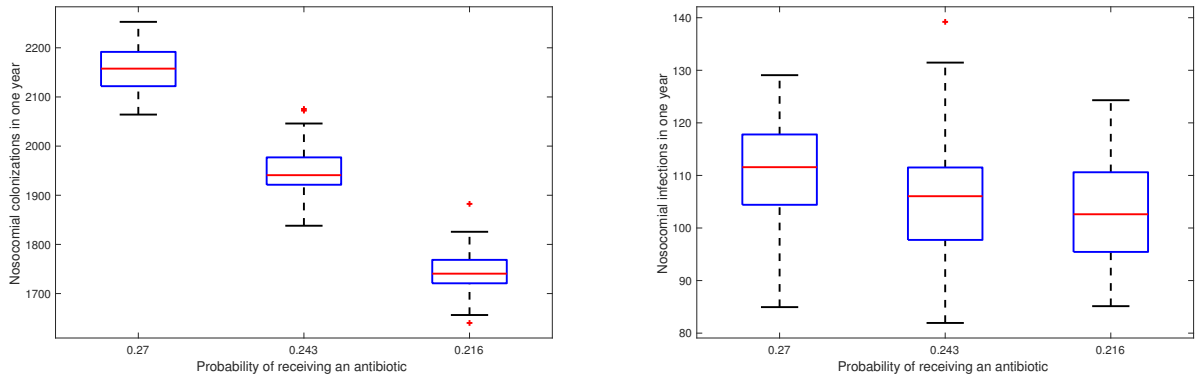
Figure 3.7: Breakdown of (a) nosocomial colonizations and (b) nosocomial infections based on disease status at admission for 100 iterations over a one-year time period with baseline parameter values

Table 3.3: Median percentage of patients admitted in each class who eventually become colonized during their hospital stay out of 100 iterations

Admitted resistant who become colonized	19.64%
Admitted susceptible who become colonized	32.87%
Admitted colonized who clear colonization but then eventually return to colonized	25.07%
Admitted diseased who return to susceptible and then become colonized again	17.37%

Table 3.4: Median percentage of patients admitted in each class who eventually become diseased during their hospital stay out of 100 iterations

Admitted resistant who become diseased	$< 1\%$
Admitted susceptible who become diseased	$< 1\%$
Admitted colonized who become diseased	5.56%
Admitted diseased who return to susceptible and then experience recurrence	$< 1\%$



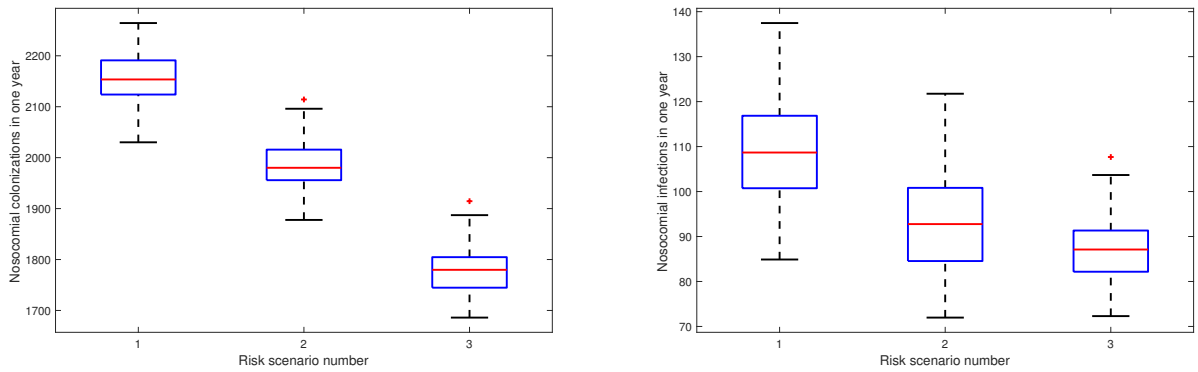
(a) Nosocomial colonizations **(b)** Nosocomial infections

Figure 3.8: Reducing the half-daily probability of receiving an antibiotic: Resulting number of (a) nosocomial colonizations and (b) nosocomial infections for baseline probability of receiving an antibiotic ($p = 0.27$) and for the the reduced probabilities of receiving an antibiotic (10% reduction and 20% reduction) described in Table 3.1, normalized to 10,000 admissions, for 100 iterations over a one-year time period

3.5.2 Single control interventions

We begin our assessment of control interventions by weighing the impact of each control strategy implemented on its own on the numbers of nosocomial colonizations and infections. In Section 3.3, we described two types of antimicrobial stewardship, and we consider these first. Figure 3.8 illustrates the impact of reducing the overall number of antibiotics prescribed, and Figure 3.9 shows the effect of reducing the proportions of very high-risk and high-risk antibiotics with respect to CDI, according to the risk scenarios described in Table 3.2. In each graph, the first box plot corresponds to the baseline scenario for comparison. Both of these antimicrobial stewardship strategies have a notable impact on reducing the nosocomial colonizations (Figures 3.8a, 3.9a), and we see that reducing the proportions of high-risk and very high-risk antibiotics has more of an impact on decreasing the nosocomial infections (Figure 3.9b) than reducing the half-daily probability of receiving an antibiotic has on reducing nosocomial infections (Figure 3.8b).

The next control strategy we implement is more effective terminal ward room cleaning. Figure 3.10a indicates that this particular strategy is not as impactful as the antimicrobial stewardship strategies at reducing nosocomial colonizations, even if 100% effective cleaning



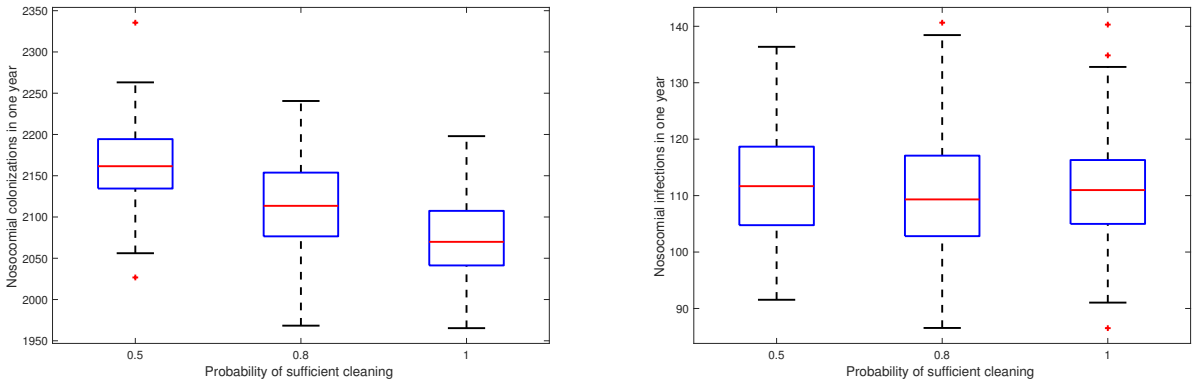
(a) Nosocomial colonizations

(b) Nosocomial infections

Figure 3.9: Reducing the proportion of very high-risk and high-risk antibiotics: Resulting number of (a) nosocomial colonizations and (b) nosocomial infections for each risk scenario (specifying proportions of low-risk, high-risk, and very high-risk antibiotics) described in Table 3.2, where Risk Scenario 1 is baseline, normalized to 10,000 admissions, for 100 iterations over a one-year time period

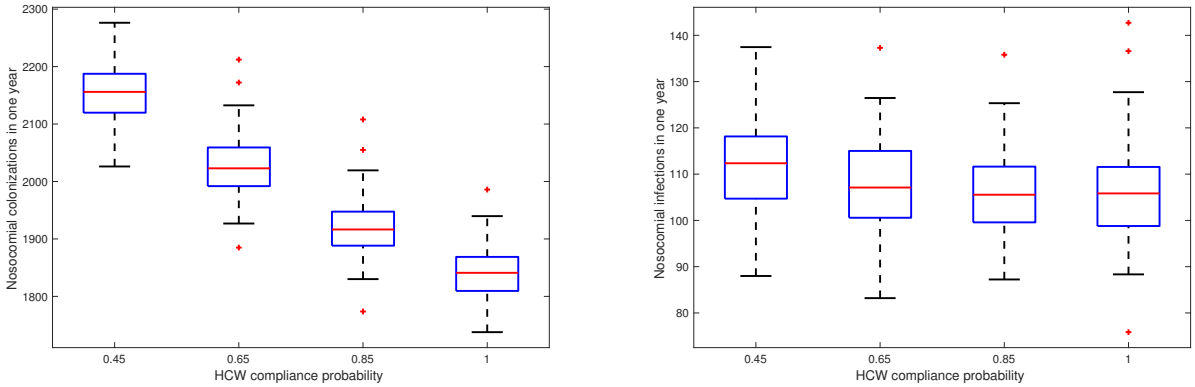
is maintained. This result is similar to the conclusions made by Bintz et al. [5]. Additionally, more effective cleaning has little impact on nosocomial infections (Figure 3.10b).

Another form of environmental decontamination is achieved by improved HCW adherence to the best hand-hygiene and contact protocol. Figure 3.11a shows that increased HCW compliance with all patients is more impactful on nosocomial colonizations than improved room cleaning is; however, this general improved HCW compliance does not have a notable impact on reducing nosocomial infections (Figure 3.11b). The results of improved HCW compliance with quarantined patients is shown separately in Figure 3.12a. If HCWs achieve 100% compliance with quarantined patients, there is an extremely noticeable decrease in nosocomial colonizations. Such a vast decrease is likely due to our model structure: if HCWs are compliant with quarantined patients, there is a 0% chance of pathogen transfer from HCW to room, or vice versa. This assumes that when fully compliant, HCWs will wear gloves and strictly follow contact protocol so that there is no chance of exposure or transfer, which is more likely to happen when HCWs know a patient is isolated due to symptomatic CDI. This control strategy also results in a nice reduction of nosocomial infections (Figure 3.12b).



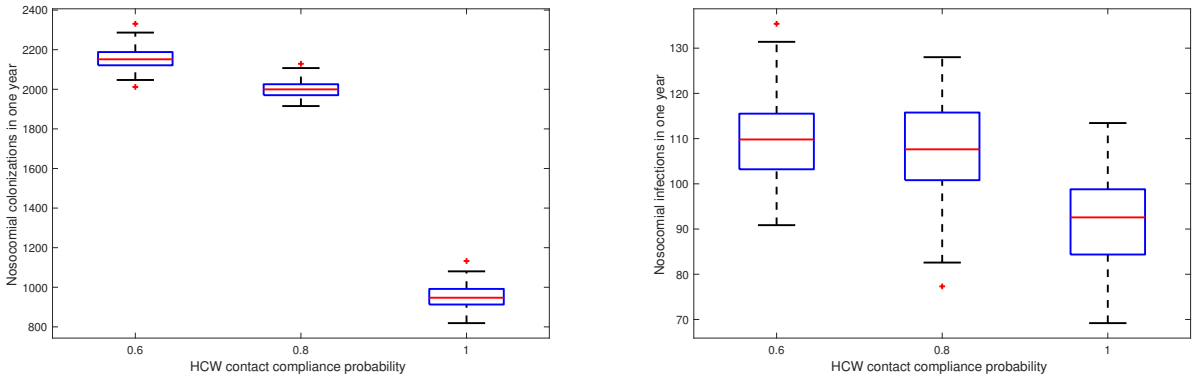
(a) Nosocomial colonizations **(b)** Nosocomial infections

Figure 3.10: Increasing the probability of sufficiently cleaning ward rooms: Resulting number of (a) nosocomial colonizations and (b) nosocomial infections for increased probabilities of sufficiently cleaning ward rooms, where 0.5 is baseline, normalized to 10,000 admissions, for 100 iterations over a one-year time period



(a) Nosocomial colonizations **(b)** Nosocomial infections

Figure 3.11: Increasing HCW compliance with all patients: Resulting number of (a) nosocomial colonizations and (b) nosocomial infections for increased probabilities of HCWs sufficiently cleaning their hands after visiting patients, where 0.45 is baseline, normalized to 10,000 admissions, for 100 iterations over a one-year time period



(a) Nosocomial colonizations **(b)** Nosocomial infections

Figure 3.12: Increasing HCW contact compliance with quarantined patients: Resulting number of (a) nosocomial colonizations and (b) nosocomial infections for increased probabilities of HCW contact compliance when visiting quarantined patients, where 0.6 is baseline, normalized to 10,000 admissions, for 100 iterations over a one-year time period

For easier comparison of individual control strategies, Table 3.5 gives the median numbers of nosocomial colonizations and infections for the most extreme cases of each of the individual strategies. We see that reducing the proportions of very high-risk and high-risk antibiotics is the most effective strategy at reducing nosocomial infections while increasing HCW contact compliance with quarantined patients has the largest impact on reducing nosocomial colonizations. However, there is not one strategy that is best at reducing both nosocomial colonizations and nosocomial infections simultaneously. It is essential for hospital policy to not only consider how to effectively reduce infection incidence, but also colonization incidence since these colonized individuals may develop CDI after leaving the hospital [5]. Discharging colonized patients may will inevitably result in a subsequent increase in the admission of diseased patients to healthcare facilities [5, 65] and to the amount of *C. difficile* in the environment. Therefore, we next to compare the impact of various combinations of these control strategies on both nosocomial colonizations and nosocomial infections.

3.5.3 Combination strategies

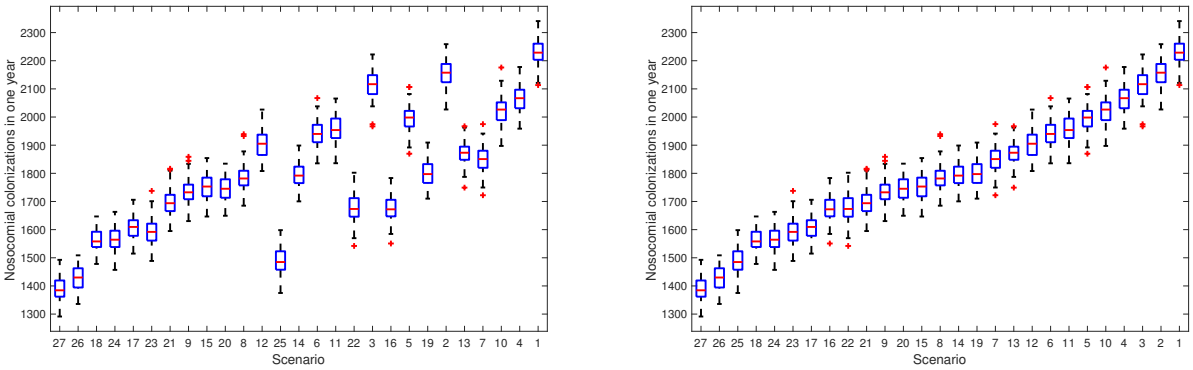
We begin this section by considering various combinations of antimicrobial stewardship and improved cleaning. Initially considering the same scenarios as Bintz et al. [5] allows us to

Table 3.5: Median numbers of nosocomial colonizations and nosocomial infections per year for 100 iterations, normalized to 10,000 admissions, for the individual control scenarios listed

	Median nosocomial colonizations	Median nosocomial infections
Baseline	2,161	111
Reduce antibs by 20%	1,740	103
Risk scenario 3	1,776	86
100% probability of effective cleaning	2,077	112
100% HCW compliance	1,843	106
100% HCW contact compliance (with quarantined patients)	952	93

compare our results to theirs and assess the impact of the modifications and extensions we made to their ABM, such as the explicit inclusion of HCWs as agents. The combinations of antimicrobial stewardship and cleaning considered were taken from [5] and are listed and numbered in Table 3.6. Figure 3.13a displays the resulting median numbers of nosocomial colonizations with the 27 strategies ordered in the way [5] determined most effective at reducing colonizations while Figure 3.13b ranks the 27 control strategies according to increasing median numbers of nosocomial colonizations resulting from our model. It is immediately noticeable that, with our model, many of these strategies have a different impact on nosocomial colonizations than they did on the resulting colonizations in [5].

First, note that the baseline scenario is indicated by Strategy 2. Comparison of Figures 3.13a and 3.13b shows that cleaning has less impact on nosocomial colonizations in our model than it did using the model in [5]. We see that for our model there is only one scenario (Strategy 1) worse than baseline at reducing nosocomial colonizations, compared to five scenarios in [5] that were worse than baseline. In both cases, the strategies worse than baseline all had less effective cleaning (specifically, a probability of effective cleaning set to 0.2). This insensitivity of less effective cleaning on nosocomial colonizations in our ABM is further illustrated by the fact that the best-ranked strategies for our model are 27, 26, and 25, which have varying levels of effective cleaning. The higher ranking of Scenario 25 for our model, even with its lower probability of effective cleaning, shows that antimicrobial stewardship is more impactful than cleaning. With the addition of HCWs, we were able



(a) Nosocomial colonizations **(b)** Nosocomial colonizations

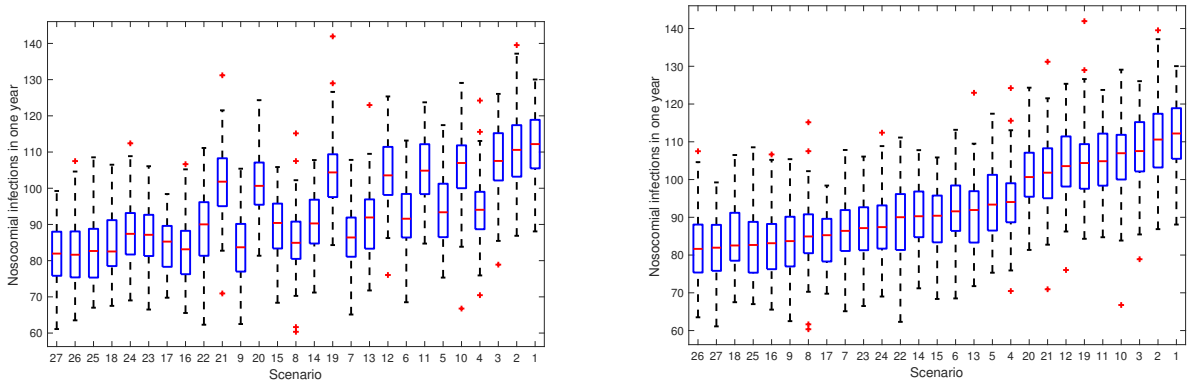
Figure 3.13: Combination strategies involving antimicrobial stewardship and ward room cleaning: Resulting number of nosocomial colonizations for each of the 27 strategies listed in Table 3.6 that incorporate both antimicrobial stewardship and ward room cleaning as control interventions, normalized to 10,000 admissions, for 100 iterations over a one-year time period, where the x-axis gives the strategies listed in order from the most effective strategy to the least effective strategy for reducing nosocomial colonizations (a) based on conclusions from Bintz et al.'s model [5] and (b) based on the results from our model

to consider room-level contamination, rather than ward-level contamination (as used in [5]), when determining the probability of patients becoming colonized due to *C. difficile* exposure. Thus, the cleanliness of the whole ward affected a patient's likelihood of becoming colonized in [5], so more effective cleaning could affect a larger number of patients' probabilities of colonization. Despite these model differences, we still come to the same conclusion as [5] with respect to this combination of control strategies: even in the event of less sufficient ward room cleaning, antimicrobial stewardship is noticeably effective at reducing nosocomial colonizations.

The numbers of nosocomial infections resulting from the 27 combination control strategies listed in Table 3.6, ordered the same way as those in Figure 3.13b (based on resulting median numbers of nosocomial colonizations), are illustrated in Figure 3.14a. For comparison, Figure 3.14b also illustrates the numbers of nosocomial infections for the 27 strategies, but they are ordered according to increasing median number of nosocomial infections. From these figures, we can conclude that Strategies 26 and 27 are the best two strategies for reducing both the nosocomial colonizations and infections simultaneously while Strategies 1 and 2 (baseline) are the worst for both.

Table 3.6: Antimicrobial stewardship and ward room cleaning combination strategies numbered for easy reference, where the specific distributions of antibiotic-risk-level probabilities for each risk scenario are given in Table 3.2

Combination number	Half-daily antibiotic probability	Risk scenario	Probability of sufficient cleaning
1	0.27	1	0.2
2	0.27	1	0.5
3	0.27	1	0.8
4	0.27	2	0.2
5	0.27	2	0.5
6	0.27	2	0.8
7	0.27	3	0.2
8	0.27	3	0.5
9	0.27	3	0.8
10	0.243	1	0.2
11	0.243	1	0.5
12	0.243	1	0.8
13	0.243	2	0.2
14	0.243	2	0.5
15	0.243	2	0.8
16	0.243	3	0.2
17	0.243	3	0.5
18	0.243	3	0.8
19	0.216	1	0.2
20	0.216	1	0.5
21	0.216	1	0.8
22	0.216	2	0.2
23	0.216	2	0.5
24	0.216	2	0.8
25	0.216	3	0.2
26	0.216	3	0.5
27	0.216	3	0.8



(a) Nosocomial infections

(b) Nosocomial infections

Figure 3.14: Combination strategies involving antimicrobial stewardship and ward room cleaning: Resulting number of nosocomial infections for each of the 27 strategies listed in Table 3.6 that incorporate both antimicrobial stewardship and ward room cleaning as control interventions, normalized to 10,000 admissions, for 100 iterations over a one-year time period, where the x-axis gives the strategies listed (a) in order of increasing resulting median number of nosocomial colonizations determined in Figure 3.13b and (b) in order of increasing resulting median number of nosocomial infections

Next, we consider the addition of improved HCW compliance to the current combinations of antimicrobial stewardship with improved cleaning. To keep the number of parameter combinations under control, we select 5 of the 27 strategies listed in Table 3.6 to be representative of their varying effects on nosocomial colonizations and infections. To these 5 strategies (Strategies 6, 15, 18, 22, and 25), we incorporate improved HCW compliance. We consider three values for HCW compliance with non-quarantined patients: 0.45 (baseline), 0.75, and 1, and we consider two values for HCW contact compliance with quarantined patients: 0.6 (baseline) and 1. The resulting 15 parameter combinations considered are listed and numbered in Table 3.7. We will consider these 15 combinations first with baseline HCW contact compliance with quarantined patients and then all 15 combinations again with the increased HCW contact compliance. The results for these 15 combinations with baseline HCW contact compliance are shown in Figure 3.15a and those with 100% contact compliance with quarantined patients are illustrated in Figure 3.15b. Similar plots are given for the resulting number of nosocomial infections (Figures 3.16a and 3.16b).

Figure 3.15a shows that scenarios 25.2, 18.2, and 18.1 are most effective at reducing

nosocomial colonizations. These four scenarios implemented Risk Scenario 3 (Table 3.2), which accounts for the most extreme reductions in high-risk and very high-risk antibiotics. The next two best scenarios, 22.2 and 15.2, surpassed Scenarios 25.0 and 18.0 (that implement Risk Scenario 3 but only consider baseline HCW compliance) in their effectiveness at reducing nosocomial colonizations. This is one example of many observations we made that often a more extreme version of one control (such as HCW compliance) can compensate for a less extreme version of another (such as a smaller reduction in the overall antibiotic probability). We do not, however, see this same trend when HCW contact compliance with quarantined patients is increased to 100% (Figure 3.15b). In this case, Scenario 25 is always better than the remaining 4 strategies for all values of general HCW compliance. This is expected since increasing HCW contact compliance with quarantined patients leads to less overall pathogen transfer between HCWs and rooms, so nosocomial colonizations are no longer as sensitive to changes in general HCW compliance.

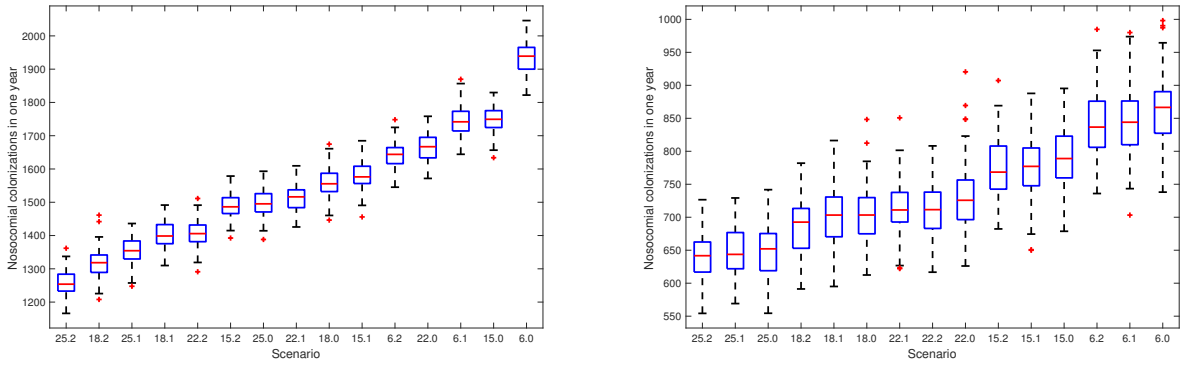
The resulting ranking of control scenarios for nosocomial infections matches what we discovered when running the control scenarios individually. In particular, we saw that Risk Scenario 3 was the most effective at reducing nosocomial infections, and we see in Figures 3.16a and 3.16b that all of the strategies from Table 3.7 with Risk Scenario 3 (18.0, 18.1, 18.2, 25.0, 25.1, 25.2) were the most effective at reducing nosocomial infections, regardless of the values of other parameters.

3.5.4 Vaccination

The control scenarios and combinations of controls considered so far were all more impactful on reducing the number of nosocomial colonizations than on reducing the number of nosocomial infections. They all targeted the reduction of *C. difficile* in the environment and the reduction of patients' susceptibility to colonization more intensely than the prevention of progression from colonized to diseased. Because there has been an increase in the percentage of patients admitted already colonized by *C. difficile*, many colonized patients will not be affected by the control scenarios we have considered. Therefore, considering a control scenario that will inhibit a patient's transition from colonized to diseased, such as a toxoid vaccine, would be a beneficial addition to the other controls considered.

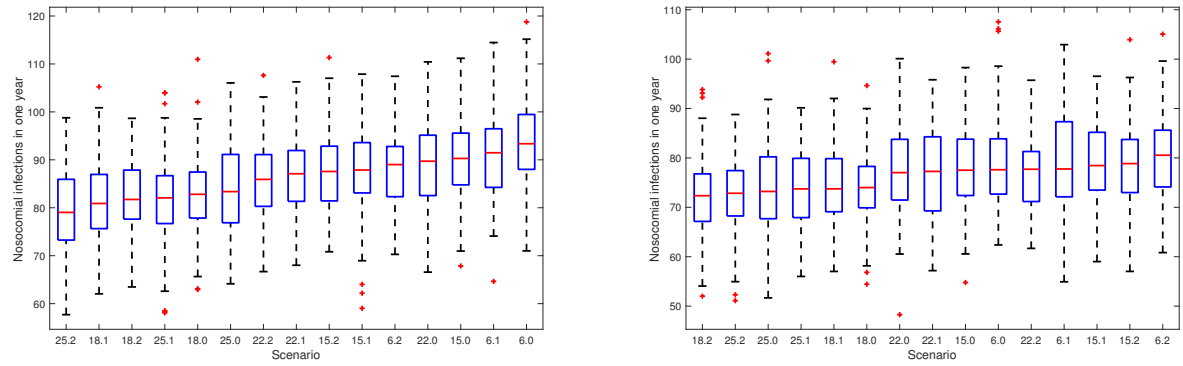
Table 3.7: Parameter combinations representing control interventions with increased HCW compliance (where 0.45 is baseline) combined with select combinations of antimicrobial stewardship and ward room cleaning (Scenarios 6, 15, 18, 22, and 25 from Table 3.6)

Combination number	Half-daily antibiotic probability	Risk scenario	Probability of sufficient cleaning	HCW compliance (all patients)
6.0	0.27	2	0.8	0.45
6.1	0.27	2	0.8	0.75
6.2	0.27	2	0.8	1
15.0	0.243	2	0.8	0.45
15.1	0.243	2	0.8	0.75
15.2	0.243	2	0.8	1
18.0	0.243	3	0.8	0.45
18.1	0.243	3	0.8	0.75
18.2	0.243	3	0.8	1
22.0	0.216	2	0.2	0.45
22.1	0.216	2	0.2	0.75
22.2	0.216	2	0.2	1
25.0	0.216	3	0.2	0.45
25.1	0.216	3	0.2	0.75
25.2	0.216	3	0.2	1



(a) HCW contact compliance = 0.6 **(b)** HCW contact compliance = 1

Figure 3.15: Combination strategies involving antimicrobial stewardship, ward room cleaning, and HCW compliance: Resulting number of nosocomial colonizations for each of the 15 strategies listed in Table 3.7 that incorporate antimicrobial stewardship, ward room cleaning, and HCW compliance as control interventions, normalized to 10,000 admissions, for 100 iterations over a one-year time period, where the x-axis (a) corresponds to the strategies in Table 3.7 with HCW contact compliance with quarantined patients equal to 0.6 and (b) corresponds to the strategies in Table 3.7 with HCW contact compliance with quarantined patients equal to 1



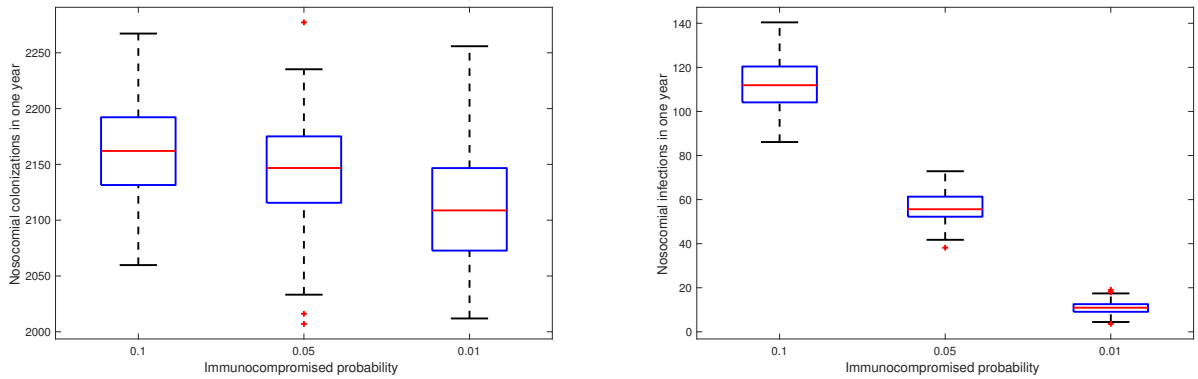
(a) HCW contact compliance = 0.6 **(b)** HCW contact compliance = 1

Figure 3.16: Combination strategies involving antimicrobial stewardship, ward room cleaning, and HCW compliance: Resulting number of nosocomial infections for each of the 15 strategies listed in Table 3.7 that incorporate antimicrobial stewardship, ward room cleaning, and HCW compliance as control interventions, normalized to 10,000 admissions, for 100 iterations over a one-year time period, where the x-axis (a) corresponds to the strategies in Table 3.7 with HCW contact compliance with quarantined patients equal to 0.6 and (b) corresponds to the strategies in Table 3.7 with HCW contact compliance with quarantined patients equal to 1

The *C. difficile* vaccine currently being tested is a toxoid vaccine, meaning that it will only fight against clinical infection and will not protect against colonization by *C. difficile*. Therefore, an effective version of this vaccine would result in a decrease in the proportion of immunocompromised patients. We perform a preliminary assessment of vaccination by making the strong assumption that a vaccination program has been successfully implemented in the hospital for a period of time such that it has already resulted in an overall reduction in the percentage of immunocompromised patients. To simulate this, we decrease the baseline value for the probability of a patient being immunocompromised from 10%, used by Bintz et al. [5], down to values such as 5% or 1%. Note that this a simplified implementation of vaccination because it relies on the major assumptions that all patients at risk will be vaccinated and will be vaccinated effectively. Our future work will involve the addition of a vaccinated disease class, a probability of patients being vaccinated, and a vaccine efficacy probability to more thoroughly assess the impact of vaccination as a control strategy.

We begin by implementing vaccination individually with no other controls. As expected, since vaccination does not prevent colonization, it has a large impact on the nosocomial infections (Figure 3.17b) and a minimal impact on the nosocomial colonizations (Figure 3.17a). To avoid an excessive number of parameter combinations, we selected 8 scenarios from Table 3.7 (6.1, 6.2, 18.1, 18.2, 22.1, 22.2, 25.1, and 25.2) to which we added vaccination. The resulting combinations are numbered and labeled in Table 3.8. Figure 3.18 shows the resulting number of nosocomial colonizations for each of the control combinations in Table 3.8.

We observed that vaccination in combination with other control techniques did not change the effectiveness of those scenarios at reducing colonizations in the absence of vaccination (Figure 3.18b). That is, the same scenarios we found to be most effective at reducing nosocomial colonizations in the absence of vaccination were still the most effective once vaccination was added. Furthermore, vaccination in combination with other control techniques had a similar impact on reducing nosocomial infections as it did when implemented in the absence of additional controls, as illustrated by Figure 3.19. Thus, if a healthcare facility is able to implement a vaccination program that would lead to a reduction in the probability of patients being immunocompromised to 5% or 1%, then they



(a) Nosocomial colonizations

(b) Nosocomial infections

Figure 3.17: Reducing probability of being immunocompromised as a form of effective vaccination: Resulting number of (a) nosocomial colonizations and (b) nosocomial infections for decreasing probabilities of being immunocompromised, where 0.10 is baseline, normalized to 10,000 admissions, for 100 iterations over a one-year time period

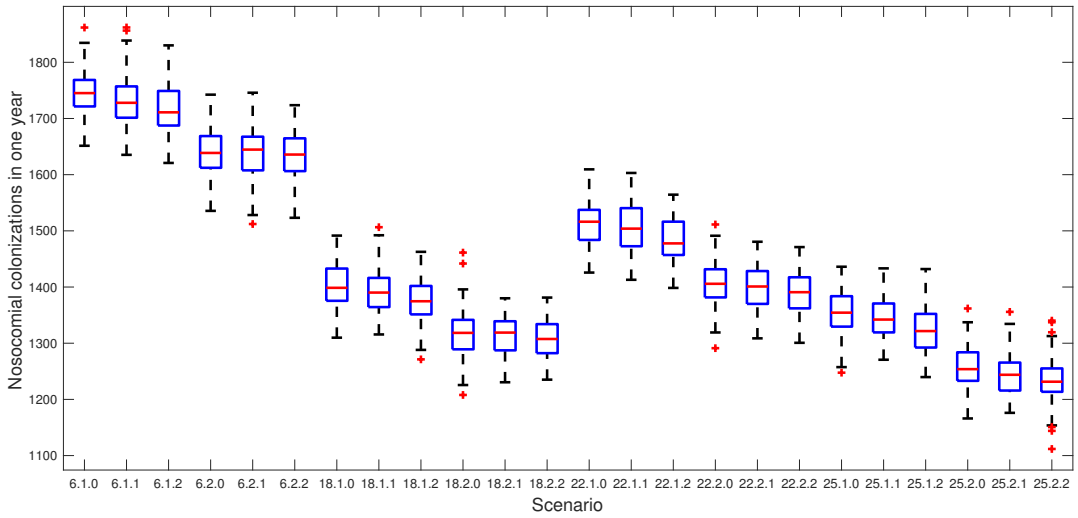
would experience a significant decrease in the number of nosocomial infections but not a notable change in nosocomial colonizations.

3.6 Discussion

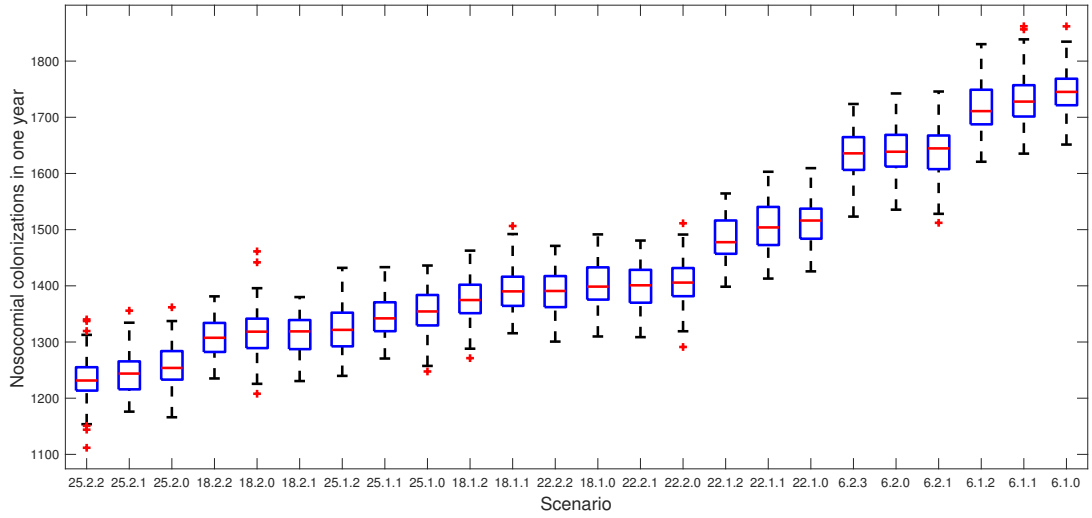
Because *C. difficile* can survive on environmental surfaces for extended time periods [28], there is benefit to incorporating environmental transmission when modeling its spread in healthcare facilities. To consider the roles of contaminated environments and of both symptomatic and asymptomatic carriers as *C. difficile* reservoirs, we developed an ABM (a modification and extension of the ABM in [5]) that explicitly incorporates HCWs as vectors of transmission, tracks individual patient antibiotic histories, incorporates varying risk levels of antibiotics with respect to CDI, and tracks contamination of ward rooms by *C. difficile*. We use this ABM to simulate and evaluate the impact of different control strategies on the resulting numbers of nosocomial colonizations and infections by *C. difficile*. The control strategies considered included two forms of antimicrobial stewardship (overall reduction in antibiotics and a reduction of specifically high-risk and very-risk antibiotics), increased environmental decontamination through room cleaning, improved HCW compliance with quarantined and non-quarantined patients, and a preliminary assessment of vaccination. To

Table 3.8: Parameter combinations representing control interventions with decreased probability of being immunocompromised (where 0.10 is baseline), combined with select combinations of improved HCW compliance, antimicrobial stewardship, and ward room cleaning (Scenarios 6.1, 6.2, 18.1, 18.2, 22.1, 22.2, 25.1, and 25.2 from Table 3.7)

Combination number	Half-daily antibiotic probability	Risk scenario	Probability of sufficient cleaning	HCW compliance	Probability of being immuno-compromised
6.1.0	0.27	2	0.8	0.75	0.10
6.1.1	0.27	2	0.8	0.75	0.05
6.1.2	0.27	2	0.8	0.75	0.01
6.2.0	0.27	2	0.8	1	0.10
6.2.1	0.27	2	0.8	1	0.05
6.2.2	0.27	2	0.8	1	0.01
18.1.0	0.243	3	0.8	0.75	0.10
18.1.1	0.243	3	0.8	0.75	0.05
18.1.2	0.243	3	0.8	0.75	0.01
18.2.0	0.243	3	0.8	1	0.10
18.2.1	0.243	3	0.8	1	0.05
18.2.2	0.243	3	0.8	1	0.01
22.1.0	0.216	2	0.2	0.75	0.10
22.1.1	0.216	2	0.2	0.75	0.05
22.1.2	0.216	2	0.2	0.75	0.01
22.2.0	0.216	2	0.2	1	0.10
22.2.1	0.216	2	0.2	1	0.05
22.2.2	0.216	2	0.2	1	0.01
25.1.0	0.216	3	0.2	0.75	0.10
25.1.1	0.216	3	0.2	0.75	0.05
25.1.2	0.216	3	0.2	0.75	0.01
25.2.0	0.216	3	0.2	1	0.10
25.2.1	0.216	3	0.2	1	0.05
25.2.2	0.216	3	0.2	1	0.01



(a) Nosocomial colonizations with scenarios in the order listed in Table 3.8



(b) Nosocomial colonizations with scenarios ordered according to increasing number of colonizations

Figure 3.18: Combination strategies involving antimicrobial stewardship, ward room cleaning, HCW compliance, and vaccination: Resulting number of nosocomial colonizations for each of the 24 strategies listed in Table 3.8 that incorporate antimicrobial stewardship, ward room cleaning, HCW compliance, and vaccination as control interventions, normalized to 10,000 admissions, for 100 iterations over a one-year time period, where the x-axis (a) lists the scenarios in the order presented in Table 3.8 and (b) lists the scenarios according to increasing number of colonizations

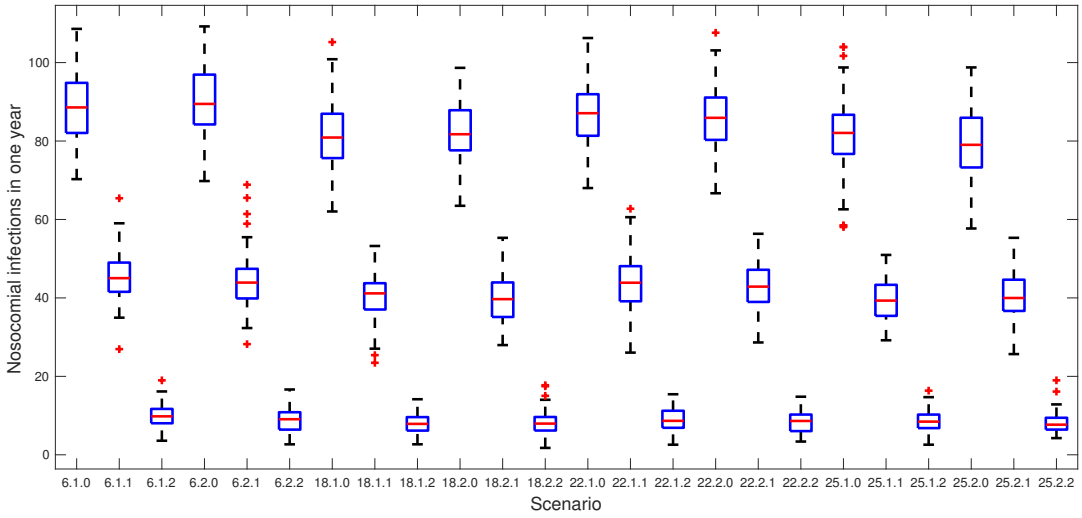


Figure 3.19: Combination strategies involving antimicrobial stewardship, ward room cleaning, HCW compliance, and vaccination: Resulting number of nosocomial infections for each of the 24 strategies listed in Table 3.8 that incorporate antimicrobial stewardship, ward room cleaning, HCW compliance, and vaccination as control interventions, normalized to 10,000 admissions, for 100 iterations over a one-year time period, where the x-axis lists the scenarios in the order presented in Table 3.8

improve HCW compliance, a hospital would need to bring in additional HCWs due to the time needed to adequately sanitize. Although our model does not explicitly account for the time HCWs spend adequately washing, this is something that could be further explored in future work.

We illustrated the efficacy of each of the control interventions individually and in various combinations on reducing the numbers of nosocomial colonizations and infections in order to determine where control efforts should be concentrated. It is important for hospitals to implement strategies that are effective at decreasing incidence of both infection and colonization by *C. difficile* [5]. However, in our modeling study, we demonstrated that there was no single strategy that was best at reducing nosocomial colonizations and nosocomial infections simultaneously. In particular, improved cleaning did not have a significant impact on either while improved HCW compliance with all patients proved to be effective at reducing colonizations but was not impactful on reducing nosocomial infections. Both forms of antimicrobial stewardship were shown to be effective at decreasing colonizations, and

both had a more notable impact on reducing nosocomial infections than did cleaning or improved HCW compliance (with all patients and specifically with quarantined patients). Increased HCW compliance with quarantined patients was more notable in its impacts on both nosocomial colonizations and infections than increased HCW general compliance. Overall, targeted reduction of high-risk and very high-risk antibiotics with respect to CDI was the most effective strategy at reducing nosocomial infections, and increased HCW compliance with quarantined patients was most effective at reducing nosocomial colonizations.

Additionally, we determined that when the control strategies are combined in various ways, a more extreme version of one control could often compensate for a less extreme version of another to effectively reduce nosocomial colonizations. We also determined that the resulting impact of the control scenarios on nosocomial colonizations and infections were not completely additive. In particular, the reduction in nosocomial colonizations (or infections) made by a particular combination strategy was not equal to the sum of the reduction made by the strategies individually.

Because an increased number of patients are coming into hospitals already colonized, we considered an additional control strategy that would prevent these patients from progressing to diseased. In particular, we performed a preliminary evaluation of vaccination in order to assess how a vaccine would impact the resulting colonizations and infections in a hospital both on its own and in combination with other control strategies. As expected, vaccination had a large impact on disease incidence with little impact on nosocomial colonizations since the *C. difficile* toxoid vaccine does not prevent colonization, but only subsequent infection. This preliminary assessment of vaccination comes with strong assumptions and is considered the best case scenario. Results such as these may help hospitals determine what kind of vaccination strategy would be necessary to achieve the desired results and the implementation feasibility of such a strategy. In the future, we would like to expand our preliminary assessment of vaccination by including vaccine efficacy at the individual patient level and a protocol efficacy to more thoroughly evaluate the impact of vaccination as a control measure.

3.7 ODD Protocol: Overview

In this section, we describe the Overview, Design concepts, and Details (ODD) of our agent-based model to provide a more complete and rigorous model description. ODD was designed by experienced modelers to create a complete, quick, and exhaustive method for describing agent-based models for the purpose of standardization and replication [72].

3.7.1 Purpose

We modified and expanded the agent-based model in [5], which simulates the transmission of *C. difficile* in a healthcare setting. In particular, we explicitly incorporated healthcare workers as vectors of transmission and then evaluated the following: (1) the efficacy of control measures such as antimicrobial and environmental stewardship and (2) the impact of HCWs on the spread of nosocomial CDI.

3.7.2 Input data

The agent behaviors, parameter values, and initial conditions are based on information from either published literature or data collected from six medicines wards at Barnes-Jewish Hospital in St. Louis, Missouri. Information about the collection of this data is described by Lanzas et al. in [45]. We also incorporated updated hospital data that was collected after the publication of [45], such as an increased admission of colonized patients, described by Alasmari et al. [1].

By varying model inputs, we simulated and compared the impact of a variety of control measures on reducing nosocomial colonization and infection. The first such strategy involved varying the probability of effective cleaning. As in the original ABM in [5], we defined effective cleaning to be "cleaning that reduces the contamination level of a ward room." The cleanliness, or lack thereof, of each ward room affects the probability that a patient will become colonized, so increasing the probability of effective cleaning serves as a disease control measure.

Because healthcare workers are the only agents that move from room to room, they are

important vectors of spore transmission, so our second control strategy involved varying healthcare worker (HCW) compliance and HCW contact compliance. HCW compliance is defined as the level of compliance that HCWs adhere to when washing their hands after visiting patients. Our baseline value for HCW compliance was based on the values given by Rubin et al. in [75].We define HCW contact compliance to be the level of compliance that HCWs adhere to after visiting a quarantined patient. Data indicates that HCWs are more compliant with hand-washing and other contact precautions when they know they are visiting an infected patient. We set the baseline value of this variable to be 0.6 to match the data for percentage of adherence to the use of contact precautions in isolation rooms given in [75].

Antimicrobial stewardship was determined in [5] to be another important control measure. One method of implementing antimicrobial stewardship involves reducing the overall number of antibiotics given to patients. We implement this in the same way that Bintz et al. do in [5]: define q to be the proportion by which we want to reduce antibiotic treatments in the hospital. Then, out of all patients who will receive an antibiotic at each time-step, determined by the probability of receiving an antibiotic, only $1-q$ of them will now receive an antibiotic. A second method of antimicrobial stewardship involves altering the relative proportions of antibiotics given. As in [5], we define three risk levels of antibiotics prescribed (low, high, or very high) based on whether they make patients more or less at risk of contracting CDI. The baseline values for the probability of receiving a low-risk, high-risk, or very-high-risk antibiotic (0.4, 0.26, and 0.34, respectively) were taken from the data and are the same as those used in [5]. Control strategies considered involve decreasing the proportion of very-high-risk antibiotics prescribed.

3.7.3 Entities, state variables, and scales

Our ABM has three entities: patients, healthcare workers, and ward rooms. The model was designed to mimic characteristics of Barnes-Jewish Hospital, from where the original data was obtained. As such, we considered a hospital with six medical wards of 35 rooms each, with at most one patient occupying a room at any given time. This allowed for a total possible capacity of 210 patients, and we set the baseline occupancy level to be 0.85. Patient

Table 3.9: Room state variable explanations and values

Room Variable	Description	Possible Value(s)
ward-number	Specifies in which ward the room is located	1, 2, ..., 6
contamination-level	Tracks the amount of contamination in room	$[0, \infty)$
quarantine-patient-here	Specifies whether or not current occupant is under quarantine	yes, no
prob-room-transfer	Gives the probability the room will transfer pathogen to an HCW	$[0, 1]$

state variables are updated on a half-day time scale, which reflects the time-step used in [5]. HCW state variables are updated every 15 minutes to reflect their movement from room to room.

Room State Variables Each ward room is characterized by four state variables, listed in Table 3.9. First, each room is assigned to a specific ward. Next, all rooms have a contamination level that is updated on the 15-minute time-step scale. HCWs can increase the contamination level of a room upon entering, depending on *prob-hcw-transfer*, the probability that an HCW will transfer pathogen to the room, described more in Section 3.8.9. Each half-day symptomatic and asymptomatic patients contribute to the contamination level of a room. Effective cleaning can reduce the contamination level of a room, and cleaning is implemented each half day only after a patient is discharged from that room. The contamination level of an individual room affects the probability that a susceptible patient in that room will become colonized.

The next state variable that governs room characteristics is whether or not a room is occupied by a patient under quarantine. According to [29], symptomatic patients are placed in quarantine to ensure proper contact precautions are implemented. Finally, a room is characterized by the state variable *prob-room-transfer*. This probability is updated each 15-minute time-step and determines the likelihood of an HCW picking up pathogen upon entering that particular room. More information about determining this probability is also described in Section 3.8.9.

Patient State Variables Patient behavior is characterized by many state variables, all of which are listed in Table 3.10. A patient's disease status is tracked beginning at admission. A patient can either be resistant to contracting CDI, susceptible to contracting CDI, colonized by *C. difficile* (asymptomatic), or diseased (symptomatic CDI). Because taking an antibiotic is the strongest risk factor for contracting CDI [48], our assumption is that any patient who has not received an antibiotic is resistant to CDI. In particular, it has been shown that more than 90% of patients of hospitalized patients with CDI recently underwent antimicrobial therapy [19]. Once an antibiotic is given, a patient becomes susceptible to colonization. Depending on a patient's probability of becoming colonized, a susceptible patient who comes into contact with *C. difficile* spores may become colonized and, therefore, become an asymptomatic carrier.

A patient either will or will not be immunocompromised. An immunocompromised patient is a colonized patient who is unable to mount his or her own immune response and, therefore, will contract CDI. Those who are not immunocompromised are able to mount an immune response and will not experience CDI symptoms. Each susceptible and asymptomatically colonized patient has a probability of his or her gut microbiota returning to normal (and therefore regaining resistance). If a colonized patient is not immunocompromised and receives an antibiotic, it is possible to revert to being susceptible; if he or she is immunocompromised and does not receive an antibiotic, it is possible to regain resistance. An immunocompromised colonized patient who receives an antibiotic will contract CDI more quickly than immunocompromised patients who do not receive antibiotics. The movement among disease states are illustrated in Figure 3.2.

Each patient that is admitted is assigned a length of stay based on his or her disease status. Patients' time since admission and time since current disease status are both tracked while, for patients who have received an antibiotic, their time since beginning antibiotics is tracked in addition to the risk level (low, high, or very high) of the antibiotic taken and the number of antibiotics taken. Diseased patients may or may not be identified as diseased upon screening, and their time since a successful screening is tracked. Additionally, diseased patients who are successfully identified may or may not be treated successfully, and their time since beginning treatment is tracked.

Table 3.10: Patient state variable explanations and values

Patient Variable	Description	Possible Value(s)
disease-status	Tracks patient disease status	R, S, C, D
disease-status-at-admission	Identifies patient disease status upon admission	R, S, C, D
length-of-stay	Specifies a patient's length of stay in the hospital (half-days)	[0, 160]
time-since-admission	Tracks amount of time since patient was admitted (half-days)	0, 1, 2, ...
time-since-current-disease-status	Tracks amount of time since patient current disease status began	0, 1, 2, ...
immunocompromised	Indicates whether or not a patient will mount an immune response to colonization	yes, no
treatment-length	Gives prescribed length of current antibiotic treatment (half-days)	14
time-to-normal	Gives time until patient's gut microbiota returns to normal (half-days) low-risk antibiotic high-risk antibiotic very-high-risk antibiotic	 28 28 70
time-since-began-antib	Tracks time since patient began current antibiotic treatment (half-days)	0, 1, 2, ...
prob-regaining-resistance	Gives the probability of regaining resistance to colonization	$[0, 1]$
prob-becoming-colonized	Gives the probability of a susceptible patient becoming colonized	$[0, 1]$
antib-risk-level	Indicates the risk level of the current antibiotic with respect to CDI	low, high, very-high
number-hosp-antibs	Tracks the number of antibiotics a patient has received	0, 1, 2, ...
length-incubation-period	Gives the length of time between colonization and becoming diseased (half-days) low-risk antibiotic high-risk antibiotic very-high-risk antibiotic	 $[20, 60]$ $[14, 40]$ $[8, 20]$
time-until-diseased	Gives the length of time until an immunocompromised, colonized patient becomes diseased (half-days)	$[0, 60]$
will-ID	Indicates whether a screening will correctly test positive for CDI	yes, no
time-since-succ-screen	Tracks the amount of time since patient correctly tested positive for CDI (half-days)	0,1,2...
will-treat-succ	Determines whether a patient will be treated for CDI successfully	yes, no

Healthcare Worker State Variables HCWs are initially assigned a ward, and it is assumed HCWs visit only patients in that same ward for the entirety of their shift. Each HCW is assigned a shift length upon entry to the hospital, and an HCW's time since beginning a shift is tracked. There is a 50% chance an HCW will have an 8-hour shift and a 50% chance an HCW will work a 12-hour shift. Healthcare workers are divided into two types: Type 1 HCWs visit many patients for short periods of time (assumed to be 15 minutes), and Type 2 HCWs visit fewer patients for longer periods of time (assumed to be 45 minutes). Type 1 HCWs move systematically from room to room, meaning that they move to the next closest occupied room at each 15-minute time-step. Type 2 HCWs move randomly from room to room within the same ward. It is assumed there will never be more than one Type 1 HCW or more than one Type 2 HCW in a given room simultaneously; however, there can be a Type 2 and a Type 1 HCW visiting the same patient at the same time. HCWs will never enter rooms not occupied by a patient.

All HCWs have individual contamination levels similar to the contamination levels tracked for each ward room. We refer to HCWs' contamination levels as their *carrier level*, which represents the amount of pathogen on their hands. For simplicity, we assume that all HCWs begin their shifts with carrier levels of zero; however, this could soon need to be increased as data indicates community-associated CDI is increasing [87]. Once in the hospital, HCW carrier levels can be increased upon picking up pathogen in contaminated rooms and can be decreased by adherence to proper hand-washing and contact precaution protocols. Each HCW has a probability of transferring pathogen to a room upon entry, referred to as *prob-hcw-transfer* (Section 3.8.9).

Not only does the time HCWs spend with patients vary, but also the type of task they perform on a patient can affect their probability of picking up *C. difficile* spores. We define three task levels (low risk, medium risk, or high risk) based on the risk of transfer. HCWs can perform any risk level task, but we assume Type 1 HCWs are more likely to perform low-risk tasks while Type 2 HCWs are more likely to perform high-risk tasks. A list of all HCW variable values along with explanations is given in Table 3.11.

Table 3.11: HCW state variable explanations and values

HCW Variable	Description	Possible Value(s)
shift-length	Specifies length of HCW's shift (hours)	8, 12
time-since-shift-began	Tracks the time since an HCW began a shift (hours)	$[0, 12]$
carrier-level	Tracks amount of contamination on an HCW's hands	$[0, \infty)$
hcw-type	Indicates whether an HCW will be Type 1 or Type 2	Type 1, Type 2
hcw-risk	Indicates the risk level of the task an HCW is performing	low, medium, high
prob-hcw-transfer	Gives the probability an HCW will transfer pathogen to a room	$[0, 1]$

Global State Variables A summary description of all global variables is given in Table 3.12. Admission proportions for each disease status (a_r, a_s, a_c, and a_d) are global variables based on the Barnes-Jewish Hospital data detailed in [45] with modifications made based on the updated data in [1]. This new data indicated that 15% of admitted patients were colonized upon arrival, so we updated a_c and thereby decreased a_s to reflect this. Thus, we set the probability of a patient being colonized upon admission to 0.15, the probability of a patient being susceptible upon admission to 0.09, the probability of a patient being resistant upon admission to 0.75, and the probability of a patient having CDI upon admission to 0.01.

The probability of an HCW complying with proper hand-washing and contact precaution protocol after leaving a room has a baseline value of 0.45. In particular, we averaged the percentage of hand-hygiene adherence for nurses and doctors in non-isolated rooms given in [75]. The probability an HCW who has just visited a quarantined patient will follow proper protocol is set slightly higher to 0.6 to match the percentage of adherence to the use of contact precautions in isolation rooms given in [75]. The percentage of total contamination that an HCW will transfer to a room after determining transfer will occur is a global variable set to 90% while the percentage of pathogen a room will transfer to an HCW is set to 10%. Assessments of hospital cleaning practices have shown that routine cleaning results in decontamination of no more than 56% of targeted surfaces [28]. If a room is effectively cleaned, we set the contamination level to be reduced by 50%.

The probability of susceptible patients becoming colonized depends on both the contamination level of their room and the risk level of their current antibiotic. Similar to antibiotic risks, room contamination levels are divided into three groups (low, medium, or high contamination). Rooms with contamination levels between 0 and 0.4 are considered low contamination while rooms with contamination levels between 0.4 and 0.8 are considered to have medium contamination. Any rooms with contamination levels higher than 0.8 are considered highly contaminated. Each probability of becoming colonized is denoted with a subscript referring to the antibiotic-risk level and a superscript referring to the room-contamination level. For example, p_l^h is the probability a patient on a low-risk antibiotic becomes colonized in a highly contaminated room. Probabilities for each combination of antibiotic-risk level and room-contamination level are denoted in a similar way. Values for each of these probabilities and for the room-contamination cut-off levels were chosen so that nosocomial colonizations accounted for 20% of admissions [11, 40]. More details about these calculations are given in Section 3.8.13.

All global variables described in the remainder of this section are kept the same as those used in the original ABM in [5]. We define the hospital occupancy level to be a global variable that is set to 0.85. The probability a patient is immunocompromised is a global variable with baseline value 0.1. To determine the probability that a susceptible or not-immunocompromised colonized patient will regain resistance, we define a global variable for the minimum probability of regaining resistance, p_{rrmin}. At each half-day, there is a 27% chance a patient will begin antibiotic therapy. Bintz et al. [5] chose this value as the baseline so that the simulated total number of antibiotic treatments per patient matched the data. The baseline values for the probabilities of receiving a low-risk, high-risk, or very-high-risk antibiotic were taken from the dataset to be 0.4, 0.26, and 0.34, respectively.

The probability of effectively cleaning a room is set to a baseline value of 0.5, described more in Section 3.8.6. Symptomatic patients are screened for CDI, and the sensitivity of this test is a global variable set to 0.91. The turnover time for this test is assumed to be 2 half days [69]. The probability of successfully treating a patient with CDI has a baseline value of 0.8, based on the dataset from Barnes-Jewish Hospital.

Table 3.12: Global variable explanations and baseline values

Global Variable	Description	Baseline value
occupancy	hospital occupancy level	0.85
a_r	probability a patient is resistant upon admission	0.75
a_s	probability a patient is susceptible upon admission	0.09
a_c	probability a patient is colonized upon admission	0.15
a_d	probability a patient is diseased upon admission	0.01
immcomp-prob	probability a colonized patient will not mount an immune response	0.1
p_{rrmin}	minimum probability of regaining resistance	0.2
prob-antib	half-daily probability of a patient beginning an antibiotic treatment	0.27
prob-low-risk	probability of a prescribed antibiotic being low-risk with respect to CDI	0.4
prob-high-risk	probability of a prescribed antibiotic being high-risk with respect to CDI	0.26
prob-vhigh-risk	probability of a prescribed antibiotic being low-risk with respect to CDI	0.34
p_l^h	probability of becoming colonized if treated with low-risk antibiotic in a highly contaminated room	1/30
prob-eff-clean	probability of effective room cleaning	0.5
sensitivity	sensitivity of the CDI screening test	0.91
turnover	turnover time (half-days) of the CDI screening test	2
prob-succ-treat	probability of successful treatment of CDI	0.8
hcw-contact-compliance	probability of an HCW following proper contact precautions when visiting a quarantined patient	0.6
hcw-compliance	probability of an HCW effectively sanitizing after visiting a non-quarantined patient	0.45
clean-reduction	proportion by which the contamination level of a room is reduced after effective cleaning	0.5
hcw-transfer-percent	proportion of an HCW's carrier level that is transferred to a room upon successful transfer	0.9
room-transfer-percent	proportion of a room's contamination level that is transferred to an HCW upon successful transfer	0.1
contam-level-low	maximum contamination level of a low-contamination room	0.4
contam-level-med	maximum contamination level of a medium-contamination room	0.8

3.7.4 Process overview and scheduling

Our model runs some processes with a 15-minute time-step and other processes with a half-day time-step. The following HCW processes occur every 15 minutes: first, some HCWs may begin a new shift, and all HCWs will perform tasks on patients. Type 1 HCWs will move from room to room every 15 minutes, and Type 2 HCWs will move every 45 minutes (3 time-steps). Once an HCW enters a room, the risk level of the task he or she will perform is determined. Then, the probability of an HCW transferring pathogen to a room and the probability of a room transferring pathogen to an HCW are determined. Based on these probabilities, HCW carrier levels and room contamination levels are updated. After HCWs leave a room, they can reduce their contamination levels if they effectively wash their hands. Finally, a shift change occurs, and those who have finished their shift will leave the hospital before the process starts again. After the shift change, HCW time characteristics are updated.

Patient behaviors and interactions are updated each half-day in the following order: patients are admitted, their disease status is updated, the room contamination levels are then updated based on contributions from asymptomatic and symptomatic patients, and then patients may be discharged. Upon discharge, vacant rooms are then cleaned. Lastly, time characteristics are updated for the patients.

3.7.5 Initialization

The hospital is initially populated by patients whose disease statuses are based on the proportions a_r, a_s, a_c, and a_d given in Table 3.12. There are 210 available rooms that are filled to 85% occupancy. This occupancy proportion remains constant because we set the number of patients admitted each half-day equal to the number of patients discharged in the previous half-day. The number of HCWs is chosen so that there is a 3:1 ratio of patients to HCWs, and this is kept constant by assuming the number of HCWs who begin their shifts at each 15-minute time-step equals the number of HCWs who left at the last time-step. Initial room contamination levels are based on the disease status of the patient in the room upon

initialization, and the initial carrier level of all HCWs is assumed to be zero. The shift-lengths of HCWs who initially populate the model are set to random lengths between 0 and 12 hours since we assume that not all of them arrived to work at the same time. We simulate a three-week time period before recording any outputs to ensure that initial conditions are not significantly affecting the results.

3.8 Submodels

In this section, we detail all the submodels that together form the overall simulation routine.

3.8.1 Admit HCWs

At the beginning of each 15-minute time-step, new HCWs arrive to replace those who left the hospital at the end of the previous time-step. The number who arrive is set equal to the number who left at the previous time-step to ensure that the ratio of 1 HCW to every 3 patients is maintained. Upon arrival, each HCW is randomly assigned to a ward, and he or she remains in that same ward for the entirety of the shift. HCWs are only initially admitted into patient-occupied rooms where no other HCWs are currently present.

Once a new HCW arrives to the hospital, he or she is assigned a Type 1 or Type 2 role with a 50% chance of each. Additionally, a HCW's pathogen level is set to 0 upon arrival, and he or she is assigned a length of shift. For simplicity, we consider two possible shift lengths: 8 hours or 12 hours. There is a 50% chance a HCW will work an 8-hour shift, and a 50% chance he or she will work a 12-hour shift; this is decided for each HCW once arriving to the hospital.

3.8.2 Admit patients

This subroutine is modeled in the same way as that described in [5] with small modifications. At the beginning of each half-day time-step, new patients are admitted to replace those discharged at the end of the previous time-step. Similar to the arrival of HCWs, the number of new patients admitted equals the number of patients discharged at the previous time-step

to maintain a constant total population. Because of the variability in the number of patients discharged at the end of each time-step, this also ensures consistency and keeps the number of patients lower than the total number of ward rooms. The assignment of disease status upon admission is determined with the same probabilities used in the initialization process: a_r, a_s, a_c, and a_d, listed in Table 3.12. That is, there is a 75% chance an admitted patient is resistant [45], a 9% chance an admitted patient is susceptible, a 15% chance an admitted patient is colonized [1], and a 1% chance an admitted patient has CDI [45]. After a patient is assigned a disease status, we set his or her time since entering this disease status to 0 so that we can track this throughout the patient's hospital stay. The only exception to this is for resistant patients; we do not track their time since becoming resistant since this time does not affect their probability of moving to another disease class or how long it will be until they move to another disease class.

When patients are admitted, we initialize their number of antibiotics received in the hospital to 0, and their time since admission is also set to 0. Patients are randomly assigned a room upon admission and will only be assigned to vacant rooms since we assume all hospital rooms are single patient rooms. Also upon arrival, each patient is assigned a length of stay, which is determined by the subroutine described in Section 3.8.16.

When a patient is admitted as susceptible, we first assign that patient an antibiotic history because of our assumption that the only way to become susceptible to colonization is through the disruption of the normal gut microbiota by antibiotics. The process for determining the type of antibiotic that we will assign is described in Section 3.8.12. We next assign the susceptible patient a time since beginning antibiotic treatment (which will vary since antibiotic treatment began prior to entering the hospital). As described in [5], we set this time to "a random integer drawn from a uniform distribution ranging from 0 to an upper limit defined as the sum of the treatment length (14 half-days) and time until microbiota recovery (28 half-days for low- and high-risk antibiotics and 70 half-days for very-high-risk antibiotics)." This mimics our assumption that patients become susceptible immediately after receiving antimicrobial treatment and remain susceptible until the restoration of their normal gut microbiota. Lastly, a susceptible patient's time since becoming susceptible is set equal to his or her time since beginning an antibiotic.

Upon admission of a colonized patient, we first must determine whether or not this patient is immunocompromised. We do so by using the global variable for the probability a colonized patient will not mount an immune response, listed in Table 3.12. Once it is determined that a patient is not immunocompromised, we then assign the patient an antibiotic, using the subroutine described in Section 3.8.12. Next, we assign a time since beginning antibiotics in the same way described in the previous paragraph for susceptible patients. Because these patients can become colonized anytime after receiving an antibiotic, we lastly set their time since becoming colonized to be a random integer chosen from a uniform distribution ranging from 0 to their time since beginning antibiotics.

If it is determined that a colonized patient is immunocompromised upon admission, this patient will contract CDI, and the time until doing so is referred to as the incubation period. The length of the incubation period for a particular patient depends on the risk level of the antibiotic assigned. Therefore, for each immunocompromised patient, we begin by assigning an antibiotic (Section 3.8.12). The minimum and maximum possible lengths of the incubation period for various antibiotic-risk levels are given in Table 3.10. In particular, for those patients assigned a low-risk antibiotic, their incubation period is assigned to be a random integer from a uniform distribution over 20 to 60 half-days. Patients on a high-risk antibiotic have a greater chance of contracting CDI more quickly, so they are assigned an incubation period ranging from 14 to 40 half-days while patients on very-high-risk antibiotics are assigned an incubation period between 8 and 20 half-days. Once an immunocompromised patient is assigned an incubation period, he or she is then assigned a time until becoming diseased, which we set to a random integer less than or equal to the incubation period. Lastly, we track their time since becoming colonized by setting it equal to the length of the incubation period minus the time until becoming diseased, as described in [5].

If a patient is diseased upon admission, we begin by setting his or her time since becoming diseased to be a random integer less than or equal to 21 half-days, as used in [5]. We then assign whether or not each diseased patient will be treated successfully by using the global variable for the probability of successful treatment, listed in Table 3.12 as 0.8 [57]. Next, we decide if the hospital will successfully identify a diseased patient as diseased upon screening. Note that all patients are screened upon admission and/or upon becoming diseased [5]. The

success of the screening depends on the sensitivity of the test for CDI, which we represent with the sensitivity global variable listed in Table 3.12 as 0.91 [69]. If a patient will be successfully identified as diseased, we initialize his or her time since a successful screening to 0. Similarly, we will set the time since an unsuccessful screening to 0 for those patients who are not successfully identified. The turnaround time for the test is set to be 2 half-days [69]; once a patient's time since a successful screening reaches this turnaround time, he or she will be quarantined and begin treatment for CDI, a procedure described in Section 3.8.15. Those diseased patients who were unsuccessfully screened for CDI will not be tested again until after the turnaround time has passed.

3.8.3 Update disease status

This subroutine is run at each half-day time-step and is implemented similarly to the update-disease-status procedure described in [5]. There is a global variable for the probability that a patient will receive an antibiotic each half-day. In [5], they determined this probability should be 0.27 so that the total number of antibiotic treatments per patient matched the data from Barnes-Jewish Hospital. All possible disease-status transitions for a patient are illustrated in Figure 3.2 and were briefly described in Section 3.7.3. In this section, we describe in more detail the transitions and how they are implemented.

Once patients transition to a new disease status, their time since entering this new status is set to 0. A resistant patient's only possible movement is to the susceptible class by taking an antibiotic. If it is determined that a resistant patient receives an antibiotic, then that patient will be assigned an antibiotic (Section 3.8.12). We also keep track of the number of antibiotics a patient receives while in the hospital, so we update this number here. Next, an updated length of stay will be determined based on the patient's new status as susceptible; more details about this are given in Section 3.8.16. If this updated length of stay is greater than the current length of stay assigned to the patient, then the patient's current length of stay will be modified to reflect the longer length of stay.

A susceptible patient can either move back to the resistant class or become colonized after being exposed to pathogen. For each susceptible patient, this subroutine begins by

determining his or her probability of regaining resistance, which varies at each half-day time-step. Details about the calculation of this probability are given in Section 3.8.14. Based on this probability, a susceptible patient may return to the resistant class. If a susceptible patient does not return to resistant, there is a 27% chance that he or she will receive an additional antibiotic, and the type of antibiotic received is determined by the procedure described in Section 3.8.12.

Each susceptible patient also has a probability of becoming colonized that depends on the local contamination level and on the risk level of the antibiotic(s) received. Details about the calculation of this probability are given in Section 3.8.13. We also keep track of the number of patients who become colonized while in the hospital. If it is determined a susceptible patient will become colonized, we count him or her in this list and then determine whether or not he or she will be immunocompromised. For those who are immunocompromised, their incubation period is set in the same way as described in the admit-patients subroutine (Section 3.8.2).

For those colonized patients who are not immunocompromised, they also have a probability of regaining resistance (Section 3.8.14), or, like susceptible patients, they may receive an additional antibiotic. If so, their total number of hospital antibiotics and time since beginning an antibiotic are updated to reflect this.

Colonized patients who are immunocompromised also have a chance of receiving an additional antibiotic. Once the type of antibiotic is determined, this additional antibiotic may decrease their incubation period. In particular, for a high-risk antibiotic, their time until becoming diseased is decreased by 10%, and for a very-high-risk antibiotic, their time until becoming diseased is decreased by 20%. Once their time until becoming diseased reaches 0, they move to the disease class and receive an updated length of stay based on this new disease status (Section 3.8.16). Now that these patients are symptomatic, they will be screened at the next half-day time-step. We then determine whether these patients will be treated and/or screened successfully (in the same manner as described in Section 3.8.2). These patients are then counted in the number of patients who become diseased while in the hospital.

The only possible transition for diseased patients is back to the susceptible class. If a

diseased patient had a successful screening, he or she will be quarantined and begin treatment once the turnover time for the screening test has elapsed. If it is determined that the treatment will be successful, then the diseased patient may move back to the susceptible class after 20 half-days [5]. If a diseased patient had an unsuccessful screening, then after the turnover time has elapsed, he or she will be re-screened for CDI.

3.8.4 Update room contamination levels

After patient disease statuses are updated, the model updates the room contamination levels based on the disease status of the patient in the room. This particular subroutine only considers patient contributions to overall room contamination levels; HCW contributions are updated every 15 minutes using a different submodel (Section 3.8.9). A colonized patient will contribute an amount in the range $[1, 2)$ to the room contamination level at each half-day time step. Because the transmission potential is higher for patients with active disease than in asymptomatic carriers [26], a diseased patient will contribute an amount in the range $[2, 3)$ at each half-day time-step. Note that these ranges are larger than the possible ranges for HCW contributions since HCW contributions are updated at every 15-minute time-step.

3.8.5 Discharge patients

Once a patient's time since being admitted reaches his or her length of stay (assigned upon admission based on the procedure described in Section 3.8.16), that patient is discharged from the hospital. Discharges can only occur at each half-day time-step. In the discharge subroutine, we also tally the total number of patients discharged, the total number of patients discharged for each disease status, and the total number of antibiotics given in the hospital. The average length of stay for all discharged patients is also calculated.

3.8.6 Clean ward rooms

After patients are discharged, their vacant room is cleaned. The probability the room will be effectively cleaned is a global variable, listed in Table 3.12 as 0.5. This baseline value was chosen because, depending on which cleaning measures are used, the cleaning could be

more or less effective, and this probability can be adjusted to mimic more or less intensive cleaning. Our model only explicitly accounts for terminal cleaning; however, daily cleaning of select rooms could be implemented in the case of an outbreak. This can be incorporated in our model by modifying the contamination level of rooms that were targeted by extra cleaning.

In this subroutine, if it is determined a room will be effectively cleaned, the contamination level of the room will decrease by 50%, which is represented by the global variable *clean-reduction*. Similar to the probability of effective cleaning, this percentage can be increased to model more targeted and intensive cleaning.

3.8.7 Update patient time characteristics

Patient time characteristics are updated at each half-day time-step. This includes their time since being admitted and, for all patients except resistant patients, their time since entering their current disease status. As mentioned in Section 3.8.2, we do not track this time for resistant patients because it does not affect whether or not they will become susceptible; this is only determined by their probability of receiving an antibiotic.

For susceptible and colonized (non-immunocompromised) patients, this submodel increases their time since beginning an antibiotic by one half-day time-step each time it is run. For the colonized (immunocompromised) patients, their time until becoming diseased is decreased by one half-day. We also update the time since a diseased patient has received a successful, or unsuccessful, screening for CDI, and for those diseased patients who have begun treatment, we update their time since beginning treatment.

3.8.8 HCW movement

This subroutine defines how HCWs move from room to room, which depends on whether or not they are Type 1 HCWs or Type 2 HCWs. HCWs are instructed to only move into rooms that are currently occupied by a patient and will never enter vacant ward rooms. We also assume that all HCWs remain in the same ward for the entirety of their shift and never move from ward to ward.

In each ward, the rooms are numbered from 1 to 35. Type 1 HCWs, skipping any rooms that are unoccupied, move every 15-minute time-step from one room to the next in order of room number. Upon reaching room 35, a Type 1 HCW will next move to room 1 of that ward (as long as it is occupied at that time). Type 2 HCWs move randomly within a ward, and only move every three 15-minute time-steps. It is not possible for two Type 1 HCWs to be in the same room at the same time or for two Type 2 HCWs to be in the same room at the same time; however, it is possible for a Type 1 and a Type 2 to visit the same patient at the same time.

3.8.9 Update HCW and room contamination levels

This subroutine defines both how an HCW will transfer pathogen *to* a room and how an HCW will pick up pathogen *from* a room. It has three parts: defining risk level of tasks being performed, determining the probability of transfer, and updating contamination levels based on that transfer. Note that in our model there is no direct pathogen transfer from an HCW to a patient or vice versa. This transfer pathway is indirectly considered by assuming that colonized patients shed pathogen and increase the contamination level of their rooms, and the contamination level of the room affects the probability of HCWs picking up pathogen from that room.

The submodel begins by determining the risk level of the task each HCW will perform at a particular time-step. Type 1 HCWs have a greater chance of performing low-risk tasks while Type 2 HCWs have a greater chance of performing high-risk tasks. The specific probabilities used are shown in Table 3.13. The risk level of the task is chosen at every 15-minute time-step for both Type 1 HCWs and Type 2 HCWs. Therefore, a Type 2 HCW may perform different risk level tasks while with the same patient.

After determining the task-risk level, this submodel determines both the probability that an HCW will transfer pathogen to a room and the probability that a room will transfer to an HCW. Both of these probabilities depend on the risk level of the task being performed and on the amount of contamination already in the room or on the HCW's hands. We use three transfer functions, one for each risk level, to determine these probabilities. Each is a function of the following form, where x represents the contamination level (of the room or

of the HCW) and k depends on the risk level of the task:

$$f(x) = \frac{1 - \exp\left(\frac{-x}{k}\right)}{1 + 300\exp\left(\frac{-x}{k}\right)}.$$

The value of k controls the steepness of the curve. In particular, we use $k = 1, 0.5$, and 0.15 for a low-risk, medium-risk, and high-risk task, respectively. The resulting transfer functions are shown in Figure 3.20. The higher the contamination level of the HCW (or the room), the higher the probability of transfer. For a high-risk task, there is a greater chance of transfer at lower contamination levels than there is for a medium-risk or low-risk task at the same contamination level. Note that this process is only used for non-quarantined patients. For those patients who are quarantined, there is either a 100% chance of transfer or a 0% chance of transfer, depending on the variable *hcw-contact-compliance*. As listed in Table 3.12, we set this value to 0.6 [75] since HCWs are more likely to comply with proper contact protocol when visiting a quarantined patient. When an HCW does comply with contact regulations with a quarantined patient, then there is a 0% chance of pathogen transfer; when an HCW does not, there is a 100% chance of transfer.

The final process in this submodel involves the actual transfer of pathogen. If is determined that an HCW will transfer pathogen to the room, then he or she will transfer 90% of his or her total contamination level to the room. This then decreases the HCW contamination level by 90% and increases the room contamination level by that same amount. This percentage is represented by the global variable *hcw-transfer-percent* listed in Table 3.12. Similarly, if it is determined that a room will transfer pathogen to an HCW, then the room contamination level will decrease by 10%, and the HCW contamination level will increase by that amount. This value for *room-transfer-percent* was chosen with the assumption that, because a room has many surfaces on which pathogen may live, one HCW will only pick up a small percentage of the total contamination in one visit.

Table 3.13: Probabilities used to determine risk level of tasks performed by HCWs

Type 1

Task Risk Level	Probability
low	0.60
medium	0.25
high	0.15

Type 2

Task Risk Level	Probability
low	0.15
medium	0.25
high	0.60

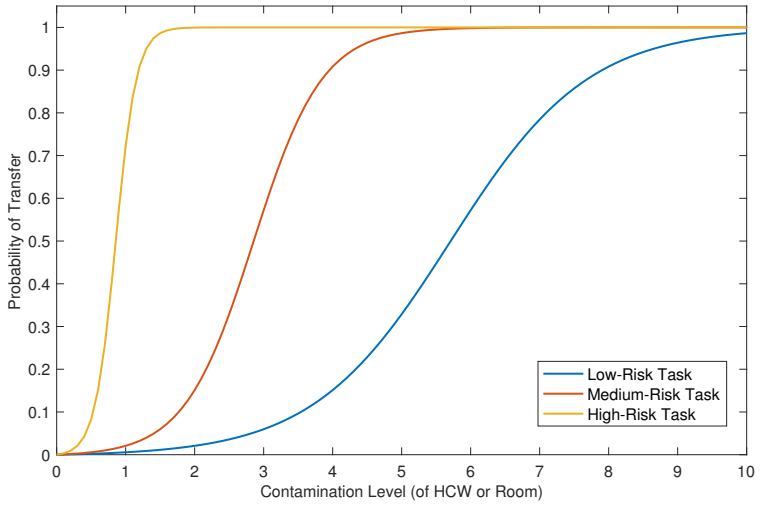


Figure 3.20: Transfer functions used to determine the probability a room (or HCW) will transfer pathogen at a particular time-step

3.8.10 HCW compliance

Each time HCWs leave a room, they wash their hands with a 45% chance of effectively doing so [75]. Based on this probability, if it is determined they will effectively do so, they reduce their total contamination level to 5% of what it was prior to washing their hands. If not, their contamination level remains the same.

3.8.11 Shift change and update of HCW time characteristics

Once an HCW's time since beginning a shift reaches the total length of his or her shift, assigned upon arrival (Section 3.8.1), he or she will leave the hospital. After this, we update the counter tracking the time since each HCW's shift began before starting the next 15-minute time-step.

3.8.12 Antibiotic assignment

The degree of microbiota disturbance (and resulting susceptibility to colonization) caused by antibiotics depends on the spectrum, duration, and number of antibiotics received [78, 14, 5]. For this reason, we maintain the three risk levels for antibiotics defined in [5]: low risk, high risk, and very high risk. This categorization of antibiotics was based on studies completed to analyze the association of particular antibiotics with *C. difficile*. In the antibiotic assignment submodel, we assign an antibiotic-risk level based on the probabilities of the antibiotic being low risk, high risk, or very high risk in terms of its association with *C. difficile*. The baseline values for these probabilities are given in Table 3.12. The risk level of an antibiotic also affects the time until microbiota returns to normal, which we assign in this subroutine based on the risk level assigned. For all patients, we set the length of treatment to one week as a simplifying assumption also used in [5].

3.8.13 Colonization probability assignment

At each half-day time-step, a susceptible patient's probability of being exposed to *C. difficile* and becoming colonized depends on two things: the contamination level of the room and

the risk level associated with the antibiotic received. To determine this probability, we divide room contamination levels into three categories: low, medium, or high contamination. Together with the three antibiotic-risk levels (low, high, or very high), this makes nine possible combinations of antibiotic-risk and room-contamination levels, which gives us nine different probabilities of colonization.

We denote p_h^l to represent the probability of a susceptible patient becoming colonized given that he or she is in a room with low contamination and has received a high-risk antibiotic. We use this notation similarly for the eight remaining probabilities, where the superscript refers to the room contamination level (l, m, or h) and the subscript refers to the risk level associated with the antibiotic (l, h, or vh).

To determine values for each of these probabilities, we began by using those calculated by Bintz et al. in [5]. Because studies have quantified the odds ratios for the risk of infection assigned to specific antibiotics [4] [23] [78], Bintz and his coauthors used odds ratios to represent the chances of becoming colonized if given a high-risk or very high-risk antibiotic compared to the odds of becoming colonized after given a low-risk antibiotic. Specifically, they were able to estimate odds ratios for high-risk and very high-risk antibiotics and then use those values, along with the data for the number of nosocomial infections, to determine the probabilities.

In our model, we used the nine probabilities calculated in [5] as a foundation but then modifed each of these values so that our number of nosocomial colonizations more closely matched the dataset. To make this match, we divided the nine probabilities used by Bintz et al. by the same scaling factor so that nosocomial colonizations accounted for 20% of all admissions [11, 40]. The final values we used for the probabilities are given in Table 3.14.

3.8.14 Resistance-restoration probability assignment

Once the microbiota returns to normal, a patient's resistance to colonization by *C. difficile* is restored. The chances of regaining resistance depend on how long a patient has been on an antibiotic and the type of antibiotic the patient received since the associated antibiotic risk affects the length of time until a normal microbiota is restored.

To determine the probability that resistance will be restored for a patient at a particular

Table 3.14: Probabilities of becoming colonized for each combination of antibiotic-risk and room-contamination level

	Antibiotic Risk Level	Room Contamination Level	Value
p_l^h	low	high	0.0333
p_h^h	high	high	0.0920
p_{vh}^h	very high	high	0.1301
p_l^m	low	medium	0.0250
p_h^m	high	medium	0.0748
p_{vh}^m	very high	medium	0.1119
p_l^l	low	low	0.0167
p_h^l	high	low	0.0544
p_{vh}^l	very high	low	0.0874

time-step, we use the same function Bintz et al. use in [5]. This function is logistic, where the input t represents the time since a patient began taking an antibiotic and T is the sum of the treatment length and the time until a normal microbiota is restored:

$$p(t,T) = \frac{1 - p_{\min}}{1 + \exp\left(-\frac{12}{T}\left(t - \frac{T}{2}\right)\right)} + p_{\min}.$$

The variable $p_{\min}$ is set to 0.2 and represents the minimum probability of regaining resistance while the parameter value of 12 controls the steepness of the curve.

3.8.15 Quarantine and treat

This submodel allows us to identify those patients who were successfully screened for CDI, mark them as quarantined, and model the effects of their isolation. Once patients are quarantined, they begin antimicrobial treatment for CDI, so we assign them an antibiotic using the procedure described in Section 3.8.12. Then, we update the patient's total number of hospital antibiotics to reflect this and initialize the time since beginning treatment to 0.

3.8.16 Patient length of stay

Depending on their disease status at admission, patients' length of stay in the hospital will vary. We assign patients a length of stay upon admission (Section 3.8.2) and determine this length in the same manner used in [5]. In their model, the authors resampled from the dataset generated by the Barnes-Jewish Hospital values for the length of stay of patients in each particular disease status. They then determined that resistant patients will stay between 0 and 16 days, susceptible and colonized patients will stay between 0 and 34 days, and diseased patients will stay between 0 and 80 days.

Chapter 4

Future work

The results we obtained in Chapter 2 are only a starting point for the analysis of vaccination against CDI. Because such a vaccine is still in testing, we were unable to incorporate data for quantities such as the monetary cost associated with this vaccination program. Once this data is obtained, we hope to carry out a more quantitative modeling study.

Additionally, the form of vaccination implemented in the ABM presented in Chapter 3 was based on the following assumptions: (1) everyone who needed to be vaccinated was able to be and (2) the vaccine was successfully implemented in such a way that the hospital experienced an overall reduction in the percentage of colonized, immunocompromised patients. Will vaccination actually result in the overall decrease in the percentage of colonized, immunocompromised patients that we assumed in Chapter 3? We would like to weaken our assumptions and observe how modeling and tracking the vaccination of individual patients in the ABM affects the overall disease prevalence. In particular, we want to incorporate age and other CDI risk factors when deciding who to vaccinate.

Future plans also include expanding our exploration of the role environmental reservoirs play in *C. difficile* transmission. Specifically, we will examine the effect of fomite touch frequency on transmission. To model these dynamics, we will utilize a stochastic model that incorporates patient and pathogen populations, where the patients are divided according to disease status with respect to *C. difficile* and the pathogen levels are divided based on high-frequency touch surfaces and low-frequency touch surfaces. Our goal is to use this

model to better understand how surfaces with varying touch frequencies affect nosocomial colonizations and infections by *C. difficile*.

Bibliography

[1] Alasmari, F., Seiler, S., Hink, T., Burnham, C., and Dubberke, E. (2014). Prevalence and risk factors for asymptomatic *Clostridium difficile* carriage. *Clinical Infectious Diseases*, 59(2):216–222. 13, 45, 77, 83, 88

[2] Asano, E., Gross, L., Lenhart, S., and Real, L. (2008). Optimal control of vaccine distribution in a rabies metapopulation model. *Mathematical Biosciences and Engineering*, 5(2):219–238. 10

[3] Barlett, J. (2006). Narrative review: the new epidemic of *Clostridium difficile*-associated enteric disease. *Annals of Internal Medicine*, 145:758–764. 39

[4] Bignardi, G. (1998). Risk factors for *Clostridium difficile* infection. *Journal of Hospital Infection*, 40(1):1–15. 98

[5] Bintz, J., Lenhart, S., and Lanzas, C. (2017). Antimicrobial stewardship and environmental decontamination for the control of *Clostridium difficile* transmission in healthcare settings. *Bulletin of Mathematical Biology*, 79(1):36–62. xvi, 8, 39, 40, 41, 42, 43, 44, 45, 46, 52, 54, 56, 57, 61, 63, 64, 65, 71, 72, 75, 77, 78, 79, 84, 87, 88, 89, 90, 92, 97, 98, 99, 100

[6] Brauer, F. (2015). Some simple nosocomial disease transmission models. *Bulletin of Mathematical Biology*, 77(3):460–469. 4, 38

[7] Carling, P. and Bartley, J. (2010). Evaluating hygienic cleaning in health care settings: what you do not know can harm your patients. *American Journal of Infection Control*, 38(5 Suppl 1):S41–50. 8

[8] Carroll, K. and Bartlett, J. (2011). Biology of *Clostridium difficile*: implications for epidemiology and diagnosis. *Annual Review of Microbiology*, 65:501–521. 39

[9] Clabots, C., Johnson, S., Olson, M., Peterson, L., and Gerding, D. (1992). Acquisition of *Clostridium difficile* by hospitalized patients: evidence for colonized new admissions as a source of infection. *Journal of Infectious Diseases*, 166(3):561–567. 2

[10] Codella, J., Safdar, N., Heffernan, R., and Alagoz, O. (2014). An agent-based simulation model for *Clostridium difficile* infection control. *Medical Decision Making*, 35(2):211–229. 40, 41

[11] Crobach, M., Vernon, J., Loo, V., Kong, L., Pèchinè, S., Wilcox, M., and Kuijper, E. (2018). Understanding *Clostridium difficile* colonization. *Clinical Microbiology Reviews*, 31(2):e00021–17. 57, 84, 98

[12] Curry, S., Muto, C., Schlackman, J., Pasculle, A., Shutt, K., Marsh, J., and Harrison, L. (2013). Use of multilocus variable number of tandem repeats analysis genotyping to determine the role of asymptomatic carriers in *Clostridium difficile* transmission. *Clinical Infectious Diseases*, 57(8):1094–1102. 41

[13] D'Agata, E., Magal, P., Olivier, D., Ruan, S., and Webb, G. (2007). Modeling antibiotic resistance in hospitals: the impact of minimizing treatment duration. *Journal of Theoretical Biology*, 249:487–499. 40, 41

[14] Dancer, S., Kirkpatrick, P., Corcoran, D., Christison, F., Farmer, D., and Robertson, C. (2013). Approaching zero: temporal effects of a restrictive antibiotic policy on hospital-acquired *Clostridium difficile*, extended spectrum β-lactamase-producing coliforms and methicillin-resistant *Staphylococcus aureus*. *International Journal of Antimicrobial Agents*, 41(2):137–142. 39, 45, 97

[15] Dancer, S., White, L., Lamb, J., Girvan, E., and Robertson, C. (2009). Measuring the effect of enhanced cleaning in a uk hospital: a prospective cross-over study. *BMC Medicine*, 7:28. 8

[16] Ding, W. and Webb, G. (2016). Optimal control applied to community-acquired methicillin-resistant staphylococcus aureus in hospitals. *Journal of Biological Dynamics*. 10

[17] Donskey, C. (2010). Preventing transmission of *Clostridium difficile*: Is the answer blowing in the wind? *Clinical Infectious Diseases*, 50(11):1458–1461. 40

[18] Dubberke, E., Carling, P., Carrico, R., Donskey, C., Loo, V., McDonald, L., Maragakis, L., Sandora, T., Weber, D., and Yokoe et al., D. (2014). Strategies to prevent *Clostridium difficile* infections in acute care hospitals: 2014 update. *Infection Control & Hospital Epidemiology*, 35(06):628–645. 2, 39, 40, 44

[19] Dubberke, E., Haslam, D., Lanzas, C., Bobo, L., Burnham, C.-A., and Grohn, Y. (2011). The ecology and pathobiology of *Clostridium difficile* infections: An interdisciplinary challenge. *Zoonoses Public Health*, 58(1):4–20. 1, 2, 3, 80

[20] Dubberke, E. and Olsen, M. (2012). Burden of *Clostridium difficile* on the healthcare system. *Clinical Infectious Diseases*, 55(suppl 2):S88–S92. 38

[21] Eckstein, B., Adams, D., and Eckstein et al., E. (2007). Reduction of *Clostridium difficile* and vancomycin-resistant *Enterococcus* contamination of environmental surfaces after an intervention to improve cleaning methods. *BMC Infectious Diseases*, 7:61. 40

[22] Faires, M., Pearl, D., Berke, O., Reid-Smith, R., and Weese, J. (2013). The identification and epidemiology of meticillin-resistant *Staphylococcus aureus* and *Clostridium difficile* in patient rooms and the ward environment. *BMC Infectious Diseases*, 13:342. 8

[23] Feazel, L., Malhotra, A., Perencevich, E., Kaboli, P., Diekema, D., and Schweizer, M. (2014). Effect of antibiotic stewardship programmes on *Clostridium difficile* incidence: a systematic review and meta-analysis. *Journal of Antimicrobial Chemotherapy*, 69(7):1748–1754. 39, 98

[24] Fister, R., Lenhart, S., and McNally, J. (1998). Optimizing chemotherapy in an hiv model. *Electronic Journal of Differential Equations*, 32:1–12. 10

[25] Friedman, A. (1982). *Foundations of Modern Analysis*. Dover Publications, Inc, New York. 22

[26] Furuya-Kanamori, L., J, M., Yakob, L., Riley, T., Paterson, D., Foster, N., Huber, C., and Clements, A. (2015). Asymptomatic *Clostridium difficile* colonization: epidemiology and clinical implications. *BMC Infectious Diseases*, 15:516. 92

[27] Gaff, H. and Schaefer, E. (2009). Optimal control applied vaccination and treatment strategies for various epidemiological models. *Mathematical Biosciences and Engineering*, 6:469–492. 10

[28] Galvin, S., Dolan, A., Cahill, O., Daniels, S., and Humphreys, H. (2012). Microbial monitoring of the hospital environment: why and how? *Journal of Hospital Infection*, 82:143–151. 7, 39, 40, 72, 83

[29] Gerding, D., Muto, C., and Owens, R. (2008). Measures to control and prevent *Clostridium difficile* infection. *Clinical Infectious Diseases*, 46(Supplement 1):S43–S49. 40, 79

[30] Ghosh-Dasitar, U. and Lenhart, S. (2015). Modeling the effect of vaccines on cholera. *Journal of Biological Systems*, 23(02):323–338. 10

[31] Goldmann, D. and Huskins, W. (1997). Control of nosocomial antimicrobial-resistant bacteria: a strategic priority for hospitals worldwide. *Clinical Infectious Diseases*, 24 Suppl 1:S139–45. 40

[32] Grimm, V., Berger, U., DeAngelis, D., Polhill, J., Giske, J., and Railsback, S. (2010). The odd protocol: a review and first update. *Ecological Modeling*, 221(23):2760–2768. 43

[33] Hackbusch, W. (1978). A numerical method for solving parabolic equations with opposite orientations. *Computing*, 20(3):229–240. 25

[34] Hota, B. (2004). Contamination, disinfection, and cross-colonization: are hospital surfaces reservoirs for nosocomial infection? *Clinical Infectious Diseases*, 39(8):1182–1189. 7

[35] Hsieh, P. and Sibuya, Y. (1999). *Basic Theory of Ordinary Differential Equations*. Springer, New York. 16

[36] Hsieh, Y., Liu, J., Tzeng, Y., and Wu, J. (2014). Impact of visitors and hospital staff on nosocomial transmission and spread to community. *Journal of Theoretical Biology*, 356(0):20–29. 38

[37] Hsu, J., Abad, C., Dinh, M., and Safdar, N. (2010). Prevention of endemic healthcare-associated *Clostridium difficile* infection: Reviewing the evidence. *The American Journal of Gastroenterology*, 105(11):2327–2339. 41

[38] Joh, R., Wang, H., Weiss, H., and Weitz, J. (2009). Dynamics of indirectly transmitted infectious diseases with immunological threshold. *Bulletin of Mathematical Biology*, 71(4):845–862. 38

[39] Johnson, S. and Gerding, D. (1998). *Clostridium difficile*-associated diarrhea. *Clinical Infectious Diseases*, 26(5):1027–1034. 11, 39

[40] Kachrimanidou, M. and Malisiovas, N. (2011). *Clostridium difficile* infection: a comprehensive review. *Critical Reviews in Microbiology*, 37:178–187. 38, 39, 45, 57, 84, 98

[41] Kujper, E., Coignard, B., and Tull, P. (2006). Emergence of *Clostridium difficile*-associated disease in north america and europe. *Clinical Microbiology and Infection*, 12 Suppl 6:2–18. 38

[42] Kwon, J., Olsen, M., and Dubberke, E. (2015). The morbidity, mortality, and costs associated with *Clostridium difficile* infection. *Infectious Disease Clinics of North America*, 29(1):123–134. 1

[43] Kyne, L., Warny, M., Qamar, A., and Kelly, C. (2000a). Asymptomatic carriage of *Clostridium difficile* and serum levels of igg antibody against toxin a. *New England Journal of Medicine*, 342(6):390–397. 9

[44] Kyne, L., Warny, M., Qamar, A., and Kelly, C. (2000b). Asymptomatic carriage of *Clostridium difficile* and serum levels of IgG antibody against toxin A. *The New England Journal of Medicine*, 342(6):390–397. 13

[45] Lanzas, C., Dubberke, E., Lu, Z., Reske, K., and Grohn, Y. (2011). Epidemiological model for *Clostridium difficile* transmission in healthcare settings. *Infection Control and Hospital Epidemiology*, 32(6):553–561. xi, 2, 3, 4, 10, 11, 12, 13, 32, 38, 43, 44, 45, 46, 77, 83, 88

[46] Leber, A., Viladomiu, M., Hontecillas, R., Abedi, V., Philipson, C., Hoops, S., Howard, B., and Bassaganya-Riera, J. (2015). Systems modeling of interactions between mucosal immunity and the gut microbiome during *Clostridium difficile* infection. *PLoS ONE*, 10(7):e0134849. 3

[47] Lee, B., Popovich, M., Tian, Y., Bailey, R., Ufberg, P., Wiringa, A., and Muder, R. (2010). The potential value of *Clostridium difficile* vaccine: an economic computer simulation model. *Vaccine*, 28(32):5245–5253. 9

[48] Leffler, D. and Lamont, T. (2015). *Clostridium difficile* infection. *The New England Journal of Medicine*, 372(16):1539–1548. 1, 2, 3, 36, 45, 47, 80

[49] Lenhart, S. and Workman, J. (2007). *Optimal control applied to biological models*. CRC Press, New York. 4, 5, 25

[50] Lessa, F., Mu, Y., Bamberg, W., Beldavs, Z., Dumyati, G., Dunn, J., Farley, M., Holzbauer, S., Meek, J., Phipps, E., Wilson, L., Winston, L., Cohen, J., Limbago, B., Fridkin, S., Gerding, D., and McDonald, L. (2015). Burden of *Clostridium difficile* infection in the united states. *New England Journal of Medicine*, 372(9):825–834. 1

[51] Leuzzi, R., Adamo, R., and Scarselli, M. (2014). Vaccines against *Clostridium difficile*. *Human vaccines & immunotherapeutics*, 10(6):1466–1477. 9

[52] Lopman, B., Gastañaduy, P., Park, G., Hall, A., Parashar, U., and Vinjé, J. (2012). Environmental transmission of norovirus gastroenteritis. *Current Opinion in Virology*, 2(1):96–102. 7

[53] Lowden, J., Beilan, R., and Yahdi, M. (2014). Optimal control of vancomycin-resistant enterococci using preventive care and treatment of infections. *Mathematical Biosciences*, 249:8–17. 10

[54] Marino, S., Hogue, I., Ray, C., and Kirschner, D. (2008). A methodology for performing global uncertainty and sensitivity analysis in systems biology. *Journal of Theoretical Biology*, 254:178–196. 115, 116

[55] Mayfield, J., Leet, T., Miller, J., and Mundy, L. (2000). Environmental control to reduce transmission of *Clostridium difficile*. *Clinical Infectious Diseases*, 31(4):995–1000. 40

[56] McDonald, L., Killgore, G., Thompson, A., Owens, R. J., Kazakova, S., Sambol, S., Johnson, S., and Gerding, D. (2005). An epidemic, toxin gene-variant strain of *Clostridium difficile*. *New England Journal of Medicine*, 353(23):2433–2441. 1

[57] McFarland, L. (2008). Update on the changing epidemiology of *Clostridium difficile*-associated disease. *Nature Clinical Practice Gastroenterology and Hepatology*, 5(1):40–48. 13, 89

[58] McFarland, L., Mulligan, M., Kwok, R., and Stamm, W. (1989). Nosocomial acquisition of *Clostridium difficile* infection. *New England Journal of Medicine*, 320(4):204–210. 11

[59] McKay, M., Beckman, R., and Conover, W. (2000). A comparison of three methods for selecting values of input variables in the analysis of output from a computer code. *Technometrics*, 42(1):55–61. 115

[60] McMaster-Baxter, N. and Musher, D. (2007). *Clostridium difficile*: Recent epidemiologic findings and advances in therapy. *Pharmacotherapy: The Journal of Human Pharmacology and Drug Therapy*, 27(7):1029–1039. 40

[61] Miller-Neilan, R., Schaefer, E., Gaff, H., Fister, K., and Lenhart, S. (2010). Modeling optimal intervention strategies for cholera. *Bulletin of Mathematical Biology*, 1(4):379–393. 10

[62] Mojica, E., Stephenson, B., Day, J., Lenhart, S., and Peterson, G. (Submitted). Papas: A lightweight and generic framework for parallel parameter studies. *PEARC18*. 57

[63] Morris, A., Jobe, B., Stoney, M., Sheppard, B., Deveney, C., and Deveney, K. (2002). *Clostridium difficile* colitis: an increasingly aggressive iatrogenic disease? *Archives of Surgery*, 137:1096–1100. 39

[64] Novoa, A., Pi-Sunyer, T., Sala, M., Molins, E., and Castells, X. (2007). evaluation of hand hygience adherence in a tertiary hospital. *American Journal of Infection Control*, 35(10):676–686. 40

[65] Otten, A., Reid-Smith, R., Fazil, A., and Weese, J. (2010). Disease transmission model for community-associated *Clostridium difficile* infection. *Epidemiology and Infection*, 138:907–914. 63

[66] Oughton, M., Loo, V., Dendukuri, N., Fenn, S., and Libman, M. (2009). Hand hygiene with soap and water is superior to alcohol rub and antiseptic wipes for removal of *Clostridium difficile*. *Infection Control and Hospital Epidemiology*, 30(10):939–944. 40

[67] Owens, R., Donskey CJ Gaynes, R., Loo, C., and Muto, C. (2008). Antimicrobial-associated risk factors for *Clostridium difficile* infection. *Clinical Infectious Diseases*, 46:S19–31. 39

[68] Pepin, J., Routhier, S., Gagnon, S., and Brazeau, I. (2006). Management and outcomes of a first recurrence of *Clostridium difficile*-associated disease in quebec, canada. *Clinical Infectious Diseases*, 42:758–764. 38

[69] Planche, T., Aghaizu, A., Holliman, R., Riley, P., Poloniecki, J., Breathnach, A., and Krishna, S. (2008). Diagnosis of *Clostridium difficile* infection by toxin detection kits: a systematic review. *The Lancet Infectious Diseases*, 8(12):777–784. 84, 90

[70] Pontryagin, L., Boltyanskii, V., Gamkrelize, R., and Mishchenko, E. (1962). *The mathematical theory of optimal processes*. Wiley, New York. 4, 5, 6, 21, 23, 24

[71] Rafii, F., Sutherland, J., and Cerniglia, C. (2008). Effects of treatment with antimicrobial agents on the human colonic microflora. *Therapeutics and Clinical Risk Management*, 4(6):1343–1358. 13

[72] Railsback, S. and Grimm, V. (2012). *Agent-based and individual-based modeling: a practical introduction*. Princeton University Press, New Jersey. 7, 40, 42, 77

[73] Rebeaud, F. and Bachmann, M. (2012). Immunization strategies for *Clostridium difficile* infections. *Expert Review of Vaccines*, 11(4):469–479. 3

[74] Romulus, B. (2013). Role of environmental persistence in pathogen transmission: a mathematical modeling approach. *Journal of Mathematical Biology*, 66(3):535–546. 38

[75] Rubin, M., Jones, M., Leecaster, M., Khader, K., Ray, W., Huttner, A., Huttner, B., Toth, D., Sablay, T., Borotkanics, R., Gerding, D., and Samore, M. (2013). A simulation-based assessment of strategies to control *Clostridium difficile* transmission and infection. *PLoS ONE*, 8(11):e80671. 39, 40, 41, 50, 51, 55, 78, 83, 95, 97

[76] Saltelli, A., Tarantola, S., and Campolongo, F. (2000). Sensitivity analysis as an ingredient of modeling. *Statistical Science*, 15(4):377–395. 115

[77] Samore, M., Venkataraman, L., DeGirolami, P., Arbeit, R., and Karchmer, A. (1996). Clinical and molecular epidemiology of sporadic and clustered cases of nosocomial *Clostridium difficile* infection. *New England Journal of Medicine*, 100(1):32–40. 11

[78] Slimings, C. and Riley, T. (2014). Antibiotics and hospital-acquired *Clostridium difficile* infection: update of systematic review and meta-analysis. *Journal of Antimicrobial Chemotherapy*, 69(4):881–891. 39, 45, 97, 98

[79] Smith, H. (1995). *Monotone dynamical systems: an introduction to the theory of competitive and cooperative systems*. American Mathematical Society, Rhode Island. 16

[80] Starr, J., Campbell, A., Renshaw, E., Poxton, I., and Gibson, G. (2009). Spatiotemporal stochastic modeling of *Clostridium difficile*. *Journal of Hospital Infection*, 71(1):49–56. 2

[81] Stephenson, B., Lanzas, C., Lenhart, S., and Day, J. (2017). Optimal control of vaccination in an epidemiological model of *Clostridium difficile* transmission. *Journal of Mathematical Biology*, 75(6-7):1693–1713. 38

[82] Talpaert, M., Gopal Rao, G., Cooper, B., and Wade, P. (2011). Impact of guidelines and enhanced antibiotic stewardship on reducing broad-spectrum antibiotic usage and its effect on incidence of *Clostridium difficile* infection. *Journal of Antimicrobial Chemotherapy*, 66(9):2168–2174. 39

[83] Tien, J. and Earn, D. (2010). Multiple transmission pathways and disease dynamics in a waterborne pathogen model. *Bulletin of Mathematical Biology*, 72(6):1506–1533. 38

[84] van Kleef, E., Deeny, S., Jit, M., Cookson, B., Goldenberg, S., Edmunds, W., and Robotham, J. (2016). The projected effectiveness of *Clostridium difficile* vaccination as part of an integrated infection control strategy. *Vaccine*, 34(46):5562–5570. 3, 38, 40, 42

[85] Viscidi, R., Laughon, B., Yolken, R., Bo-Linn, P., Moench, T., Ryder, R., and Bartlett, J. (1983). Serum antibody response to toxins a and b of *Clostridium difficile*. *Journal of Infectious Diseases*, 148(1):93–100. 9

[86] Webb, G., Blaser, M., Zhu, H., Ardal, S., and Wu, J. (2004). Critical role of nosocomial transmission in the toronto sars outbreak. *Mathematical Biosciences and Engineering*, 1(1):1–13. 38

[87] Wilcox, M., Mooney, L., Bendall, R., Settle, C., and Fawley, W. (2008). A case-control study of community-associated *Clostridium difficile* infection. *Journal of Antimicrobial Chemotherapy*, 62:388–396. 82

[88] Yahdi, M., Abdelmageed, S., Lowden, J., and Tannenbaum, L. (2012). Vancomycin-resistant *enterococci* colonization-infection model: parameter impacts and outbreak risks. *Journal of Biological Dynamics*, 6(2):645–662. 38

Appendices

A Sensitivity analysis

Sensitivity analysis is used to quantify uncertainty by evaluating how variations in model outputs can be attributed to different input sources, such as parameter values and initial conditions [54, 76]. Because a few of our parameters in Chapter 2 were numerically estimated and did not come directly from data or the literature, it is useful to quantify the impact of each of our parameters on the objective functional value, $J(v^*)$, in (2.8). If our output is notably sensitive to a particular parameter value, it becomes more important for us to estimate that parameter as accurately as possible.

We use Latin Hypercube Sampling (LHS) and partial rank correlation coefficients (PRCCs) to perform our sensitivity analysis. LHS is a sampling technique that requires fewer samples than many other sampling methods, but with equivalent accuracy [54]. This sampling process involves taking the assigned interval for each parameter, dividing it into n intervals of equal probability, and then sampling each of the intervals to obtain n values for each parameter. We then use the vector of n values for each of the k parameters being evaluated to create an $n \times k$ matrix, referred to as the LHS matrix. As a result, the i^{th} row of the LHS matrix contains a specific value for each of the k parameters to be used on the i^{th} run of the computer model.

For our analysis, we aim to quantify the impact of 11 inputs, in this case parameter values, on the objective functional value $J(v^*)$. The 11 parameters of interest are listed, with their corresponding baseline values and intervals sampled, in Table A.1, and we assume the parameters are uniformly distributed across the their specified intervals, which were chosen so that the baseline value used in Chapter 2 is the average of the lower and upper bound of the interval. For LHS to be used correctly, it is required that the output be monotonic with respect to each of the parameters [59]. Before begin the sampling process, we ensure that this monotonicity requirement is met for each parameter, and any parameter that does not satisfy this criteria cannot be included in the sensitivity analysis. To verify monotonicity, we vary one parameter while fixing the remaining parameters at baseline and then solve our optimal control problem several times across the assigned interval for the parameter being varied. We were able to illustrate that the objective functional value $J(v^*)$ was monotonic

with respect to each of the 11 parameters being considered.

Next, we created the $n \times 11$ LHS matrix. The number of trials, n, that we used was 100. Each column of our LHS matrix then represents 100 different values for a particular parameter that were chosen from 100 different subintervals of equal probability between the lower bound and upper bound for that parameter. The 100 chosen values for each parameter are permuted so that they are randomly ordered. Each row of the LHS matrix then represents one particular parameter combination to be used to solve our optimal control problem and then to calculate the resulting objective functional. Thus, we solve the optimal control problem 100 times for 100 different parameter combinations contained in each row of the LHS matrix.

Correlation quantifies the strength of a linear association between an input and an output while controlling for the impact of the remaining inputs [54] . We calculate PRCCs for each of our parameters and then use significance tests to assess if the PRCC is significantly different from zero and if two PRCCs are significantly different from each other. To calculate the PRCCs and corresponding p-values of the significance tests, we use the *partialcorr()* function in MATLAB. The resulting values are illustrated for easy comparison in Figure A.1 and are listed in Table A.2.

Using a significance level of 0.01, we conclude that α, β_c, β_d, k_r, and k have PRCCs that are significantly different from 0. Thus, the antibiotic prescription rate, transmission coefficients (for both asymptomatic and symptomatic patients), and discharge rates for all patients except diseased patients have a significant impact on the objective functional value $J(v^*)$.

Table A.1: List of parameters considered in the sensitivity analysis procedure with their corresponding intervals sampled and baseline values

Parameter	Interval	Baseline value
α	$[0.35, 0.65]$	0.5
θ	$[0.023, 0.043]$	0.033
β_c	$[10^{-8}, 10^{-4}]$	10^{-6}
β_d	$[10^{-8}, 10^{-4}]$	10^{-6}
f	$[0.45, 0.75]$	0.6
ε	$[0.07, 0.13]$	0.1
p	$[0.6, 1]$	0.8
ϕ	$[0.03, 0.1]$	0.06
k_r	$[0.23, 0.43]$	0.33
k	$[0.105, 0.195]$	0.15
k_d	$[0.048, 0.088]$	0.068

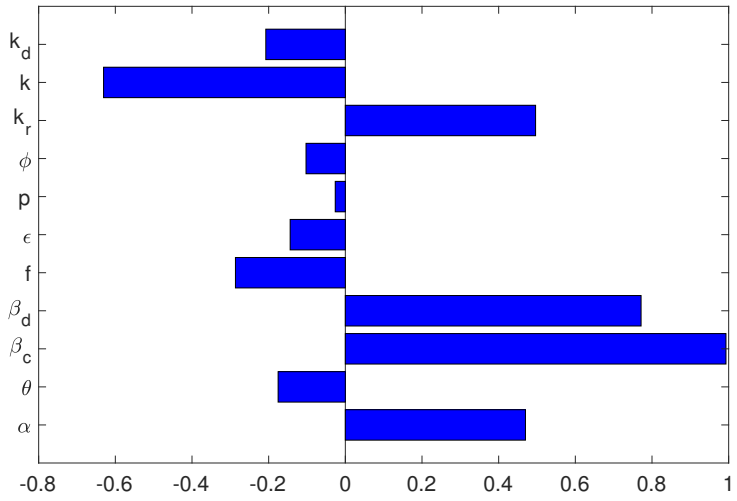


Figure A.1: Resulting PRCCs for each of the parameters considered

Table A.2: PRCCs and corresponding p-values for each parameter

Parameter	PRCC	p-value
α	0.54	< 0.01
θ	-0.18	0.08
β_c	0.99	$<< 0.01$
β_d	0.76	< 0.01
f	-0.12	0.28
ε	-0.10	0.34
p	-0.18	0.09
ϕ	0.03	0.81
k_r	0.64	< 0.01
k	-0.63	< 0.01
k_d	-0.18	0.10

Vita

Brittany Christine Stephenson was born in Jackson, Mississippi on October 3, 1989. She was raised by Chris and Jud Stephenson in Madison, Mississippi with her two siblings, Matt and Kayla. There she attended Madison Central High School, from which she graduated in 2008. After graduating, she moved to Starkville, Mississippi to attend Mississippi State University. Following in the footsteps of her mother, aunts, and older brother, she majored in mathematics and worked with Dr. Ratnasingham Shivaji, with whom she began her research involving population dynamics. She obtained her Bachelor of Science degree in Mathematics in May 2012.

In August 2012, Brittany moved to Knoxville, Tennessee to begin her pursuit of a PhD in Mathematics with a concentration in Mathematical Ecology. While there, she was supported by a teaching assistantship and through funding as a graduate student on NIH award #R01GM113239. At UT, Brittany taught many mathematics classes, including Calculus I, Mathematics for Life Sciences, Finite Mathematics, and Statistical Reasoning. From 2015 to 2018, she worked with Drs. Judy Day, Suzanne Lenhart, and Cristina Lanzas on the modeling of *C. difficile* transmission. In August 2018, Brittany graduated with her PhD in Mathematics.

Brittany will continue sharing her love for mathematics as an Assistant Professor of Mathematics at Lewis University in Romeoville, Illinois, beginning August 2018.